LEUKOCYTE AND ENDOTHELIAL GENE EXPRESSION: RESPONSE TO ENDOTHELIAL STIMULATION AND LEUKOCYTE TRANSMIGRATION

A Dissertation
Presented to
The Academic Faculty

by

Marcie R. Williams

In Partial Fulfillment
of the Requirements for the Degree
Doctor of Philosophy in Biomedical Engineering

Georgia Institute of Technology
Emory University

May, 2009

LEUKOCYTE AND ENDOTHELIAL GENE EXPRESSION:
RESPONSE TO ENDOTHELIAL STIMULATION AND LEUKOCYTE TRANSMIGRATION

Approved by**:**

Dr. Larry V. McIntire, Advisor
Wallace H. Coulter Department of Biomedical Engineering
Georgia Institute of Technology

Dr. Suzanne G. Eskin
Wallace H. Coulter Department of Biomedical Engineering
Georgia Institute of Technology

Dr. Julia E. Babensee
Wallace H. Coulter Department of Biomedical Engineering
Georgia Institute of Technology

Dr. C. Wayne Smith
Department of Pediatrics and Immunology
Baylor College of Medicine

Dr. Leonard M. Anderson
Cardiovascular Research Institute
Morehouse School of Medicine

Date Approved: 2/19/09

To my family who supported me from beginning to end.

ACKNOWLEDGEMENTS

This project could not have been completed without the assistance of many people. Within the lab I would like to thank Dr. Noriyuki Kataoka, who served as my mentor and sounding board during the first two years of the project; Dr. Lisa Schildmeyer, who provided assistance, training, and advice; Leslie Coburn, who was a great study partner and conference roommate; Yumiko Sakurai, who did much of the protein analysis described here; and finally Daniel Conway, who worked with me to develop the reversing flow system and performed many of the experiments described in Chapter 4. I would also like to thank a number of undergraduate students who have assisted in this project; Christina Powers, Matt Goette, Blaise MacEachern, and Courtney Mitchell.

I am also grateful to a number of collaborators from outside the biomedical engineering department. Morehouse School of Medicine Functional Genomics Core Facility performed the microarray hybridization and scanning in addition to providing assistance with data analysis. The Biomolecular Computing Resource (BimCore) at Emory University allowed me access to important microarray analysis software. I have also been greatly assisted by highly skilled and knowledgeable scientists from Baylor College of Medicine and Rice University with whom we participated in a Bioengineering Research Partnership supported by the National Institute of Health.

I would also like to thank Dr. Wayne Smith, Dr. Leonard Anderson, and Dr. Julia Babensee who served as members of my committee and have offered me valuable

advice on my project. My advisors, Dr. Larry McIntire and Dr. Suzanne Eskin, have been a great blessing. They have provided me with abundant freedom to define my own project, support in my personal and scientific endeavors, and guidance for future pursuits and goals.

My parents, Mark and Sherry Plunkett, have provided endless assistance and support throughout all of my endeavors. Certainly, none of this would be possible without my wonderful husband, Arthur Williams, who is endearingly patient when I am distracted, supportive when I am upset, and kind when I am not. I am also greatly blessed by my daughter Caiden who giggles with delight when I play with her, smiles with joy when I walk in the room, and gives me kisses in the morning as I leave for work.

Finally, I would like to thank my Lord and Savior, Jesus Christ, who has given me hope and a future.

TABLE OF CONTENTS

LIST OF TABLES

LIST OF FIGURES

LIST OF ABBREVIATIONS

ACIN	Apoptotic Chromatin Condenstation Inducer 1
ANOVA	Analysis of Variance
APOL3	Apolipoprotein L-III
BFL1	BCL2 Related Protein A1
BrdU	Bromodeoxyuridine
C5a	Complement Component 5a
CAD	Caspase Activated DNAse
CAMP	Cathelicidin Antimicrobial Peptide
CASP3	Caspase 3
CCL	Chemokine (C-C motif) ligand
CCL2	Monocyte Chemotactic Protein 1
CCL7	Monocyte Chemotactic Protein 3
CCNB3	Cyclin B3
CCNE2	Cyclin E2
CDC20	Cell Division Cycle 20
CDK2	Cyclin-dependent Kinase 2
cDNA	Complementary Deoxyribonucleic Acid
CRIP1	Cysteine-rich Intestinal Protein 1
cRNA	Complementary Ribonucleic Acid
CTP	Cytidine 5’ Triphosphate
CTSG	Cathepsin G

Cy3	Cyanine 3
Cy5	Cyanine 5
CXCL	Chemokine (C-X-C motif) ligand
CX3CL1	Chemokine (C-X3-C motif) ligand 1
CXCR5	Chemokine (C-X-C motif) receptor 5
CYP1A1	Cytochrome P450, Family 1, Subfamily A, Member 1
CYP1B1	Cytochrome P450, Family 1, Subfamily B, Member 1
DAVID	Database for Annotation, Visualization and Integrated Discovery
DEFA3	Defensin Alpha 3
EBM-2	Endothelial Cell Basal Media-2
EC	Endothelial Cells
ECL	Enhanced Chemiluminescence
EDTA	Ethylenediaminetetraacetic acid
EGM-2	Endothelial Cell Growth Media-2
FITC	Fluorescein Isothiocyanate
FMLP	Formyl-Methionyl-Leucyl-Phenylalanine
GAS2	Growth Arrest Specific 2
GCSF	Granulocyte Colony-Stimulating Factor
GEO	Gene Expression Omnibus
GO	Gene Ontology
GM-CSF	Granulocyte-Macrophage Colony-Stimulating Factor
HBB	Hemoglobin Beta
HSA	Human Serum Albumin

HSS	High Steady Shear Stress
HUVEC	Human Umbilical Vein Endothelial Cells
Hz	Hertz
ICAM1	Inter-Cellular Adhesion Molecule 1
IgG	Immunoglobulin G
IL1	Interleukin 1
IL1RN	Interleukin Receptor Antagonist
IL6	Interleukin 6
IL8	Interleukin 8
IL10	Interleukin 10
IL17	Interleukin 17
IL19	Interleukin 19
IL1β	Interleukin 1 beta
JAK-STAT	Janus Kinase - Signal Transducers and Activators of Transcription
kDa	Kilodalton
KEGG	Kyoto Encyclopedia of Genes and Genomes
KLF2	Kruppel-like Factor 2
LFA1	Lymphocyte Function Associated Antigen 1
LDL	Low-density Lipoprotein
LSS	Low Steady Shear Stress
LTF	Lactoferrin
M-CSF	Macrophage Colony Stimulating Factor
MEF2A	Mads Box Transcription Enhancer Factor 2, Polypeptide A

MEM	Minimal Essential Media
MMP	Matrix Metalloproteinase
mRNA	Message RNA
MT1F	Metallothionein 1F
NAIP	NLR Family Apoptosis Inhibitory Protein
NCBI	National Center for Biotechnology Information
NF-κB	Nuclear Factor Kappa-Light-Chain-Enhancer of Activated B cells
NPR1	Natriuretic Peptide Receptor A
p	P-value
p38 MAPK	Mitogen-activated protein kinase p38
PBEF	Pre-B-Cell Colony Enhancing Factor 1
PBMC	Peripheral Blood Mononuclear Cells
PBS	Phosphate Buffered Solution
PDGF	Platelet-Derived Growth Factor
PECAM1	Platelet/Endothelial Cell Adhesion Molecule 1
PET	Poly(Ethylene Terephthalate)
PLA2G3	Phospholipase A2, Group III
PLA2G4A	Phospholipase A2, Group IVA
PRIM2A	Primase Polypeptide 2A
PTHLH	Parathyroid Hormone-like Hormone
PVDF	Polyvinylidene Fluoride
qRT-PCR	Quantitative Real Time Polymerase Chain Reaction
Rac	Ras-related C3 botulinum toxin substrate, subfamily of Rho GTPases

RBC	Red Blood Cell
RF	Reversing Flow
RNA	Ribonucleic Acid
R-PE	R-phycoerythrin
RT-PCR	Real Time Polymerase Chain Reaction
SDS-PAGE	Sodium Dodecyl Sulfate Polyacrylamide Gel Electrophoresis
SEM	Standard Error of the Mean
siRNA	Small Interfering Ribonucleic Acid
SOCS3	Suppressor of Cytokine Signaling 3
STAT	Static
TEER	Transendothelial Electrical Resistance
TGFβ	Transforming Growth Factor Beta
THP-1	Human Acute Monocytic Leukemia Cell Line
TLR4	Toll Like Receptor 4
TM	Transmigrated Monocytes
TNFα	Tumor Necrosis Factor α
TRAF1	TNF Receptor Associated Factor 1
VCAM1	Vascular Cell Adhesion Molecule 1
UMA	Unmigrated Monocytes Above stimulated ECs
UMB	Unmigrated Monocytes Below stimulated ECs
UNT	Untreated Monocytes
VEGF	Vascular Endothelial Growth Factor

SUMMARY

Leukocyte transmigration is a critical step of the inflammatory process. In this project I have examined leukocyte responses to transmigration and endothelial responses to both chemical and mechanical stimuli which are known to be involved in leukocyte transmigration. My work has identified ~2500 differentially expressed genes following endothelial exposure to interleukin-1 beta (IL1β). Interestingly, IL1β induces up-regulation of claudin-1 and pre-b-cell colony enhancing factor and down-regulation of claudin-5 and occludin, which are all involved in maintaining endothelial cell-cell junctions. Analysis of endothelial cell (EC) transcriptional changes following neutrophil transmigration found few differentially expressed genes in comparison to IL1β treated ECs; indicating that the effects of transmigration on ECs are minimal in comparison to the global transcriptional changes induced by IL1β.

Atherosclerosis, characterized by monocyte accumulation within the vessel lumen, is found in regions of flow reversal and low time averaged oscillatory shear stress. I have examined the effects of this type of shear stress on endothelial cell gene expression. My data indicates that most genes differentially expressed under these conditions are controlled by low average shear stress rather than flow reversal. These differentially expressed genes are involved in regulating the cell cycle and the immune response. My work shows that cell proliferation is increased following exposure to low steady shear stress or exposure to reversing oscillatory flow in comparison to high steady shear

stress. Additionally monocyte adhesion is increased following exposure of ECs to reversing oscillatory flow.

My work has also examined the impact of transmigration on monocyte gene expression. I have identified genes which are differentially expressed in monocytes by exposure to EC secretions, monocyte/EC contact, and diapedesis. I have also shown that freshly isolated human monocytes have reduced apoptosis following transmigration. Surprisingly, I also found that monocytes had reduced expression of anti-microbial peptides following transmigration.

Overall my work identifies important endothelial and leukocyte transcriptional responses to the process of transmigration which extends from cytokine stimulation through diapedesis.

CHAPTER 1: THESIS RATIONALE

The immune system maintains a variety of innate and adaptive mechanisms in order to protect the body from infection as well as to maintain cellular health by removing apoptotic and diseased host cells. One of the first events in the immune response is the recruitment of leukocytes to sites of infection or inflammation. In order for leukocytes to migrate out of the vasculature and into surrounding tissues, endothelial cells (ECs) lining the vessel lumen must first be stimulated to up-regulate adhesion molecules on the endothelial cell surface. EC stimulation occurs through mechanical and chemical mechanisms, often involving cytokine exposure through autocrine, paracrine, and endocrine signaling events.

Numerous cytokines function in EC activation, many of which have redundant function. Some of the most commonly studied cytokines involved in EC activation include IL1β, TNFα, and lipopolysaccharide. Cytokines interact with ECs by binding to specific cell surface receptors, causing intracellular signaling events which can induce transcriptional changes, post-translational protein modifications, as well as protein translocation. Upon cytokine stimulation, leukocytes begin to roll along adhesion molecules up-regulated to the surface of ECs. Leukocyte rolling leads to firm adhesion followed by transmigration across the endothelium. This process of EC stimulation and leukocyte transmigration elicits intracellular signaling events in both ECs and leukocytes ([1,2]).

I have undertaken the following aims in order to better understand the response of ECs and leukocytes to chemical and mechanical stimulation involved in the immune response.

Aim 1: Analyze Endothelial Cell Responses to IL1β Stimulation and Neutrophil Transmigration

Transcriptional Effects of IL1β Stimulation of Endothelial Cells

Interleukin-1 is a cytokine whose inflammatory function has been studied since the early 1980's. Many studies over the last thirty years have examined the effects of IL1 on endothelial cells. These studies have primarily examined functional changes in ECs as well as changes in RNA and protein levels of individual genes, which could be hypothesized based on observed functional differences. More recently researchers have been able to examine the effects of IL1 on a more global scale, using microarrays to test for transcriptional changes induced by the cytokine.

Three research groups have published microarray data in which EC were treated with IL1β [3-5]. These studies have a number of limitations. For example, these three studies have used microarray platforms which contain probes for 4000 [3], 7050 [5], and ~18,000 [4] human genes, only representing a fraction of the whole human genome. Bandman et al. and Zhao et al. examined differential gene expression in response to both IL1β and TNFα and have reported them in a single list, making analysis of individual effects of IL1β difficult. In addition, all three of these groups used very stringent statistical analysis techniques such that all together these three groups reported only 377 genes which were differentially expressed by IL1β stimulation of HUVEC. In my work, I have used a

whole human genome microarray to analyze expression of ~40,000 RNA sequences in combination with less stringent statistical techniques. This allowed me to identify over 2500 differentially expressed genes following IL1β treatment of HUVEC. In my work I have used qRT-PCR and western blotting to further verify differential expression of specific genes relevant to leukocyte transmigration.

Impact of Neutrophils on Endothelial Cells

Neutrophil transmigration occurs in a series of stages in which neutrophils first begin to roll along stimulated endothelium. They then firmly adhere and finally begin to transmigrate across the endothelium. Direct cell-cell contact between ECs and neutrophils as well as cytokine release from the neutrophils may cause changes in EC function.

A number of groups have examined the impact of leukocyte firm adhesion on endothelial cell function (Reviewed by Van Buul et al. [6]). Neutrophil firm adhesion is mediated primarily by integrin binding of ICAM1 and VCAM1 on the endothelial surface. In early work, Etienne et al. examined the impact of ICAM1 cross-linking on EC tight junction molecules [7]. This group showed that three proteins which localize at focal adhesions (focal adhesion kinase, paxillin, and p130CAS) exhibited increased tyrosine phosphorylation after ICAM1 cross-linking. van Wetering et al. performed similar experiments to examine the impact of VCAM1 cross-linking. VCAM1 cross-linking was shown to induce intercellular gaps as well as stress fiber formation. VCAM1 cross-linking activates cell-signaling molecules as evidenced by Rac activation and increased

phosphorylation of p38 MAPK. Inhibition of Rac was also shown to cause a decrease in transmigration of a monocytic cell line across IL1β treated HUVEC in response to the chemokine C5a.

Other studies have more directly investigated the impact of neutrophils on EC function. Huang et al. showed that transmigration of neutrophils in response to the cytokine FMLP caused a 5 to 8 fold increase in cytosolic Ca levels of HUVEC [8]. These high ratios of neutrophil transmigration ensured that almost every EC had been involved in at least one neutrophil transmigration event. Increased cytosolic Ca levels were not seen in the presence of neutrophils without the addition of FMLP or in the presence of FMLP alone. This indicates that the transmigration process itself or possibly the induction of cytokine release from neutrophils as stimulated by FMLP causes an increase in EC cytosolic Ca levels. Changes in cytosolic Ca have been linked to a number of cell signaling events which can cause eventual changes in transcription as well as protein expression [9].

Marcus et al. examined the impact of neutrophil contact versus neutrophil cytokine release on the transendothelial electrical resistance (TEER) of an endothelial cell layer [10]. This group showed that direct contact of ECs with neutrophils caused a drop in the TEER. However, the incubation of neutrophils with ECs without allowing neutrophils to actually contact the ECs did not elicit the same response. This study indicates that cell-cell contact between ECs and neutrophils can elicit changes within the EC. This EC response to neutrophil contact may allow for increased neutrophil transmigration by reducing EC cell-cell adhesion and thus allowing increased diapedesis to occur.

A more recent study by Cepinskas et al. examined the effect of neutrophil transmigration on nuclear NFκb levels within ECs [11]. Neutrophil transmigration resulted in a dose dependent reduction of nuclear NFκb levels. When neutrophil adhesion and transmigration were blocked via CD18 blocking antibodies, this reduction in nuclear NFκb levels was not seen. Nuclear localization of NFκb has been closely tied to IL1β stimulation in HUVEC [12]. Nuclear localization of NFκb has been shown to cause up-regulation of a number of adhesion molecules as well as stimulation of cytokine production and transcriptional changes [13]. Thus, Cepinskas et al. have provided evidence that neutrophil transmigration may act as negative feedback in order to reduce neutrophil transmigration once it has already occurred.

Previous studies provide substantial evidence that neutrophil transmigration does indeed affect EC function. To date none of these studies have shown a direct impact on EC transcription. My work examines how neutrophil transmigration specifically affects EC gene expression. My data indicate that the transcriptional effects of neutrophil transmigration are far overshadowed by the EC transcriptional response to IL1β.

Aim 2: Analysis of Monocyte Responses to Transmigration across Stimulated HUVEC

Atherosclerosis is an extremely common disease characterized by plaque formation within the arteries. Rupture of an atherosclerotic plaque can cause myocardial infarctions, strokes, aneurysms, as well as many other serious conditions. Atherosclerotic plaque

formation begins with up-regulation of adhesion molecule expression on the vascular endothelium [14]. The stimulus which causes this up-regulation is currently under a great deal of debate. Many researchers have hypothesized that the accumulation of lipids within the intima may lead to lipid oxidation which then leads to EC stimulation. Interestingly, this increased adhesion molecule expression associated with the initial stages of atherosclerosis is primarily located at branching points within the arteries which experience disturbed blood flow patterns [15]. Thus it is also suggested that mechanical stimulation of ECs may lead to increased or decreased atheroprotective mechanisms as well as altered adhesion molecule expression.

Upon exposure to EC adhesion molecules, leukocytes become adherent and begin to penetrate into the intima. As monocytes enter the atherosclerotic plaque, these cells begin to differentiate into macrophages. Macrophages express scavenger receptors for lipoproteins, thus allowing them to ingest lipids and become foam cells [16]. Macrophages also express increased levels of toll-like receptors which have been linked to down stream secretion of pro-inflammatory cytokines and matrix metalloproteinases (MMPs) [17]. MMPs are of particular importance because these proteolytic enzymes may play a role in degradation of the fibrous cap which protects the plaque from rupture [18]. Since many of the most life-threatening clinical events are related to plaque rupture, plaque stabilization is especially important for developing clinically relevant therapies.

Monocytes play an extremely important role in atherosclerotic plaque formation and rupture. Thus, it is important to understand the changes which occur within monocytes

during this process. In 1999, Hashimoto et al. used serial analysis of gene expression to investigate transcriptional differences between monocytes and monocyte derived macrophages [19]. In this study, monocyte derived macrophages were obtained by incubating fresh monocytes with either granulocyte-macrophage colony-stimulating factor (GM-CSF) or macrophage colony-stimulating factor (M-CSF) for seven days. Over 300 differentially expressed genes were identified following GM-CSF or M-CSF treatment. A number of the up-regulated genes, such as apolipoproteinE, osteopontin, CD9, and lysosomal acid lipase, were associated with proteins involved in lipid metabolism. This suggests that development of the lipid metabolism system may be important for macrophage differentiation and thus links macrophages even more closely with atherosclerosis.

Li et al. used cDNA microarrays to examine differences between monocytes, monocyte-derived macrophages via M-CSF, and primary human alveolar macrophages [20]. Some of the most highly down-regulated genes in this study are involved in important intracellular signaling pathways. Similar to previously described data from Hashimoto et al. [19], some of the most highly up-regulated genes in macrophages were associated with lipid metabolism, e.g. fatty acid binding protein 4, fatty acid binding protein 5, and lipoprotein lipase. This group also found a number of differences in gene expression levels between macrophages derived *in vitro* via M-CSF and human alveolar macrophages. These differences indicate that *in vivo* macrophages could be very heterogeneous, depending upon individual activation methods for each cell population.

These studies have examined gene expression levels in mature macrophages obtained from alveoli or from in vitro cultivation methods. Comparison to freshly isolated monocytes is important for discovering modes of differentiation and functional capabilities of macrophages compared to monocytes. However, none of these studies have examined monocytes at very early stages of macrophage differentiation. Monocytes may begin the process of differentiation during the initial stages of cytokine stimulation and interaction with the endothelium. In particular, the process of monocyte transmigration may greatly impact monocyte gene expression.

My work examines differential gene expression in monocytes which have transmigrated across the endothelium as compared to freshly isolated monocytes. Use of careful controls has allowed for determination of specific transcriptional effects induced by monocyte exposure to secretions from stimulated ECs, monocyte/endothelial cell contact, and monocyte diapedesis.

Aim 3: Impacts of Reversing Flow Patterns on HUVEC Inflammation and Monocyte Transmigration

Atherosclerosis primarily occurs within the large and medium sized arteries and develops at specific regions of the vasculature which are characterized by low shear stress, oscillatory flow, or turbulent flow patterns [21]. These disturbed blood flow patterns occur most often at branching points and the inner wall of vessel curvatures [22]. Endothelial cells act as one of the primary cell types to sense mechanical forces within the

vasculature. Thus, a number of researchers have examined transcriptional changes in ECs in response to various types of hemodynamic forces [23-27].

My work examines differential gene expression in ECs following exposure to reversing oscillatory shear stress modeled after the wall shear stress found at the carotid sinus. Use of a low shear stress control has allowed for identification of genes regulated by low time average shear stress and genes regulated by flow reversal. I have also examined monocyte adhesion following EC exposure to reversing flow.

CHAPTER 2: GENE EXPRESSION OF ENDOTHELIAL CELLS DUE TO INTERLEUKIN-1 BETA STIMULATION AND NEUTROPHIL TRANSMIGRATION

N.B. This chapter is published (Marcie R. Williams, Noriyuki Kataoka, Yumiko Sakurai, Christina M. Powers, Suzanne G. Eskin, and Larry V. McIntire. Endothelium. 2008;15:73-165.).

To reach a site of infection, neutrophils must move out of the blood vessels and into the surrounding tissue. The initial event in this inflammation cascade is the activation of ECs. Cytokines, such as interleukin-1 beta (IL1β) and tumor necrosis factor α (TNFα), are key mediators in stimulating ECs at sites of inflammation. EC activation by cytokines is characterized by release of chemokines [28], expression of adhesion molecules on the endothelial cell surface [29], alteration of endothelial cell shape [30] and alteration of cytoskeletal distribution [31]. These responses to cytokine stimulation facilitate neutrophil adhesion to ECs and transendothelial migration.

Leukocyte emigration is classified into three steps, i.e. rolling, firm adhesion and migration [32]. These steps involve a number of different types of molecules and signaling events within the ECs [8,33-37]. Despite the fact that many adhesion molecules have been studied, new adhesion molecules implicated in leukocyte migration are still being identified [38-40]. Moreover, new steps other than rolling, firm adhesion and migration, have also been proposed [41]. To understand the process of inflammation, we need to elucidate cellular responses, i.e., gene and protein expression in both ECs and neutrophils,

signal transduction within and between ECs and neutrophils, adhesion molecule expression, and cellular behavior. Changes in gene expression occur during the initial phase of the cellular response, thus making gene expression analysis relevant for understanding this process. However, currently there is little known about changes in EC gene expression due to neutrophil transmigration.

DNA microarrays are a powerful screening tool for identifying genes which are differentially expressed following cellular exposure to various stimuli. Our own lab has used this technique to analyze the gene expression of ECs in response to mechanical forces [23,26,42]. Several DNA microarray studies have also examined the effect of inflammatory stimuli on EC transcription [3-5]. These studies identified approximately 350 genes which are differentially regulated by IL1β, or IL1β and TNFα. We hypothesized that transmigration of neutrophils through an activated EC monolayer would stimulate further transcriptional changes in the ECs. To elucidate the role of neutrophil transmigration we compared gene expression in IL1β stimulated ECs to gene expression in IL1β stimulated ECs following neutrophil transmigration.

Materials and Methods

Cell culture and materials

Pooled human umbilical vein endothelial cells (HUVEC) were purchased from Lonza. EGM-2 media was made from EBM-2 media (Lonza) with the addition of an EGM-2 bullet kit (Lonza) containing 2% fetal bovine serum, gentamicin sulfate, amphotericin, vascular endothelial growth factor, recombinant human fibroblast growth

factor basic, ascorbic acid, R^3 insulin-like growth factor 1, hydrocortisone, heparin, and recombinant human epidermal growth factor. For microarray experiments, passage 3-4 HUVEC were seeded at 50,000 cells/cm^2 onto fibronectin coated (2.5μg/cm^2) six well polyethylene terephthalate (PET) membrane cell culture inserts (diameter = 23mm) containing 3 μm pores (BD Falcon) and cultured in EGM-2 until confluent at 37 ^oC in the presence of humidified 5% CO_2. HUVEC used in time course experiments were cultured in supplemented M199 (Mediatech) containing 20% fetal bovine serum (Hyclone), 50 U/mL penicillin (Gibco), 50 μg/ml streptomycin (Gibco), 2mM L-glutamine (Mediatech), 2.5 U/ml heparin (American Pharmaceutical Partners), and 50 μg/ml endothelial mitogen (Biomedical Technologies).

Isolation of neutrophils

Human neutrophils were isolated from whole blood obtained from healthy adult donors after obtaining informed consent [43]. Briefly, whole blood was drawn into citrate buffer anticoagulant and red blood cells were allowed to settle out in a 6% Dextran 70 solution (B. Braun). Red blood cells remaining in the supernatant were lysed with a 0.2% NaCl solution for 20 seconds. Cells were centrifuged over a layer of lymphocyte separation media (1.078 g/mL, Cellgro) and pellets were resuspended in MEM with 0.5% human serum albumin (National Hospital Specialties). Isolated neutrophils were maintained in MEM with 0.5% human serum albumin at 37 ^oC until application to HUVECs and used within four hours after isolation.

Microarray experimental protocol

HUVEC treatment was begun approximately 24 hours after the cells reached confluence, at which time the media was replaced with EGM-2 media containing 100 pg/ml IL1β. Four hours later, the media was replaced with MEM containing 0.5% human serum albumin (HSA) and 100 pg/mL IL1β. In some conditions, 1 million freshly isolated neutrophils were applied. Neutrophil treatment and further IL1β stimulation was performed for 1 hours or 3 hours, as shown in Figure 1. Control and control + MACS samples were treated for 6 hours with fresh EGM-2 media without IL1β.

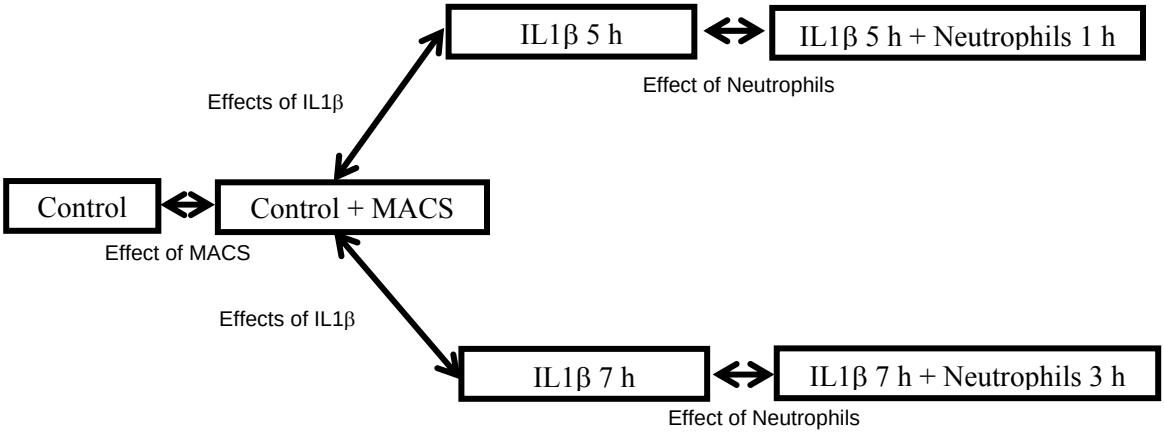

Figure 1: Experimental Conditions.
"Control" samples were cultured on cell culture inserts in EGM-2, trypsinized, pelleted, and lysed for RNA isolation. "Control + MACS" samples were treated similarly with an additional step of anti-CD45 MACS purification. "IL1β 5 h" samples were treated with 100 pg/mL IL1β in EGM-2 for 4 h, then with 100 pg/mL IL1β in MEM + 0.5% HSA for 1 h, and followed up with anti-CD45 MACS purification. "IL1β 7 h" samples were treated similarly except that the final IL1β treatment in MEM + 0.5% HSA was performed for 3 h. Comparison of "IL1β 5 h" and "IL1β 7 h" to "Control + MACS" allows determination of the effects of IL1β. "IL1β 5 h + Neutrophils 1 h" samples were treated with 100 pg/mL IL1β in EGM-2 for 4 h followed by the addition of 1 million neutrophils in MEM + 0.5% HSA containing 100 pg/mL IL1β for 1 h. Anti-CD45 MACS purification was used to remove contaminating neutrophils from the HUVEC samples prior to cell lysis for RNA isolation. "IL1β+Neutrophils 3 h" samples were treated similarly except that neutrophils were applied for 3 h.

Transmigrated neutrophils were collected from beneath cell culture inserts and counted with a Beckman Coulter Z2 Particle Count and Size Analyzer to determine percent transmigration. To obtain RNA from HUVEC after neutrophil transmigration, it was first necessary to magnetically remove neutrophils which remained adherent to the HUVEC. Cells were tryspinized off the cell culture inserts, and were incubated with CD45 Microbeads (Miltenyi) for 15 minutes at 4 ^{o}C. Neutrophils were removed from HUVEC by passing the cell mixture over a MS column placed in a miniMACS Magnetic Separator (Miltenyi). HUVEC were collected in the flow-through from the magnetic column. This step, in which CD45 antibodies were used to remove neutrophils, was applied to all conditions except the control in order to account for any differential gene expression which might be induced by magnetic cell sorting. RNA was isolated for each of 6 conditions a total of three times from three different blood donors.

In some studies performed subsequent to microarray analysis anti-glycophorin A magnetic beads were used to remove contaminating red blood cells (RBCs) and reticulocytes prior to RNA isolation. These beads were used to purify neutrophils prior to addition to ECs or to purify trypsinized ECs just prior to RNA isolation.

Time course experimental protocol

HUVEC were cultured on 75 mm tissue culture inserts in supplemented M199 media until confluent. Approximately 24 hours after the cells reached confluence, the media was replaced with supplemented M199 containing 100 pg/ml IL1β for either 0, 5, 7, 12, or 24 hours. HUVEC were trypsinized off the cell culture inserts and lysed with either

M-PER (Pierce) or Buffer RLT (Agilent) for the collection of either protein or RNA, respectively. This experimental protocol was repeated 7 times with separate HUVEC lots.

RNA isolation

RNA was isolated from purified HUVEC with an RNEasy Micro Kit (Qiagen), according to the manufacturer's instructions. RNA quantity and quality were assessed by loading 1 µl of sample RNA onto a RNA 6000 Nano chip (Agilent) and analyzing with an Agilent 2100 Bioanalyzer to determine the amount and integrity of RNA recovered (Table 1). RNA Integrity Scores can range from 0 to 10 with 10 indicating the highest quality of RNA.

Table 1: Average RNA amounts and RNA Integrity Numbers.

Treatment	**RNA Amount (µg)***	**RNA Integrity Number***
Control	7.4 +/- 2.4	9.9 +/- 0.03
Control + MACS	6.8 +/- 0.6	9.4 +/- 0.4
IL1β 5 h	8.1 +/- 2.0	9.9 +/- 0.1
IL1β 5 h + Neutrophils 1 h	8.1 +/- 2.4	9.9 +/- 0.05
IL1β 7 h	7.9 +/- 2.3	9.9 +/- 0.05
IL1β 7 h + Neutrophils 3 h	5.7 +/- 1.2	9.9 +/- 0.03

*****mean +/- SEM, n=3 for each treatment

Microarrays

Microarray hybridization and imaging were performed at the Morehouse School of Medicine Functional Genomics Core Facility. Briefly, RNA and Universal Human Reference RNA (Stratagene) were linearly amplified to cRNA using a Low RNA Input Fluorescent Linear Amplification Kit (Agilent) according to the manufacturer's instructions. Cy5-labeled cRNA for each sample was competitively hybridized with

Cy3-labeled reference cRNA to a 44k Whole Human Genome Microarray (Agilent) according to the manufacturer's instructions. Slides were dried under nitrogen and scanned on an Agilent DNA Microarray Scanner. Microarray images were analyzed with Agilent Feature Extraction Software according to the manufacturer's instructions. GeneSpring software was used to further analyze the microarray data. One way ANOVA assuming equal variances was applied using Benjamini and Hochberg multiple testing correction at a false discovery rate of 5%. Differentially expressed genes were identified as those genes which had fold changes of at least 1.5 fold and adjusted p-values of less than 0.05.

A list of differentially expressed genes was uploaded to the Database for Annotation, Visualization and Integrated Discovery (DAVID) and subjected to Functional Annotation Clustering at Medium Class Stringency in order to identify enriched biological themes [44]. Gene Ontology (GO) Biological Process annotations were used to perform this functional clustering. Clusters which had an enrichment score greater than 1.5 and specific gene functions were identified. Lists of up-regulated and down-regulated genes were uploaded separately to DAVID in order to identify enriched KEGG Pathways and map differentially expressed genes to these pathways.

Quantitative Real Time PCR

1 μg of total RNA from each sample was reverse transcribed into cDNA using SuperScript II (Invitrogen). cDNA was purified with Micro Bio-Spin P-30 Chromatography Columns (BioRad), and diluted in RT-PCR Grade Water (Ambion) 1:80.

Pre-designed PCR primers and Quantitect SYBR Green PCR Master Mix were purchased from Qiagen. Primers were added to the master mix at a ratio of 1:5. Each reaction was performed with 4 μl of diluted cDNA and 6 μl of primers in the master mix. The qRT-PCR reactions were performed on a LightCycler 2.0 (Roche Applied Science) with a 15 minute activation step at 95 ^{o}C; 50 cycles at 94 ^{o}C for 15 seconds, 55 ^{o}C for 20 seconds, 72 ^{o}C for 20 seconds; and a ramped melting cycle. Fold changes were determined using the ΔΔCt method. Statistical differences between ΔCts were assessed using a paired Student's t-test. qRT-PCR was used to verify gene expression from RNA isolated from three microarray experiments. RNA from seven time course experiments was used to examine the temporal effects of IL1β.

Western blots

Protein (65 μg) was resolved by SDS-PAGE in 10% Tris-HCL precast polyacrylamide gels (Bio-Rad) with Laemmli sample buffer and electro-transferred onto PVDF membranes (Hybond-P, GE Bioscience). After blocking with 5% nonfat dry milk, membranes were probed with rabbit polyclonal claudin-1 antibodies (Zymed), mouse monoclonal claudin-5 antibodies (Zymed), goat polyclonal PBEF antibodies (Santa Cruz), and mouse monoclonal β-actin antibodies (Sigma). Bound primary antibodies were labeled with horseradish peroxidase conjugated secondary antibodies and detected with enhanced chemiluminescence (ECL Plus, Amersham Biosciences). Band densities were quantified by densitometry with the Kodak EDAS 1D Imaging System (Kodak). Western blots were performed using protein isolated from 6 separate time course experiments and statistical significance was assessed using a paired Student's t-test.

Results

Neutrophil transmigration

The percentage of neutrophils which transmigrated was quantified after 1 and 3 hours of neutrophil application by counting the number of neutrophils collected from beneath the cell culture inserts (Figure 2). After one hour, 8 +/- 4 %, and after three hours, 35 +/- 3%, of the applied neutrophils had transmigrated (n=3).

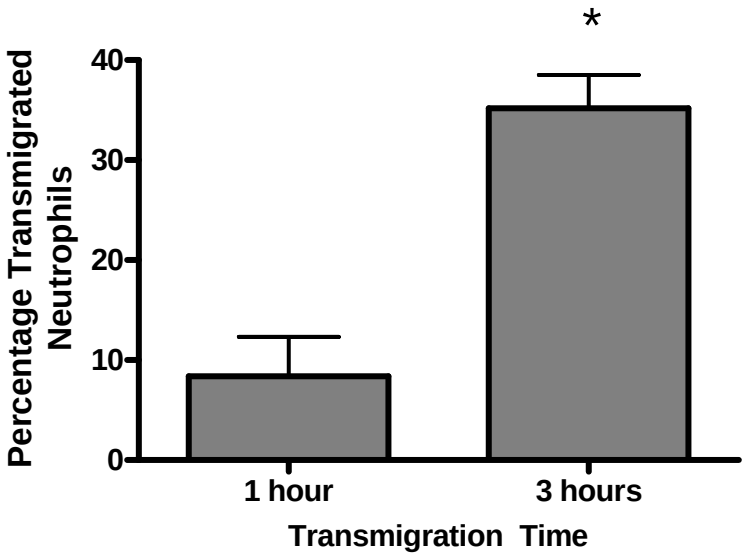

Figure 2: Neutrophil percent transmigration.
1 million neutrophils in MEM + 0.5% HSA were applied to IL1β stimulated HUVEC grown on a cell culture insert. Neutrophils were allowed to transmigrate across the activated HUVEC for either 1 hour or 3 hours. Transmigrated neutrophils were collected from the cell culture dish beneath the HUVEC and counted. The percentage of transmigrated neutrophils was calculated as the number of neutrophils collected below the HUVEC divided by the number of neutrophils applied to the HUVEC. *$P<0.05$ versus 1 hour transmigration. n = 3

Following neutrophil transmigration, unmigrated neutrophils were rinsed off the HUVEC layer; however, some of the applied neutrophils remained adherent to the HUVEC. The

HUVEC were trypsinized and contaminating neutrophils removed using CD45 Microbeads prior to isolating HUVEC RNA. RNA was collected from HUVEC under six different treatment conditions. Table 1 (page 15) shows the quantity and quality of RNA collected from all conditions, with high average RNA integrity scores as assessed by the Agilent Bioanalyzer.

Microarray condition tree

Microarray data were analyzed using a Pearson Correlation to generate a condition tree, which indicates that gene expression in HUVEC treated with IL1β alone (Figure 3, columns 3 & 5) is very similar to gene expression in HUVEC exposed to neutrophil transmigration and treated with IL1β for the same total time (Figure 3, columns 4 & 6). HUVEC treated with the MACS system without IL1β clustered with untreated HUVEC, indicating that the MACS system had negligible impact on gene expression (Figure 3, columns 1-2). All samples treated with IL1β clustered on a separate branch from cells not treated with IL1β. A comparison of the 5 hour IL1β treatment (Figure 3, columns 3-4) to the 7 hour IL1β treatment (Figure 3, columns 5-6) reveals the transient nature of IL1β stimulation, as there are several groups of genes which are differentially expressed after 5 hours of IL1β treatment compared to 7 hours of IL1β treatment.

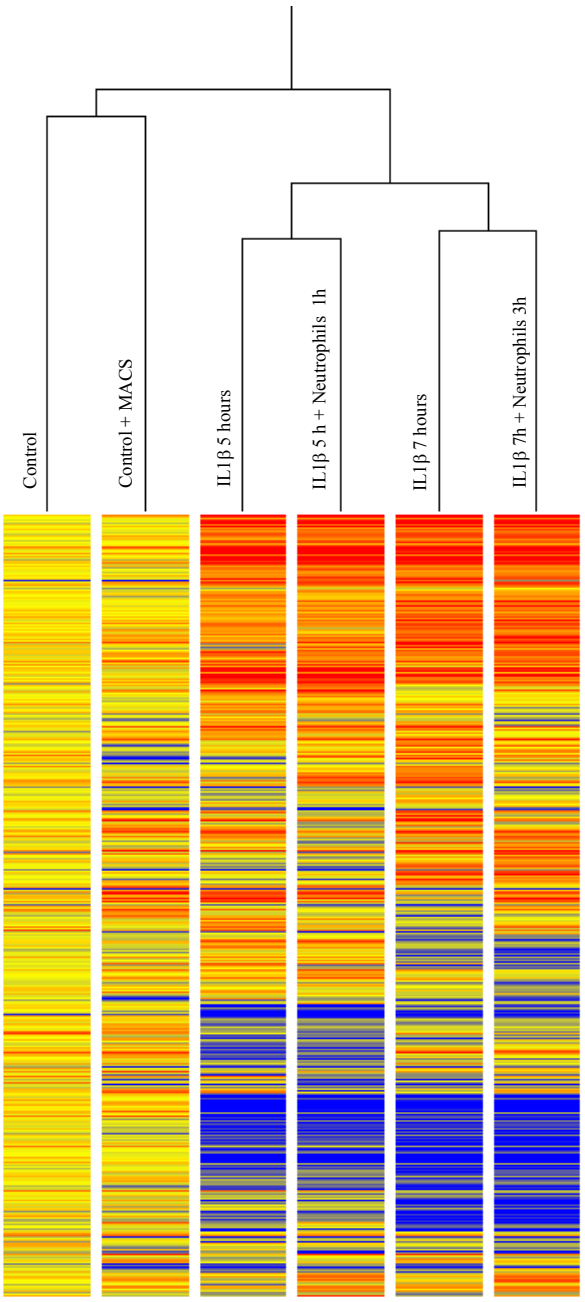

Figure 3: Condition tree.
A condition tree was generated using Genespring GX 7.3.1 to cluster microarray data based on Pearson's correlation. Red indicates 1.5 fold or greater up-regulation in comparison to the median expression level for each gene in the control samples, blue indicates 1.5 fold or greater down-regulation, and yellow represents genes which did not change expression level. This condition tree separates the 6 conditions of this experiment into two branches. The branch on the left contains the conditions which were not treated with IL1β. The branch on the right contains conditions which were treated with IL1β. IL1β treated samples also branched according to the length of time the HUVEC were treated with IL1β. This condition tree indicates that the primary effector of differential gene expression in this experiment is IL1β with neutrophil transmigration being relatively minor.

IL1β treatment effects

Analysis of microarray data identified 2716 genes and 2972 genes as being differentially expressed following 5 or 7 hours of IL1β stimulation, respectively relative to control + MACS (Supplemental Table 1). DAVID was used to functionally group these differentially expressed genes according to Gene Ontology: Biological Processes. This analysis revealed functional groups of genes associated with apoptosis, cell cycle, NF-κB cascade, chemotaxis, immune response, proteoglycan metabolism, chromosome organization and biogenesis, angiogenesis, and hemopoiesis. Table 2 lists these functional groups along with their annotation cluster enrichment score which is used to rank these functional groups according to biological significance.

Table 2: Functional Clustering.

Functional Annotation Cluster	**Enrichment Score**
Apoptosis	6.36
Cell Cycle	4.59
NF-κB Cascade	4.47
Chemotaxis	3.75
Immune Response	3.64
Proteoglycan Metabolism	1.98
Chromosome Organization and Biogenesis	1.96
Angiogenesis	1.86
Hemopoiesis	1.66

Using DAVID we also identified KEGG pathways containing a significant number of genes which are differentially expressed by IL1β. Pathways enriched with up-regulated genes include Cytokine-Cytokine Receptor Interaction, MAPK Signaling, Cell Adhesion Molecules, JAK-STAT Signaling, Toll-Like Receptor Signaling, Apoptosis, Epithelial Cell Signaling in Helicobacter Pylori Infection, Antigen Processing and Presentation,

Adipocytokine Signaling, TGF-Beta Signaling, T Cell Receptor Signaling, and Type I Diabetes Mellitus. Pathways enriched with down-regulated genes include WNT Signaling, Purine Metabolism, and Tight Junctions. Up and down-regulated genes are overlayed on the Cytokine-Cytokine Receptor Interaction pathway in Figure 4. Genes within this pathway are divided into chemokines, hematopoetins, PDGF family, interferon family, IL10 family, TNF family, TGFβ family, IL17 family, and IL1 family. Thirteen chemokine ligands were up-regulated by IL1β while one chemokine ligand and one chemokine receptor were down-regulated by IL1β. Chemokine ligands attract leukocytes to sites of infection through interaction with chemokine receptors and establishment of a chemokine gradient. Overall, thirty cytokine ligands were up-regulated by IL1β and 5 ligands were down-regulated. In addition, fourteen cytokine receptors were up-regulated by IL1β and 6 receptors were down-regulated. Mapping differentially expressed genes to the cytokine-cytokine receptor pathway offers a visual image of the important role IL1β plays in leukocyte recruitment, hematopoiesis, and other inflammatory processes. Overlays of differentially expressed genes within the Apoptosis and MAPK signaling pathways are shown in Supplemental Figures 1 and 2 respectively. (All supplemental figures and tables are located on included CD.)

Comparison of our data with other microarray studies on IL1β stimulated HUVEC revealed similar patterns of expression. There were 6 genes which were shown to be differentially expressed by three previous microarray studies. Our microarray data confirmed 100% of these genes, as shown in Table 3, in which fold changes are calculated for each condition versus control + MACS. An additional 47 genes were

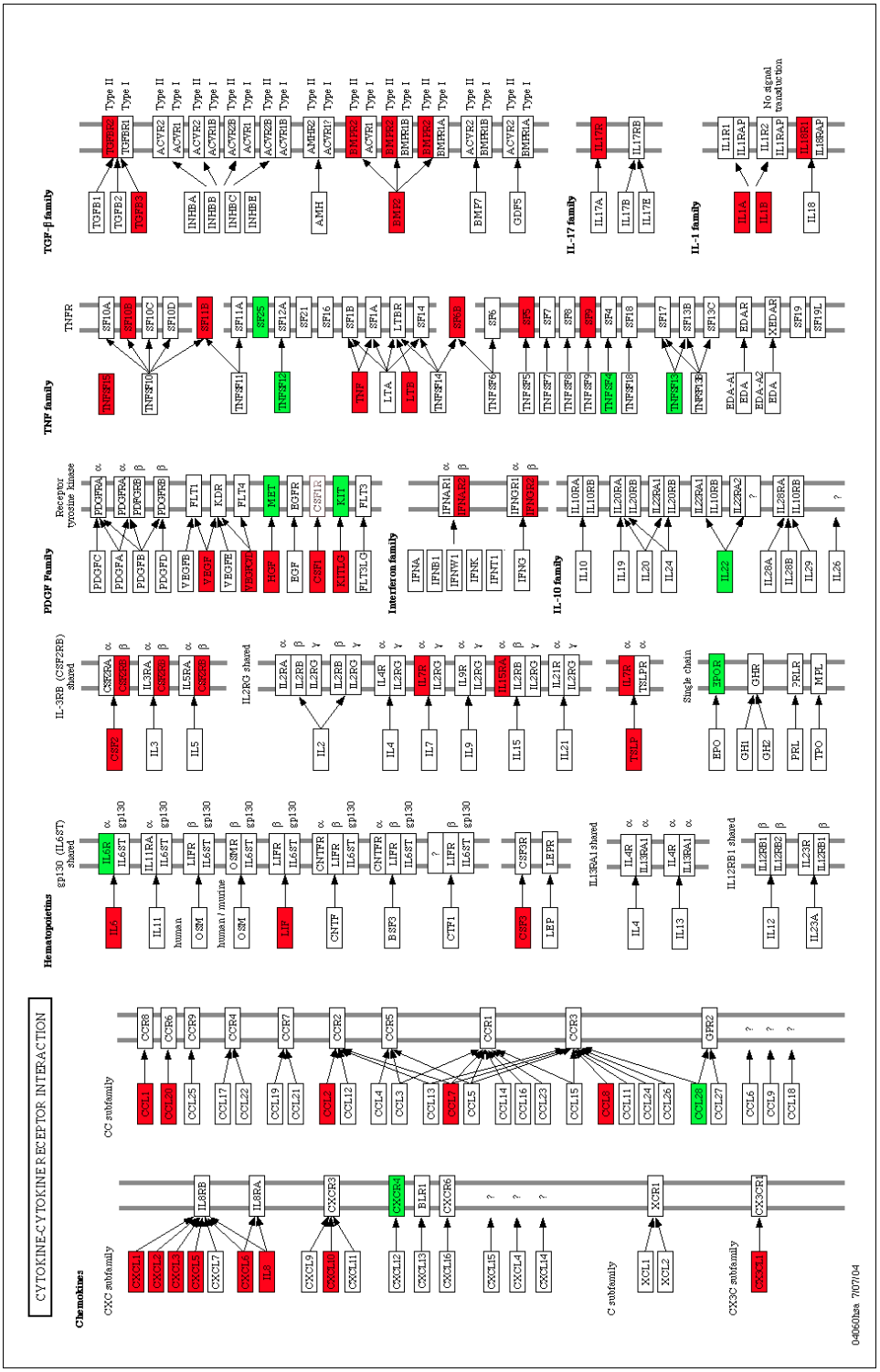

Figure 4: Cytokine-Cytokine Receptor Interaction KEGG pathway.
A number of genes which were differentially expressed following IL1β treatment are cytokines or cytokine receptors. These differentially expressed genes are shown on the the Cytokine-Cytokine Receptor Interaction KEGG pathway downloaded from DAVID. Red genes are upregulated by IL1β and green genes are downregulated by IL1β.

shown to be differentially expressed in two of the three previous microarray studies of IL1β stimulated HUVEC and our data confirmed 81% of these genes (Supplemental Table 2). Finally, there were 324 genes which were shown by only one of the previous studies to be differentially expressed by IL1β treated HUVEC. Our microarray data confirmed differential expression at either 5 or 7 hours of IL1β treatment for 46% of these genes (Supplemental Table 3).

Table 3: Established gene responses to IL1β.

Gene	Symbol	IL1β 5 hours Fold Change	IL1β 5 hours + Neutrophils 1 hour Fold Change	IL1β 7 hours Fold Change	IL1β 7 hours + Neutrophils 3 hours Fold Change
Interleukin 8	IL8	109	113	99	98
E-selectin	SELE	57	64	60	56
Cyclooxygenase 2	COX2	49	58	35	34
Vascular Cell Adhesion molecule 1	VCAM1	13	11	9	9
Ubiquitin D	UBD	14	15	14	15
Fractalkine	CX3CL1	19	20	12	11

qRT-PCR was used to confirm differential expression of 4 genes which had not been previously described as being affected by IL1β treatment in HUVEC microarray literature. These genes were chosen for qRT-PCR verification based on their known functions as cytokines and cell structural components. Table 4 contains a list of verified genes along with fold changes as determined by both microarray and qRT-PCR. Of particular interest were claudin-1, claudin-5, and occludin which are all tight junction associated molecules. Fold changes determined by qRT-PCR confirmed either up-regulation or down-regulation as found in the microarray results, with results from qRT-PCR showing larger fold changes.

Table 4: Comparison of microarray and qRT-PCR findings.

Gene	Method	5 Hour Fold Change	7 Hour Fold Change
Claudin-1	Microarray	2.8x	3.8x
Claudin-1	PCR	23.5 +/- 7.7*	47.8 +/- 34.2
PBEF	Microarray	7.2x	3.9x
PBEF	PCR	8.9 +/- 1.8*	4.8 +/- 0.6*
Claudin-5	Microarray	0.41x	0.49x
Claudin-5	PCR	0.24 +/- 0.04*	0.25 +/- 0.04*
Occludin	Microarray	0.38x	0.39x
Occludin	PCR	0.10 +/- 0.01*	0.19 +/- 0.03*

*Fold changes calculated versus control + MACS, $p < 0.05$ n=3

Time course analysis of IL1β effects

To further analyze the impact of IL1β on endothelial cells, a time course of IL1β treatment was performed. Endothelial cells were treated with 100 pg/ml IL1β for either 0, 5, 7, 12, or 24 hours. mRNA levels were examined for claudin-1, claudin-5, occludin, and PBEF using qRT-PCR. Claudin-1 is up-regulated 32 +/- 18 fold following 7 hours of IL1β treatment, with expression returning to basal levels after 24 hours of HUVEC exposure to IL1β (Figure 5). PBEF up-regulation peaks at 5.2 +/- 1.5 fold after 5 hours of IL1β treatment with PBEF mRNA levels returning to original levels after 24 hours of IL1β exposure (Figure 6). Both claudin-5 and occludin mRNA are down-regulated in IL1β stimulated HUVEC, with maximum down-regulation occurring at 0.37 +/- 0.07 and 0.27 +/- 0.08 folds, respectively, following 5 hours of IL1β treatment (Figure 6).

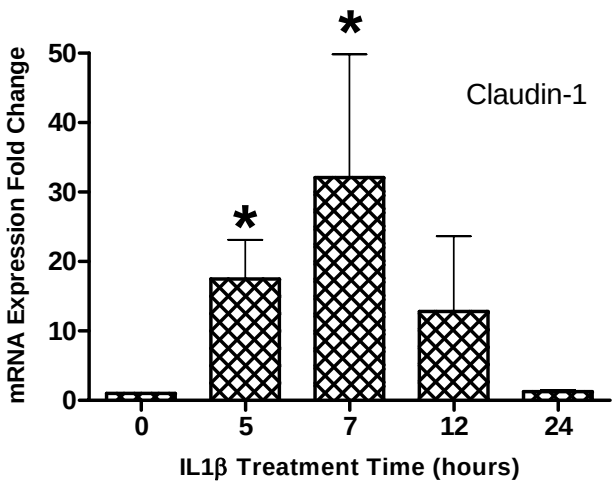

Figure 5: Claudin-1 mRNA fold change as a function of IL1β treatment time.
Confluent HUVEC were treated with 100 pg/ml IL1β for either 0, 5, 7, 12, or 24 hours. qRT-PCR was used to quantify mRNA expression of claudin-1. Fold changes were obtained by normalizing all expression levels to expression levels at the 0 hour time point. Claudin-1 mRNA is up-regulated 32 fold after 7 hours of IL1β treatment with an approximate 30x fold change in comparison to untreated HUVEC. After 24 hours of IL1β treatment, mRNA expression of claudin-1 returned to its original value. *$p<0.05$ versus 0 hours of IL1β treatment. n = 4-7

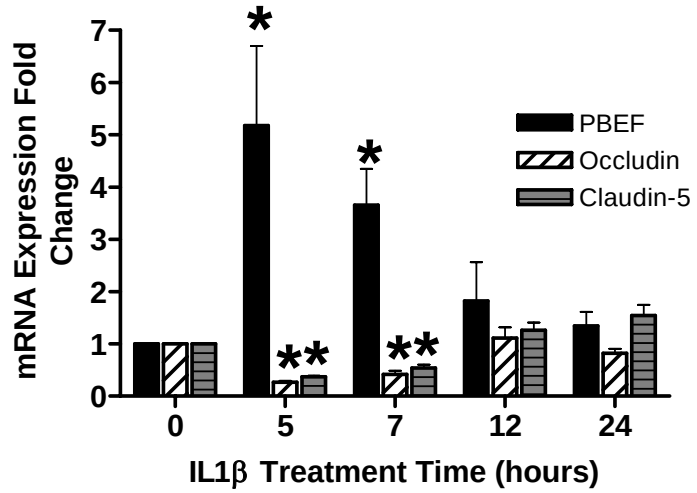

Figure 6: PBEF, occludin, and claudin-5 mRNA expression as a function of IL1β treatment time.
Confluent HUVEC were treated with IL1β for either 0, 5, 7, 12, or 24 hours. qRT-PCR was used to quantify mRNA expression of PBEF, occludin, and claudin-5. Fold changes were obtained by normalizing all expression levels to expression levels at the 0 hour time point. PBEF mRNA is up-regulated 5 fold after 5 hours of IL1β treatment with mRNA expression returning to original levels after 24 hours of IL1β treatment. Occludin and claudin-5 experienced peak down-regulation after 5 hours of IL1β treatment with expression levels returning to original values after 24 hours of IL1β. *$p<0.05$ versus 0 hours of IL1β treatment. n = 4-7

Western blotting verification of IL1β effects

To better understand the functional changes in HUVEC after IL1β treatment, we examined protein expression of claudin-1, claudin-5, and PBEF. Western blot analysis was performed on protein isolated from HUVEC after 0, 5, 7, 12, or 24 hours of treatment with IL1β (Figure 7). Fold changes in protein expression of these genes closely follows fold changes seen in mRNA expression.

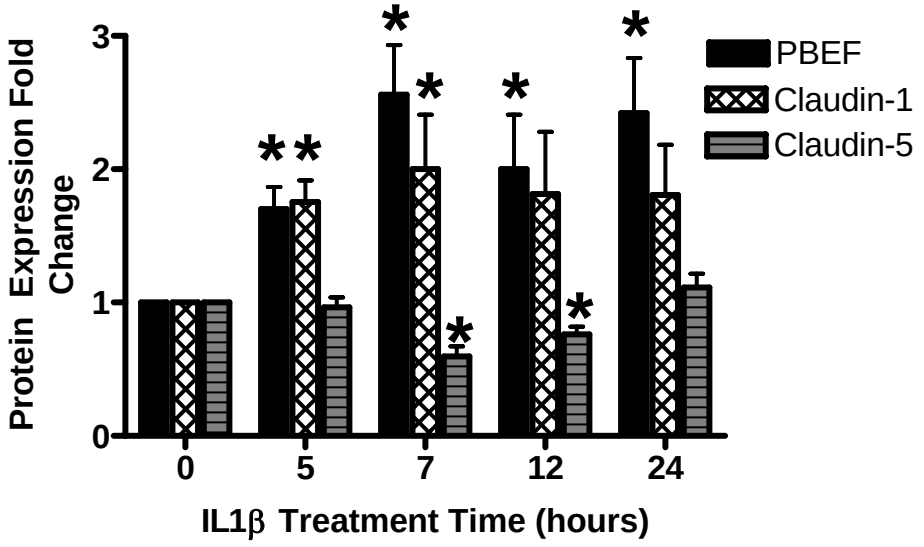

Figure 7: Protein expression fold changes for claudin-1, PBEF, and claudin-5 as a function of IL1β treatment time.
Band densities were quantified by densitometry with the Kodak EDAS 1D Imaging System and normalized to β-actin expression levels. Claudin-1 and PBEF protein levels remain elevated (1.5-2 fold) following 5 hours of IL1β stimulation and throughout the rest of the 24 hour time course. Claudin-5 protein expression was maximally down-regulated at 7 hours of IL1β treatment and then returns to original levels after 24 hours of IL1β. *$p<0.05$ versus 0 hours of IL1β treatment. $n = 6$

Neutrophil transmigration effects on EC gene expression

After allowing neutrophils to transmigrate in the presence of IL1β for one hour (with previous IL1β treatment for 4 hours), 19 genes were differentially expressed with fold

changes greater than 1.5 as compared to IL1β treatment alone for 5 hours . After three hours of neutrophil transmigration, 22 genes were differentially expressed with fold changes greater than 1.5 versus IL1β treatment for 7 hours. Table 5 contains a list of fold changes for differentially expressed genes in IL1β treated HUVEC after neutrophil transmigration as compared to IL1β treatment alone. Fold changes represented by dashes (--) indicate that these genes were not differentially regulated by neutrophil transmigration at the indicated time point. At both one and three hours of transmigration, hemoglobin beta (HBB) was the most highly up-regulated gene.

Differential expression of HBB following neutrophil transmigration was confirmed using qRT-PCR. qRT-PCR revealed no gene expression of HBB prior to neutrophil transmigration; however, expression of HBB could be detected following neutrophil transmigration. After neutrophil transmigration, the ECs were trypsinized and purified using anti-CD45 magnetic beads to remove contaminating neutrophils. Because HBB protein is a component of hemoglobin in red blood cells, we investigated the possibility that HBB gene expression was derived from red blood cell contamination of the neutrophils. Red blood cells do not express CD45 and therefore would not bind to anti-CD45 magnetic beads. Thus some RBCs found in the neutrophil population would not be removed from the trypsinized ECs following purification with anti-CD45 magnetic beads. Mature RBCs do not contain mRNA; however, reticulocytes, immature red blood cells which make up about 1% of the total red blood cell population, do contain mRNA. Therefore, a small population of reticulocytes may be responsible for the HBB gene expression found in RNA samples from ECs following neutrophil application.

Table 5: Differentially expressed genes following neutrophil transmigration.

Gene ID	Gene Name	IL1β 5 hours + Neutrophils 1 hour Fold Change	IL1β 7 hours + Neutrophils 3 hours Fold Change
NM_000518	hemoglobin, beta	5.647	4.009
NM_000359	transglutaminase 1	1.928	--
AF216583	Unannotated	1.671	--
XM_059318	RUN and TBC1 domain containing 2	1.662	--
NM_024614	hypothetical protein FLJ13197	1.622	--
NM_000399	early growth response 2 (Krox-20 homolog, Drosophila)	1.601	--
NM_003407	zinc finger protein 36, C3H type, homolog (mouse)	1.596	--
AL038125;	Unannotated	1.552	--
NM_024636	tumor necrosis factor, alpha-induced protein 9	1.55	0.559
NM_181644	hypothetical protein DKFZp761N1114	1.547	--
NM_152556	hypothetical protein FLJ31818	1.53	--
NM_173491	LSM11, U7 small nuclear RNA associated	0.666	--
BC035180;	Unannotated	0.656	--
NM_032441	zinc finger, matrin type 1	0.638	1.819
AK097587	Homo sapiens chromosome 10 open reading frame 82	0.637	0.559
BM676597	SET and MYND domain containing 4	0.614	--
THC2406165	Unannotated	0.596	0.641
NM_194449	pleckstrin homology domain containing, family E (with leucine rich repeats) member 1	0.587	--
THC2344910	Unannotated	0.583	--
THC2431122	Voltage-dependent sodium channel alpha subunit protein (Fragment), partial (18%	--	2.178
AF213987;	ALL1 fused gene from 5q31	--	1.892
NM_001010860	Chromosome 14 open reading frame 174	--	1.891
NM_033516	protein kinase NYD-SP25	--	1.797
THC2278570	Unannotated	--	1.78
NM_021807	SEC8-like 1 (S. cerevisiae)	--	1.707
NM_024873	TNFAIP3 interacting protein 3	--	1.69
AK022016	Myosin 1E	--	1.67
THC2278570	Unannotated	--	1.574
NM_020971	spectrin, beta, non-erythrocytic 4	--	1.552
NM_020211	RGM domain family, member A	--	0.665
NM_030649	centaurin, beta 5	--	0.646
BC043255	Unannotated	--	0.592
NM_005674	zinc finger protein 239	--	0.58
NM_020203	matrix, extracellular phosphoglycoprotein with ASARM motif (bone)	--	0.545
NM_019023	protein arginine N-methyltransferase 7	--	0.526
NM_004352	cerebellin 1 precursor	--	0.507

Further studies were performed to determine whether reticulocyte contamination was responsible for the detected expression of HBB. Anti-glycophorin A magnetic beads were used to remove contaminating RBCs and reticulocytes from neutrophils prior to application to stimulated ECs. Studies were also performed in which RBCs and reticulocytes were removed from trypsinized ECs just prior to RNA isolation in order to investigate whether RBC interaction with ECs could lead to HBB expression in ECs. In both cases, qRT-PCR revealed that over 99% of the HBB expression found in ECs following neutrophil transmigration was actually derived from contaminating reticulocytes rather than an actual up-regulation of HBB expression within the ECs.

Discussion

We found 3617 differentially expressed genes following 5 or 7 hours of IL1β stimulation that had not been previously reported in microarray data of IL1β stimulated HUVEC. Grouping all of the differentially expressed genes into categories using DAVID revealed prominent biological responses which occur as a result of IL1β stimulation (Table 2). As differential expression of 3617 genes constitutes over 5% of the human genome, the global impact that IL1β stimulation has on HUVEC mRNA expression is revealed.

Previous microarray studies of IL1β treatment of ECs used either smaller array sets or more stringent cutoffs for identifying differentially expressed genes [3-5]. In this study we chose to use a 1.5 fold change in gene expression as well as a 95 % confidence interval to identify differentially expressed genes from within the Agilent Whole Human Genome array set. Based on these criteria, our study identified numerous differentially expressed

genes which had not been previously reported and confirmed the data of previous microarray studies on IL1β stimulated ECs.

Table 3 shows highly up-regulated genes that have previously been reported as up-regulated by IL1β [3-5]. IL8, which was the most up-regulated gene at ~100 fold, is a chemokine known to cause neutrophil chemotaxis, degranulation, and adhesion molecule expression [45]. E-selectin and VCAM1 are also highly up-regulated at ~60 fold and ~10 fold, respectively. These molecules are surface adhesion molecules, with E-selectin acting as an adhesion molecule during the initial rolling stage of leukocyte transmigration and VCAM1 binding during the adherent phase of leukocyte transmigration [46]. COX2 was up-regulated over 30 fold in ECs following IL1β stimulation. COX2 is an enzyme which produces prostaglandin H2, a powerful mediator of inflammation [47]. Ubiquitin D, also known as FAT10 or diubiquitin, is up-regulated ~10 fold by IL1β stimulation. Ubiquitin D marks proteins for proteasomal degradation and may play a role in modulating apoptosis [48]. Fractalkine is up-regulated 10-20 fold by IL1β stimulation of endothelial cells. A recent study suggests that fractalkine expression on the EC surface stimulates P-selectin expression on adherent platelets which then leads to firm adhesion of leukocytes under arterial shear stresses [49].

We used DAVID to identify overrepresented functional groups which were differentially regulated by IL1β treatment (Table 2). IL1β is well known to activate the NF-κB pathway. The NF-κB pathway induces transcription of a number of anti-apoptotic genes including BFL1 and TRAF1 [50]. Other studies have shown that IL1β induces apoptosis

when protein synthesis is impaired [51]. In our study both apoptotic (e.g. up-regulation of CASP3, up-regulation of TNF) and anti-apoptotic (e.g. up-regulation of BFL1 and TRAF1) gene regulation was observed. Our study showed similar regulation of genes involved in control of the cell cycle. Cozzolino et al. reported halting of endothelial cells in the G_1 phase following IL1β treatment [52]; however, a recent proteomics study reported that the cytokine TNFα, but not IL1β, halts cell cycle progression [53].

IL1β signaling through the IL1β receptor is well known to activate the transcription factor NF-κB [54]. In our study a number of genes related to NF-κB activation and downstream signaling were differentially regulated. IL1β signaling is also well known to induce chemotaxis through the expression of chemokines. In our study we found up-regulation of CCLs 1, 2, 7, 8, and 20, CXCLs 1, 2, 3, 5, 6, 10, and CX3CL1 following IL1β treatment (Figure 4).

Through DAVID we also identified genes related to proteoglycan metabolism as being an overrepresented functional group. Our results showed down-regulation of a number of sulfotransferases and other enzymes involved in proteoglycan synthesis. This is consistent with reduced proteoglycan synthesis in porcine endothelial cells following IL1β treatment as shown by Skop et al. [55]. Genes related to chromosome organization are also overrepresented among our list of genes differentially expressed following IL1β treatment. Studies have shown that IL1β affects histone acetylation in regulating downstream gene expression [56]. Our study showed up-regulation of a number of histone

genes as well as chromosome binding genes which may play a role in chromosome organization.

The relationship between IL1β stimulation and angiogenesis has been studied both in vitro and in vivo with most studies indicating that IL1β is pro-angiogenic [57]. In our study a number of genes related to angiogenesis were differentially expressed, including VEGF up-regulation and neuropilin down-regulation. One of the most well characterized examples of IL1β involvement in hemopoiesis is IL1β -mediated production of GCSF, which stimulates progenitor cell differentiation to granulocytes [58]. In our study GCSF was up-regulated ~30 fold along with other differentially regulated molecules related to hemopoiesis.

Our study has shown IL1β induced up-regulation of claudin-1 mRNA expression along with down-regulation of claudin-5 and occludin mRNA expression. qRT-PCR was used to confirm differential expression of these 3 genes which are known to localize to cell-cell junctions. These genes were chosen for further study based on the importance of cell-cell junctions in endothelial barrier function and neutrophil transmigration. IL1β increases endothelial cell layer permeability [59] and decreases transendothelial resistance [60]. Cell-cell junction associated proteins, such as occludin and members of the claudin family, have been shown to be involved in regulation of endothelial barrier properties (Reviewed by Bazzoni [61]). Other studies have shown similar results in retinal pigment epithelial cells and astrocytes, indicating that claudin-1 is up-regulated by IL1β while occludin is down-regulated [62,63]. These findings suggest that altered claudin and occludin

expression may play a role in IL1β induced changes in endothelial permeability and transendothelial resistance in HUVEC.

Claudin-5 has been shown to be important in establishing barrier function within the blood brain barrier [64]. However, Fontijn et al. recently published data suggesting that the role of claudin-5 may be limited in establishing barrier function in endothelial cells which are not associated with the blood brain barrier [65]. This group found that silencing of claudin-5 expression in HUVEC did not alter endothelial permeability.

Up-regulation of PBEF following HUVEC treatment with IL1β was confirmed by qRT-PCR and western blotting. PBEF, also known as visfatin, is a protein which is believed to exhibit both extracellular cytokine activity as well as intracellular enzymatic activity [66]. PBEF mRNA expression is up-regulated in amniotic epithelial cells by mechanical stretch [67] as well as by IL1β, TNFα, and IL6 [68]. PBEF siRNA has been shown to attenuate PBEF protein expression in thrombin stimulated human pulmonary artery endothelial cell monolayers [69]. Thrombin treated endothelial cells normally exhibit decreased barrier function in the form of decreased transendothelial resistance; however, pretreatment of ECs with PBEF siRNA prior to thrombin stimulation resulted in a smaller drop in transendothelial resistance as compared to ECs treated with scrambled siRNA followed by thrombin [69]. These results indicate that PBEF is up-regulated by inflammatory mechanisms and contributes to changes in EC function as a result of these inflammatory stimuli.

Differential regulation of claudin-1, claudin-5, occludin, and PBEF is transient, with mRNA expression levels returning to those of control HUVEC following 24 hours of IL1β stimulation (Figures 5 and 6). This finding is indicative of the adaptive response of HUVEC to IL1β in order to prevent persistent activation of the endothelium which could lead to numerous vascular disorders. Persistent endothelial activation in long term pathological conditions is likely sustained by participation of a combination of stimulating cytokines released from leukocytes and platelets [70].

Our study also examined the impact of magnetic cell separation on EC gene expression. Endothelial cells were negatively selected by removing neutrophils from the EC population using CD45 Microbeads (Miltenyi). This negative selection process had very little impact on EC gene expression as compared to ECs which were not exposed to CD45 Microbeads. These results provide further validation for the use of magnetic cell separation in sample preparation for gene expression studies.

A number of studies have investigated the impact of leukocyte-EC interactions on endothelial cell signaling. Etienne et al. showed increased phosphorylation of focal adhesion molecules following ICAM1 cross-linking [7]. In a similar study, van Wetering et al. showed RAC activation and increased phosphorylation of p38 MAPK following cross-linking of VCAM1 [71]. Huang et al. found a 5 to 8 fold increase in the cytosolic calcium levels of HUVEC following neutrophil transmigration [8]. Marcus et al. showed that direct contact of neutrophils with ECs resulted in a decrease in transendothelial resistance while Cepinskas et al. showed that neutrophil transmigration results in a dose

dependent reduction of NF-κB levels [10,11]. Based on these and similar studies, van Buul and Hordijk hypothesized that leukocyte binding of ICAM1 and VCAM1 could lead to endothelial cell signaling which results in loss of endothelial cell-cell adhesion [72].

Microarray analysis revealed that relatively few differentially expressed genes could be identified following neutrophil transmigration. These results were unexpected based on previous studies of neutrophil adhesion and transmigration which identified a number of signaling events within ECs, which would be expected to be linked to transcriptional changes. We suggest that transcriptional changes resulting from neutrophil adhesion and transmigration are overshadowed in comparison to the large background of differential expression induced by IL1β.

Our study has revealed a number of global transcriptional changes occurring within ECs in response to IL1β stimulation. These differentially expressed genes represent important pathways within the cell including apoptosis, cell cycle regulation, NF-κB cascade, chemotaxis and the immune response. Differential expression of claudin-1, claudin-5, occludin, and PBEF were confirmed following IL1β stimulation of ECs. Claudin-5, claudin-1, and occludin are all found at endothelial cell-cell junctions and differential expression may play a role in altered endothelial permeability following IL1β stimulation. In addition the cytokine PBEF has been shown to affect endothelial permeability in thrombin stimulated HUVEC and may have a similar role in IL1β stimulated HUVEC. Studies on post-transcriptional changes, particularly the relationship among the tight

junction proteins, will be required to elucidate the functional impact of IL1β on ECs, and how cytokine responses of ECs lead to inflammation and presage cardiovascular disease.

CHAPTER 3: TRANSMIGRATION ACROSS ACTIVATED ENDOTHELIUM INDUCES TRANSCRIPTIONAL CHANGES IN MONOCYTES

Monocytes are phagocytic cells that play a key role in inflammation. In response to infection, these cells migrate out of the blood stream and differentiate into either macrophages which activate the innate immune response or dendritic cells which activate the adaptive immune response. Monocyte migration to a site of inflammation begins with rolling along activated endothelial cells (ECs), followed by firm adhesion to ECs, and finally diapedesis across the endothelium towards a chemoattractant. One mechanism of EC activation is exposure to interleukin 1 beta (IL1β) which induces expression of E-selectin, intercellular adhesion molecule 1 (ICAM1), and vascular cell adhesion molecule 1 (VCAM1) on the endothelial surface [73]. Monocytes interact with these adhesion molecules, leading to rolling and firm adhesion to the endothelium [74-76]. Interaction with adhesion molecules has been shown to induce outside-in signaling events within leukocytes which may lead to downstream changes in leukocyte transcription [72,77,78].

Activation of ECs through exposure to IL1β also induces release of cytokines and other secreted factors (e.g. macrophage inflammatory proteins, monocyte chemotactic proteins, and fractalkine) [73], which have been shown to stimulate monocyte activation and recruitment [79-81]. During diapedesis, monocytes undergo changes in shape and interact with molecules found in EC junctions. Monocytes bind to junctional adhesion molecules and platelet/endothelial cell adhesion molecule (PECAM1) on the EC surface during diapedesis via lymphocyte function-associated antigen 1 (LFA1) and PECAM1,

respectively [76]. This binding may induce inside-out signaling within the monocyte [82]. All of the steps in transmigration may contribute to downstream changes in monocytes which lead to either inflammatory resolution or pathogenesis.

To understand the effects of transmigration on monocyte gene expression, we used microarrays to identify transcriptional changes in freshly isolated human monocytes that had transmigrated across a layer of IL1β-stimulated ECs. Control conditions were used to further characterize which steps of transmigration are responsible for inducing these changes. Microarray analysis revealed that monocyte transmigration promotes further leukocyte recruitment, induces expression of genes involved in the inhibition of apoptosis, and reduces gene expression of anti-microbial proteins. These findings were confirmed with qRT-PCR, immunoblots, and apoptosis assays.

Materials and Methods

Cell culture and monocyte isolation

Pooled human umbilical vein endothelial cells (HUVEC) were purchased from Lonza and cultured in HUVEC media, composed of M199 media (Mediatech) containing 20% fetal bovine serum (Hyclone), 50 U/mL penicillin (Gibco), 50 μg/ml streptomycin (Gibco), 2mM L-glutamine (Mediatech), 2.5 U/ml heparin (American Pharmaceutical Partners), and 50 μg/ml endothelial mitogen (Biomedical Technologies). Passage 3-4 HUVEC were seeded at 50,000 cells/cm^2 onto porcine gelatin coated (0.2% wt/vol in phosphate buffered saline (PBS)) polycarbonate cell culture inserts (diameter = 75mm)

containing 3 μm pores (Corning) and cultured until confluent at 37 ^{o}C in the presence of humidified 5% CO_2.

Monocytes were isolated from whole blood obtained from healthy adult donors according to an institutional review board approved protocol in which all participants gave written informed consent. Blood was drawn into citrate buffer anticoagulant and combined with an equal volume of 6% Dextran 70 solution (B. Braun). This mixture was layered over lymphocyte separation media (1.078 g/mL, Cellgro) and centrifuged for 30 minutes at 400g. Following centrifugation, peripheral blood mononuclear cells (PBMCs) were obtained from the interface which formed between the lymphocyte separation media and saline solution. To remove platelets, PBMCs were rinsed twice by centrifugation in PBS at 250g for 10 minutes. Monocytes were negatively selected from the PBMCs using a MACS Monocyte Isolation Kit II (Miltenyi) with slight modifications to the manufacturer's protocol. For 30 mL of blood, PBMCs were pelleted and resuspended in 88 uL of MACS buffer (0.5% human serum albumin and 2 mM EDTA in PBS). Thirty μL each of FcR solution and antibody cocktail as provided in the monocyte isolation kit were added to the PBMCs. In addition 1 μL each of biotinylated CD2 (BD Biosciences) and CD42b (Genetex) antibodies were added to the PBMCs and the mixture was incubated at 4 ^{o}C for 10 minutes. Following this incubation period, 65 uL magnetic beads, as provided by Miltenyi, and 85 μl MACS buffer were added to the PBMCs with an additional 15 minute incubation period at 4 ^{o}C. PBMCs were then rinsed and resuspended in MACS buffer. Other cell types were removed from the monocytes by passing the cell mixture over a LS column placed in a MACS Magnetic Separator

(Miltenyi). Monocytes were collected in the flow-through from the magnetic column. Purified monocytes were maintained in minimal essential media (MEM) with 0.5% human serum albumin at 37 ^{o}C until application to HUVEC and used within two hours following isolation. In this procedure CD2 and CD42b antibodies were necessary additions to the antibody cocktail in order to remove platelets and a small number of lymphocytes which remained when the unmodified manufacturer's protocol was used. Monocyte populations were assessed by Wright-Geimsa staining of cytospin preparations and found to be greater than 95% pure (Shandon Cytospin).

Experimental protocol

Twenty-four hours after the endothelial cells reached confluence, the media was replaced with HUVEC media containing 100 pg/ml IL1β. Seven hours later, stimulated ECs were washed thoroughly 3 times with MEM. Then the insert with the ECs was transferred to a new agarose-coated tissue culture dish. Ten million freshly isolated monocytes in MEM with 0.5% HSA were placed above the stimulated ECs for 1.5 h. Following a 1.5 h incubation, monocytes that successfully transmigrated were collected (Figure 8C "TM"). As a control, monocytes that were applied above ECs but failed to transmigrate were collected (Figure 8C "UMA"). As another control, monocytes that were placed beneath stimulated ECs for 1.5 h, but never allowed to physically contact the ECs, were collected (Figure 8B "UMB"). As a final control, untreated monocytes were collected from an agarose-coated tissue culture dish following a 1.5 h incubation period (Figure 8A "UNT").

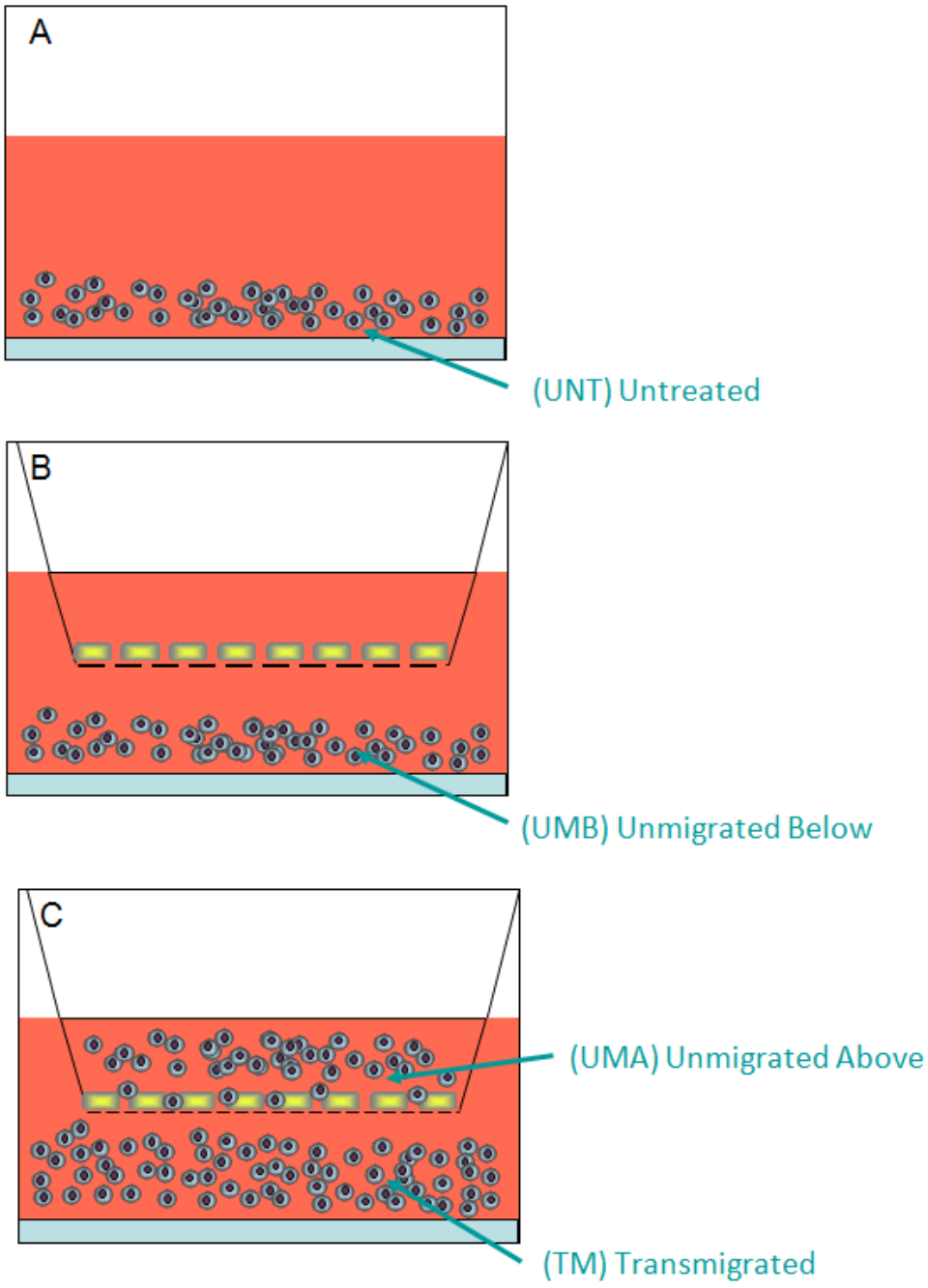

Figure 8: Four monocyte populations collected for microarray and downstream analysis.
A) Untreated monocytes (UNT) were collected following 1.5 hour incubation on agarose coated tissue culture dishes in MEM with 0.5% HSA. B) Monocytes (UMB) were collected following 1.5 hour incubation on agarose coated tissue culture dishes beneath IL1β stimulated HUVEC grown on polycarbonate cell culture inserts containing 3 μm pores. These monocytes have been exposed to EC secretions that have diffused into the lower chamber, but have not directly contacted ECs. C) Monocytes that failed to transmigrate (UMA) during a 1.5 hour incubation with IL1β stimulated HUVEC grown on cell culture inserts were collected. These monocytes have contacted stimulated ECs and been exposed to EC secretions. Monocytes that transmigrated (TM) during 1.5 hour incubation with IL1β stimulated HUVEC grown on cell culture inserts were collected. These monocytes have undergone the process of diapedesis in addition to being exposed to EC secretions and directly contacting stimulated ECs.

Prior to RNA isolation, monocyte populations were further purified using CD105 Microbeads (Miltenyi) according to the manufacturer's protocol to remove contaminating ECs which made up 3-5% of the cell population. Effectiveness of this purification step was measured by performing the transmigration protocol using freshly isolated monocytes labeled with Cell Tracker Orange (Invitrogen) and ECs labeled with Cell Tracker Green (Invitrogen). Flow cytometry was used to assess purity of the monocyte population and indicated less than 1% contamination following the EC removal step.

Following this purification step, cells were counted with a Beckman Coulter Z2 Particle Count and Size Analyzer to determine percent transmigration. RNA and protein were isolated with TRI-zol (Invitrogen) according to the manufacturer's instructions, followed by DNA removal using an RNA Cleanup Kit (Qiagen). RNA quantity and quality were assessed by loading 1 μl of sample RNA onto a RNA 6000 Nano chip (Agilent) and analyzing with an Agilent 2100 Bioanalyzer to determine the amount and integrity of RNA recovered. Monocyte samples having an RNA Integrity Number of 7.5 or greater and at least 250 ng of total RNA were used for microarray experiments.

Microarrays

Microarray hybridization and imaging were performed at the Morehouse School of Medicine Functional Genomics Core Facility. Briefly, RNA and Universal Human Reference RNA (Stratagene) were linearly amplified to cRNA using a Low RNA Input Fluorescent Linear Amplification Kit (Agilent). Cy5-labeled cRNA for each sample was competitively hybridized with Cy3-labeled reference cRNA to a 44k Whole Human

Genome Microarray (Agilent) according to the manufacturer's instructions. Slides were dried under nitrogen and scanned on an Agilent DNA Microarray Scanner. Microarray images were analyzed with Agilent Feature Extraction Software. GeneSpring 7.3 software was used to analyze the microarray data with one way ANOVA assuming equal variances followed by a post hoc Student-Neuman-Keuls test. Differentially expressed genes were identified as those which had changes of at least 2 fold and adjusted p-values of less than 0.05. Microarray data has been deposited in NCBI's Gene Expression Omnibus (GEO, http://www.ncbi.nlm.nih.gov/geo/) and is accessible through GEO Series accession number GSE14027.

Functional Grouping of Differentially Expressed Genes

Lists of differentially expressed genes were uploaded to the Database for Annotation, Visualization and Integrated Discovery (DAVID) and subjected to Functional Annotation Clustering at medium class stringency in order to identify enriched biological themes [44]. Gene Ontology (GO) Biological Process annotations were used to perform this functional clustering. Lists of up-regulated and down-regulated genes were uploaded separately to DAVID in order to identify enriched pathways and map differentially expressed genes to these pathways.

Quantitative Real Time PCR

Total RNA from each sample was reverse transcribed into cDNA using SuperScript II (Invitrogen). cDNA was purified with Micro Bio-Spin P-30 Chromatography Columns (BioRad), and diluted in RT-PCR Grade Water (Ambion). Pre-designed PCR primers

and Quantitect SYBR Green PCR Master Mix were purchased from Qiagen. Primers were added to the master mix at a ratio of 1:5. Each reaction was performed with 4 μl of diluted cDNA and 6 μl of primers in the master mix. The qRT-PCR reactions were performed on a LightCycler 2.0 (Roche Applied Science) with a 15 minute activation step at 95 ^{o}C; 50 cycles at 94 ^{o}C for 15 seconds, 55 ^{o}C for 20 seconds, 72 ^{o}C for 20 seconds; and a ramped melting cycle. Fold changes were determined using the ΔΔCt method. Statistical differences in fold changes were assessed with one way ANOVA followed by a post-hoc Tukey multiple comparison test. qRT-PCR was used to verify gene expression from RNA isolated from three independent monocyte transmigration experiments.

Immunoblotting

For detection of α-defensin or β-actin protein expression, 15 μg of protein or 5 μg of protein, respectively, was blotted onto a nitrocellulose membrane (Pall Life Science). After blocking with 5% nonfat dry milk, membranes were probed with mouse monoclonal α-defensin antibodies (GeneTex), or mouse monoclonal β-actin antibodies (Sigma). Bound primary antibodies were labeled with horseradish peroxidase conjugated secondary antibodies and detected with enhanced chemiluminescence (ECL Plus, Amersham Biosciences). Net intensities of α-defensin expression were quantified by densitometry with the Kodak EDAS 1D Imaging System (Kodak) and normalized to β-actin net intensities. Immunoblots were performed using protein isolated from 4 separate time course experiments and statistical significance was assessed using one way ANOVA followed by a post hoc Tamhane test for unequal variances. The post hoc Tamhane test

was chosen over the Tukey multiple comparison test because Bartlett's test for equal variances showed unequal variances, indicating that the Tukey test is inappropriate [83,84].

Apoptosis Assays

Cells were collected from each of the four experimental conditions and washed in cold PBS. Freshly isolated monocytes were treated for 3 hours with 2 μM staurosporine or 2 mM hydrogen peroxide as positive controls for apoptosis and necrosis, respectively. Cells were then stained with R-phycoerythrin (R-PE) conjugated Annexin V and SYTOX Green using the Vybrant Apoptosis Kit no. 8 (Molecular Probes, Eugene, OR) according to the manufacturer's instructions. Samples were analyzed by flow cytometry, measuring the fluorescence emission at 530 nm and 575 nm. The percentage of apoptotic cells was calculated using FlowJo software (Tree Star, Inc.).

Results

Monocyte Transmigration and Recovery

In control conditions, approximately 70% of the monocytes placed on agarose-coated dishes were collected after a 1.5 h incubation period. When monocytes were placed above stimulated ECs for 1.5 h, 23 +/- 7% of the applied monocytes were collected from the dish beneath the ECs. An additional 25 +/- 13% of the applied monocytes failed to transmigrate and were collected from above the stimulated ECs. The remaining monocytes which were not recovered following incubation with ECs may have become adherent to the ECs, failed to completely move across the polycarbonate cell culture inserts, or been lost in the monocyte purification steps.

Table 6: Top 10 Up- and Down-Regulated Genes in Transmigrated Monocytes

Gene Symbol	Gene Name	Fold Change (TM vs UNT)
CCL2	Monocyte Chemotactic Protein 1	14.8
CCL7	Monocyte Chemotactic Protein 3	14.4
TNIP3	TNFAIP3-Interacting Protein	13.6
EMP1	Epithelial Membrane Protein 1	13.6
BATF	Activating Transcription Factor B	9.1
DMD	Dystrophin	9.1
IL2RA	IL2 Receptor A	8.7
CTSL1	Cathepsin L	8.3
THEX1	Three Prime Histone Exonuclease	7.9
LMNB1	Lamin B 1	7.7
CST6	Cystatin 6	0.21
NTF3	Neurotrophin 3	0.20
CNTROB	Centrobin	0.19
NKX2-3	NK2 Transcription Factor related, locus 3	0.19
MUC8	Mucin 8	0.18
PLA2G4A	Phospholipase A2 Group IVA	0.17
VIL1	Villin	0.17
FANCI	Mitochondrial Polymerase Gamma	0.17
CAMP	Cathelicidin Antimicrobial Peptide	0.11
DEFA3	Defensin A 3	0.02

Global Effects of the Transmigration Process

Comparison of gene expression in transmigrated monocytes to gene expression in untreated monocytes revealed up-regulation of 489 genes and down-regulation of 203 genes following transmigration. The top 10 up-regulated and down-regulated genes are shown in Table 6. Interestingly the most highly up-regulated genes, monocyte chemotactic proteins 1 and 3, are both chemokines known to strongly attract monocytes. Thus, transmigrating monocytes may be involved in recruiting other monocytes through the production of chemokines. The most highly down-regulated genes, α-defensin 3 and cathelicidin antimicrobial peptide, are both peptides which have known antimicrobial activity. A list of all of the differentially expressed genes in transmigrated monocytes compared to untreated monocytes can be found in Supplemental Table 4.

Functional annotation clustering was performed using the Database for Annotation, Visualization, and Integrated Discovery (DAVID) to identify enriched biological themes or functional groups among these 692 up- and down-regulated genes. Genes identified as being down-regulated are involved in cell cycle arrest, DNA metabolism, and actin filament depolymerization. Up-regulated genes are involved in the immune response, the protein kinase cascade, and inhibition of apoptosis. Genes associated with these functional groups are shown in Figure 9 with red indicating up-regulation, yellow indicating no significant change in expression, and blue indicating down-regulation. It should be noted that some genes are differentially expressed in all of the monocyte

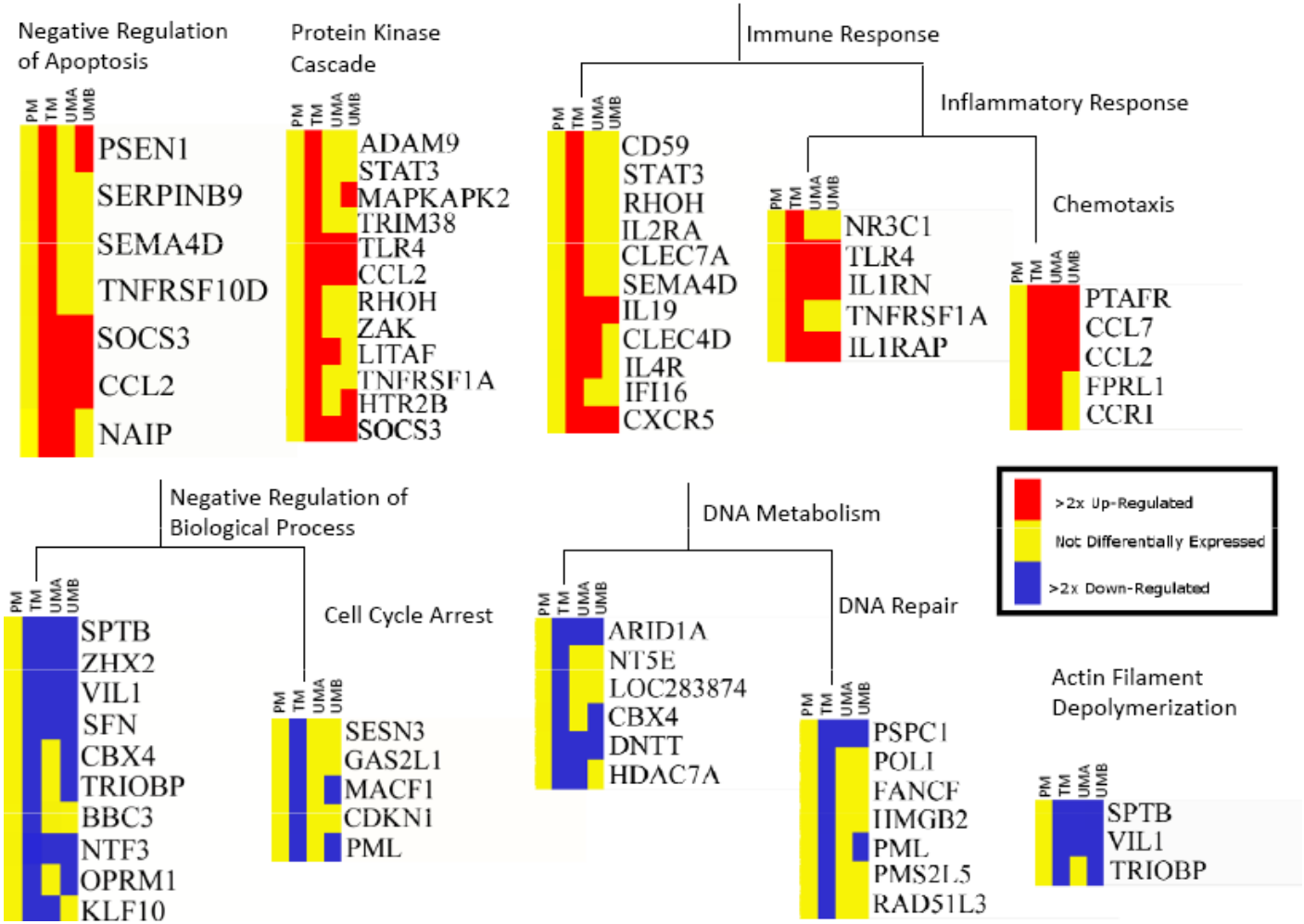

Figure 9: The process of transmigration affects genes belonging to a variety of functional groups.
Over-represented functional groups up- or down-regulated by monocyte transmigration as compared to untreated monocytes are shown. Functional groups were identified by analysis of lists of up- or down-regulated genes with DAVID. Heat maps of genes belonging to identified functional groups were generated in Genespring 7.3. Yellow indicates no significant change in gene expression. Red indicates up-regulation and blue indicates down-regulation of gene expression.

treatment conditions as compared to untreated monocytes (e.g. monocyte chemotactic protein 1 (CCL2) and suppressor of cytokine signaling 3 (SOCS3)) while other genes are differentially expressed in only one or two of the monocyte treatment conditions as compared to untreated monocytes. This result indicates that some differentially expressed genes are responding to a stimulus that is found in all of the monocyte treatment conditions (i.e. cytokine secretions from IL1β stimulated HUVEC) while other differentially expressed genes are responding to stimuli that are only found in some of the monocyte treatment conditions (i.e. EC contact or diapedesis). A more complete examination of the individual effects of these stimuli follows.

qRT-PCR Confirmation

Five up-regulated genes and 4 down-regulated genes were selected for qRT-PCR confirmation of the microarray results. The 5 up-regulated genes were chosen for confirmation because of their inclusion in the negative regulation of apoptosis functional group (Figure 9). The 4 down-regulated genes were chosen for confirmation because of their inclusion in the defense response functional group (See "Effects of Diapedesis" below). Patterns of differential expression as observed by microarray analysis closely resembled patterns of differential expression detected by qRT-PCR. A comparison of fold changes as detected by microarray analysis and qRT-PCR is shown in Table 7.

Table 7: Comparison of microarray and qRT-PCR fold changes

Gene	Method	Transmigrated	Unmigrated Above	Unmigrated Below
CCL7	Microarray PCR	14.4 25.0 +/- 12.8	5.4 14.7 +/- 9.4	8.3 16.2 +/- 7.1
CCL2	Microarray PCR	14.8 24.0 +/- 7.3	8.6 11.4 +/- 3.0	11.4 29.9 +/- 7.3
SOCS3	Microarray PCR	5.0 4.4 +/- 0.3	6.7 9.7 +/- 4.6	9.0 7.3 +/- 0.7
TNFRSF10D	Microarray PCR	3.8 3.1 +/- 0.2	1.1 3.4 +/- 0.9	1.5 2.0 +/- 0.3
NAIP	Microarray PCR	3.0 3.3 +/- 0.01	2.5 1.6 +/- 0.3	1.5 1.8 +/- 0.1
CTSG	Microarray PCR	0.38 0.26 +/- 0.21	2.7 2.4 +/- 0.6	1.2 1.3 +/- 0.2
LTF	Microarray PCR	0.21 0.045 +/- 0.017	2.6 2.7 +/- 0.7	1.2 1.1 +/- 0.1
CAMP	Microarray PCR	0.11 0.11 +/- 0.03	3.0 2.5 +/- 0.5	1.2 1.1 +/- 0.1
DEFA3	Microarray PCR	0.019 5.4E-3 +/- 4E-3	2.1 3.5 +/- 1.3	0.9 1.2 +/- 0.2

Average fold changes for microarray data were obtained from Genespring 7.0 following normalization procedures. For qRT-PCR data, fold changes represent the average +/- SEM for 3 experiments. Red genes indicate up-regulation of at least 2 fold and green genes indicate down regulation of at least 2 fold.

Transmigration Inhibits Apoptosis

Ingenuity Pathways Analysis was used to map up-regulated genes belonging to the gene ontology term "Negative Regulation of Apoptosis" to the apoptosis pathway. A portion of this pathway is shown in Figure 10, for the complete pathway, please see Supplemental Figure 3.

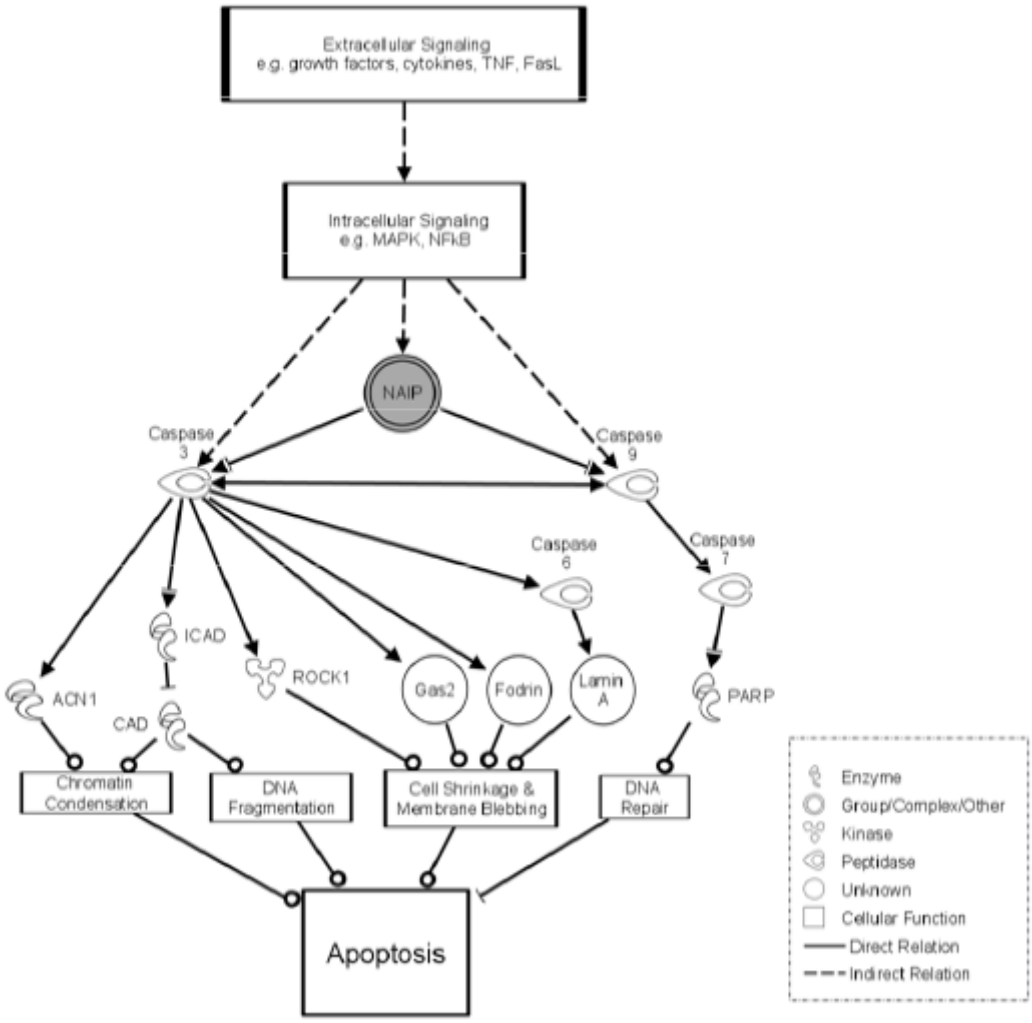

Figure 10: Transmigration Causes Differential Expression of Genes in the Apoptosis Pathway. Genes belonging to the "Negative Regulation of Apoptosis" functional group were mapped to the apoptosis pathway. Apoptosis is shown at the bottom of the pathway. Caspase 3 and caspase 9 are key enzymes in promoting apoptosis by activation through enzymatic cleavage of a number of proteins which control apoptotic functions such as chromatin condensation, DNA fragmentation, and membrane blebbing. Both of these caspase genes are inhibited by neuronal apoptosis inhibitory protein (NAIP) which is up-regulated in transmigrated monocytes compared to untreated monocytes as indicated by the gray coloring. Various intracellular and extracellular signaling pathways are involved in expression and inhibition of caspase 3, caspase 9, and NAIP.

Apoptosis is shown at the bottom of Figure 10 and is preceded by chromatin condensation, DNA fragmentation, cell shrinkage, and membrane blebbing. These cellular activities are mediated by various proteins including ACIN1 (apoptotic chromatin condensation inducer 1), CAD (caspase activated DNAse), and GAS2 (growth arrest specific 2). The activity of each of these proteins is regulated by caspase 3 and caspase 9. Further examination of Figure 3 reveals that NAIP (neuronal apoptosis inhibitory protein) inhibits caspase 3 and caspase 9 activity. The gray coloring of NAIP indicates that in our microarray data this gene was up-regulated in transmigrated monocytes compared to untreated monocytes. qRT-PCR confirmed up-regulation of NAIP in transmigrated monocytes as compared to untreated monocytes (Table 7). Significant increases in NAIP expression were not seen in monocytes incubated below stimulated ECs or in monocytes which failed to transmigrate.

Functional Assay of Apoptosis

Apoptosis assays were performed on monocyte populations using AnnexinV binding to phosphatidyl serine on the outside of the cell membrane as an indicator of monocyte apoptosis. SYTOX green labeling of DNA in monocytes having a compromised cell membrane was used as an indicator of late stage apoptosis or necrosis. Representative flow cytometry dot plots are shown in Figure 11A-D. Approximately 20% of untreated monocytes were found in the apoptotic quadrant, Q4, with positive staining for Annexin V binding and without uptake of SYTOX green (Figure 11A). Monocytes which failed to transmigrate (Figure 11C) and monocytes incubated beneath stimulated ECs (Figure 11B) contained 18% and 16% apoptotic cells, respectively. Following monocyte

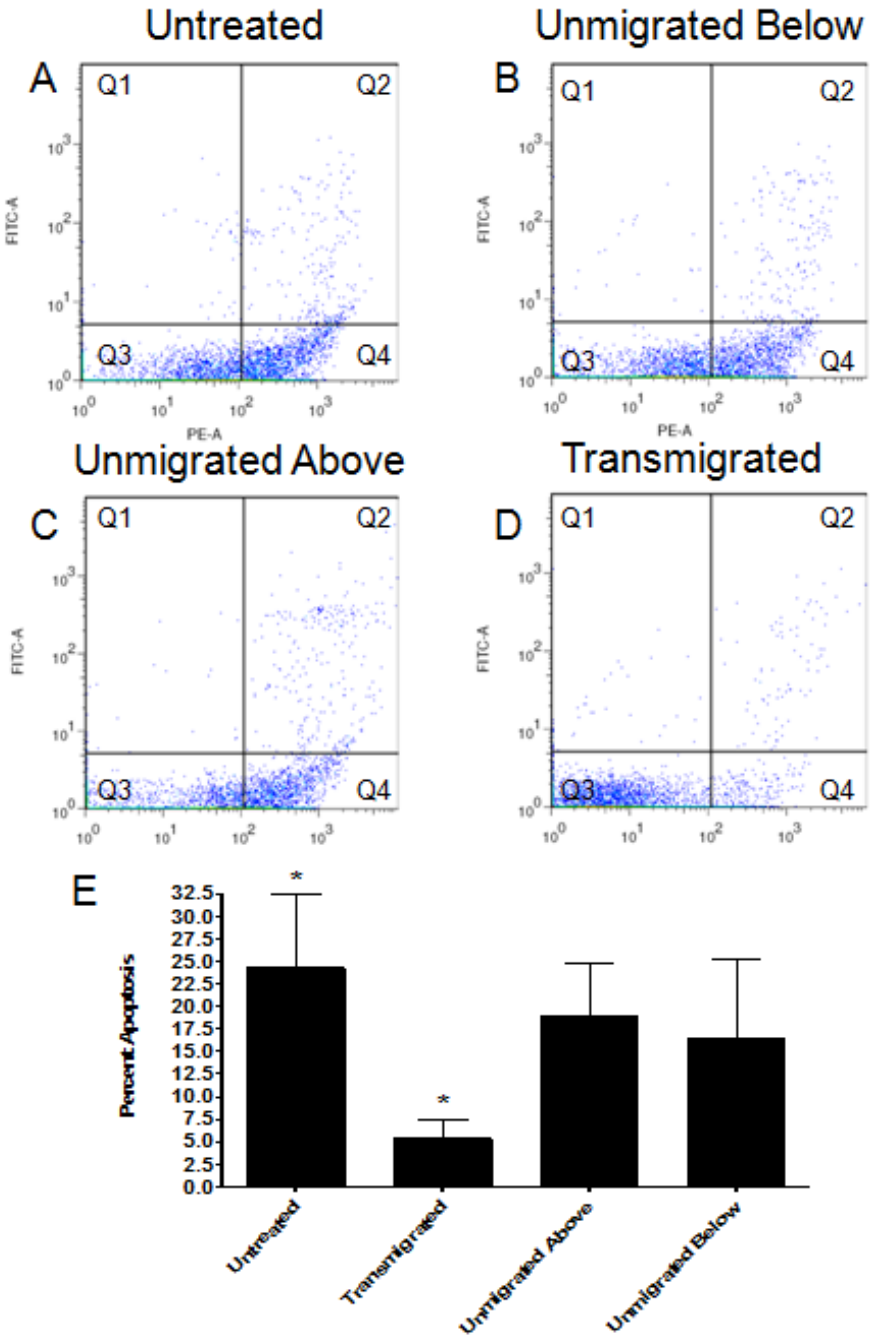

Figure 11: Apoptosis is reduced in monocytes following transmigration.
(A-D) Representative dot plots of R-PE labeled-annexinV and SYTOX green labeled monocytes from each of the four monocyte populations. Q1 – No cells. Q2 – Necrotic or late apoptotic cells. Q3 - Live monocytes. Q4 - Apoptotic monocytes. (E) Quantitation of monocyte apoptosis in four experiments, bars indicate mean +/- SEM. * $p<0.05$

transmigration only about 5% of the monocytes were apoptotic (Figure 11D), indicating that transmigration reduces monocyte apoptosis. Quantification of apoptosis in each of the four monocyte treatment conditions from four experiments is shown in Figure 11E, indicating that transmigrated monocytes have a significant reduction in apoptosis as compared to untreated monocytes.

Steps in Transmigration Process

Comparison of gene expression in transmigrated monocytes and untreated monocytes indicates that the monocyte transcriptome is altered by the process of transmigration; however, it does not allow for determination of which specific steps in the transmigration process are responsible for these changes. Control conditions were used to identify which steps of transmigration (i.e. exposure to endothelial secretions, monocyte-endothelial contact, or diapedesis) are responsible for altered monocyte gene expression.

Effects of IL1β-Induced Endothelial Secretions

We expected that a number of gene changes seen between transmigrated monocytes and untreated monocytes were induced by exposure to EC secretions resulting from IL1β treatment of the ECs. In our studies transmigrated monocytes (Figure 8 "TM"), monocytes which failed to transmigrate (Figure 8 "UMA"), and monocytes incubated beneath stimulated ECs (Figure 8 "UMB") were all exposed to EC secretions. We identified 119 genes which were differentially expressed in all of the monocyte conditions that were exposed to EC secretions as compared to untreated monocytes (Supplemental Table 5). Fold changes were similar among all of the conditions for 99%

Table 8: Functional groups associated with up-regulation by EC secretions.

IMMUNE SYSTEM RESPONSE	**FOLD CHANGE** (TM/UNT)	(UMA/UNT)	(UMB/UNT)
CCL2, monocyte chemotactic protein 1	14.8	8.6	11.4
CCL7, monocyte chemotactic protein 3	14.4	5.4	8.3
IL1RN, interleukin-1 receptor antagonist	6.9	4.8	3.5
IL19, interleukin-19	3.6	2.9	2.2
CXCR5, chemokine (c-x-c motif) receptor 5	2.5	2.3	3.5
TLR4, toll-like receptor 4	2.8	2.4	2.2
CELLULAR COMPONENT ORGANIZATION			
EMP1, epithelial membrane protein 1	13.6	6.4	5.5
CISH, cytokine inducible sh2-containing protein	7.1	9.0	8.4
SOCS3, suppressor of cytokine signaling 3	5.0	6.7	9.0
PDSS1, prenyl diphosphate synthase, subunit 1	6.2	3.5	2.8
KIF15, kinesin family member 15	2.5	3.2	4.6
FGD4, five, rhogef and ph domain containing 4	3.0	2.3	2.2
SIGNAL TRANSDUCTION			
RSPO3, r-spondin 3 homolog	3.9	4.3	2.5
CCL2, monocyte chemotactic protein 1	14.8	8.6	11.4
CCL7, monocyte chemotactic protein 3	14.4	5.4	8.3
TLR4, toll-like receptor 4	28	2.4	2.2
IL19, interleukin-19	3.6	2.9	2.2
CISH, cytokine inducible sh2-containing protein	7.1	9.0	8.4
FGD4, five, rhogef and ph domain containing 4	3.0	2.3	2.2
SOCS3, suppressor of cytokine signaling 3	5.0	6.7	9.0
MCTP2, multiple c2 domains, transmembrane 2	6.5	4.1	2.8
CXCR5, chemokine (c-x-c motif) receptor 5	2.5	2.3	3.5
CD69, cd69 antigen, early t-cell activation antigen	4.8	4.9	5.7

Table 9: Functional groups associated with down-regulation by EC secretions.

	FOLD CHANGE		
SIGNAL TRANSDUCTION	(TM/UNT)	(UMA/UNT)	(UMB/UNT)
OPRK1, opiod receptor, kappa 1	0.28	0.35	0.21
MAP4K5, mitogen-activated protein kinase kinase kinase kinase 5	0.31	0.28	0.39
guanine nucleotide-binding regulatory protein	0.30	0.30	0.40
SFN, stratifin	0.35	0.36	0.39
MED16, thyroid hormone receptor associated protein 5	0.40	0.32	0.43
CENTG2, centaurin, gamma 2	0.46	0.34	0.35
GRM5, glutamate receptor, metabotropic 5	0.37	0.46	0.37
SPTB, spectrin, beta, erythrocytic	0.40	0.45	0.38
DAB2IP, ngap-like protein	0.45	0.43	0.41
NTRK2, neurotrophic tyrosine kinase, receptor, type 2	0.46	0.38	0.44
FRAT2, frequently rearranged in advanced t-cell lymphomas 2	0.43	0.45	0.48
REGULATION OF TRANSCRIPTION			
ZNF367, zinc finger protein 367	0.24	0.29	0.35
SETD2, huntingtin interacting protein b	0.30	0.24	0.35
HOXC5, homeobox C5	0.31	0.35	0.32
BHLHB5, basic helix-loop-helix domain containing, class b, 5	0.32	0.37	0.33
KIAA2018	0.47	0.36	0.29
ZHX2, zinc fingers and homeoboxes 2	0.35	0.44	0.35
MED16, thyroid hormone receptor associated protein 5	0.40	0.32	0.43
PSPC1, paraspeckly component 1	0.40	0.31	0.50
GLIS2, glis family zinc finger 2	0.44	0.42	0.41
ARID1A, at rich interactive domain 1a	0.45	0.48	0.47

of the differentially expressed genes, indicating that exposure to EC secretions is responsible for differential expression of these genes. Functional grouping using DAVID revealed that monocyte exposure to EC secretions causes up-regulation of genes involved in a number of biological processes including the immune response, cellular component organization, and signal transduction (Table 8). Of particular interest is up-regulation of CCL2, CCL7, TLR4, IL19, and CXCR5 which are all cytokines or cytokine receptors that may be involved in further leukocyte recruitment and activation. Exposure to EC secretions causes down-regulation of genes involved in intracellular signaling and transcription (Table 9).

Effects of Monocyte-Endothelial Contact

In our system both transmigrated monocytes (Figure 8 "TM") and monocytes that failed to transmigrate (Figure 8 "UMA") had contact with ECs, while monocytes placed beneath ECs (Figure 8 "UMB") and untreated monocytes (Figure 8 "UNT") had no EC contact. Sixty-one genes were differentially expressed in monocytes that contacted ECs as compared to untreated monocytes (Supplemental Table 6). Of these 61 genes, 34 are up-regulated and 27 are down-regulated. Signal transduction and the immune response are some of the functional groups associated with genes up-regulated by monocyte endothelial cell-contact (Table 10). Lipid metabolism is one of the functional groups associated with the down-regulated genes (Table 10).

Table 10: Functional groups associated with genes differentially expressed by monocyte/EC contact.

SIGNAL TRANSDUCTION	**FOLD CHANGE** (TM/UNT)	(UMA/UNT)
GBG10, guanine nucleotide binding protein, gamma 10	5.6	3.0
MCTP2, multiple c2 domains, transmembrane 2	5.0	3.5
SUCNR1, succinate receptor 1	2.4	3.5
CCR1, chemokine (c-c motif) receptor 1	2.6	2.5
FPRL1, formyl peptide receptor-like 1	2.5	2.6
IL4R, interleukin 4 receptor	2.5	2.4
LITAF, lipopolysaccharide-induced tnf factor	2.7	2.0
PBEF, pre-b-cell colony enhancing factor 1	2.3	2.1
IMMUNE RESPONSE		
CCR1, chemokine (c-c motif) receptor 1	2.6	2.5
IL4R, interleukin 4 receptor	2.5	2.4
CLEC4D	2.4	2.0
LIPID METABOLISM		
PLA2G3, phospholipase a2, group iii	0.49	0.48
ST3GAL6, st3 beta-galactoside alpha-2,3-sialyltransferase 6	0.41	0.48
PLA2G4A, phospholipase a2, group iva	0.17	0.23

Effects of Diapedesis

In our system the only sample which went through diapedesis was transmigrated monocytes (Figure 8 "TM"). Comparing transmigrated monocytes to all of the other conditions provides information about how the process of diapedesis alters monocyte transcription. The Venn diagram in Figure 12 indicates that when transmigrated monocytes are compared to untreated monocytes, monocytes which failed to transmigrate, and monocytes incubated beneath stimulated endothelial cells there are 89 differentially expressed genes which are found to overlap in all of these lists. Eighty of these genes were up-regulated while only nine were down-regulated (Supplemental Table 7). Functional grouping of these genes shows up-regulation of genes involved in cell differentiation and down-regulation of anti-microbial proteins (Table 11).

Anti-Microbial Proteins

Of the nine genes down-regulated by diapedesis, four of these are anti-microbial genes which are involved in non-oxidative killing of bacteria. These genes include defensin alpha 3 (DEFA3), cathelicidin anti-microbial peptide (CAMP), lactoferrin (LTF), and cathepsin G (CTSG). DEFA3, CAMP, and CTSG, are all peptides which have molecular weights of less than 30 kDa. Lactoferrin is a larger iron binding protein with a molecular weight of 78 kDa. qRT-PCR confirmed down-regulation of these genes as shown in Table 7. Of these four anti-microbial genes, DEFA3 was the most down-regulated with a change of approximately 50 fold.

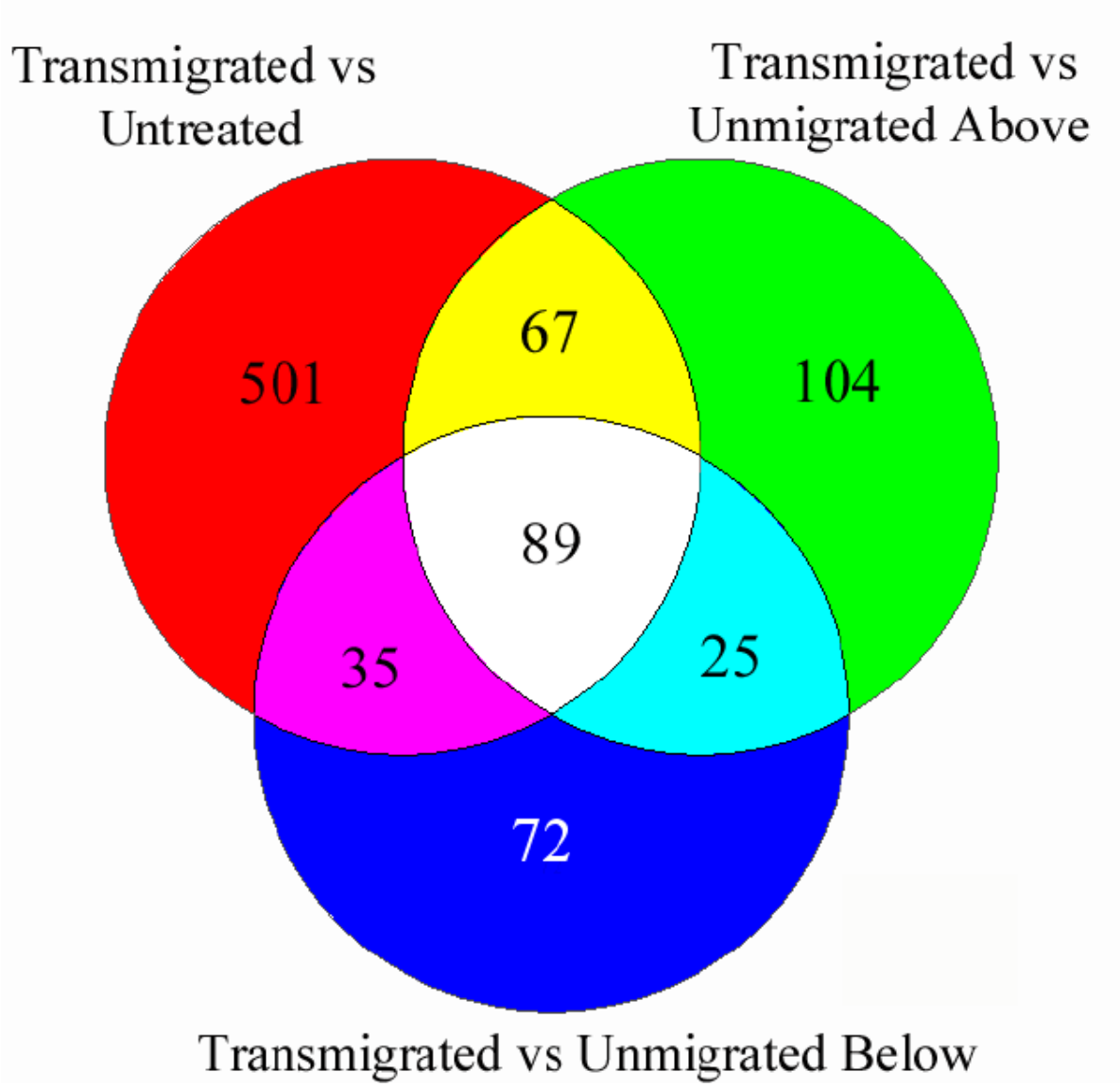

Figure 12: Monocyte transmigration induces differential gene expression in comparison to untreated monocytes, monocytes that failed to transmigrate (Unmigrated Above), or monocytes incubated below stimulated ECs (Unmigrated Below).
This Venn diagram of genes that are differentially expressed in transmigrated cells as compared to other treatment conditions shows the overlapping genes in each of the comparisons. The 89 genes in the center of this Venn diagram are differentially expressed in transmigrated monocytes as compared to all of the other conditions. The primary difference between transmigrated monocytes and the other three monocyte populations is that transmigrated monocytes have gone through the process of diapedesis. This indicates that expression of these 89 genes is likely to be controlled by diapedesis.

Table 11: Functional groups associated with genes differentially expressed by diapedesis.

CELL DIFFERENTIATION	**FOLD CHANGE** (TM/UNT)
DICER1, dcr-1 homolog	4.8
PMCH, pro-melanin-concentrating hormone	4.2
TNFRSF10D, tumor necrosis factor receptor superfamily, member 10d	3.8
ERBB4, v-erv-a erythroblastic leukemia viral oncogene homolog 4	3.8
GLDN, gliomedin	3.5
RTN4RL1, reticulon 4 receptor-like 1	3.4
HLA-DOA, major histocompatibility complex, class ii, do alpha	2.1
SIGNAL TRANSDUCTION	
FCGR2B, fc fragment of igg, low affinity iib, receptor	6.4
CD59, CD59 antigen, complement regulatory protein	4.8
PMCH, pro-melanin-concentrating hormone	4.2
RBJ, ras-associated protein rap1	3.9
TNFRSF10D, tumor necrosis factor receptor superfamily, member 10d	3.8
ERBB4, v-erv-a erythroblastic leukemia viral oncogene homolog 4	3.8
GPR112, g protein-coupled receptor 112	3.7
IL1RAP, interleukin-1 receptor accessory protein	3.6
RASA2, ras p21 protein activator 2	3.3
ADCY2, adenylate cyclase 2	2.1
TRIM38, tripartite motif-containing 38	3.2
MUSK, muscle, skeletal, receptor tyrosine kinase	2.7
FGD4, five, rhogef and ph domain containing 4	2.3
DEFENSE RESPONSE	
DEFA3, defensin, alpha 3	0.02
CAMP, cathelicidin antimicrobial peptide	0.11
LTF, lactotransferrin	0.21
CTSG, cathepsin G	0.38

α-defensin Protein Expression

Because DEFA3 is the most down-regulated gene on the microarray, immunoblots were used to assess protein expression of DEFA3 and β-actin in each of the monocyte treatment conditions. Representative immunoblots are shown in Figure 13A. As with mRNA expression, protein expression of DEFA3 is decreased following transmigration and increased in monocytes which failed to transmigrate. Protein expression from 5 separate experiments was quantified and normalized to β-actin expression (Figure 13B). This reveals ~4.5 fold up-regulation of α-defensin expression in monocytes which failed to transmigrate as compared to untreated monocytes and ~2 fold down-regulation of α-defensin expression in transmigrated monocytes.

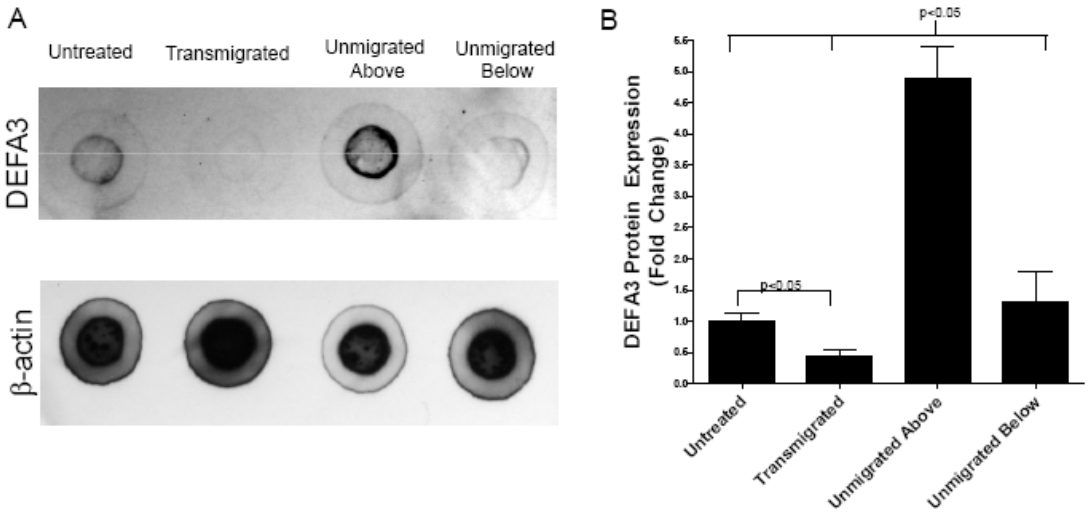

Figure 13: α-defensin protein expression is decreased in transmigrated monocytes and increased in monocytes which failed to transmigrate (unmigrated above) as assessed by immunoblots.
(A) Representative α-defensin and β-actin immunoblots. (B) Quantitation of α-defensin protein expression normalized to β-actin expression followed by normalization to expression in untreated monocytes. Bars represent mean expression +/- SEM for 5 experiments. *p<0.05

Discussion

We found differential expression of 692 genes following monocyte transmigration across activated ECs. These differentially expressed genes indicate that transmigration induces transcription of cytokines, cytokine receptors, cell signaling genes, and genes which inhibit apoptosis (Figure 14A). All of these findings indicate that transmigration induces a monocyte phenotype that is primed for response to extracellular cues which alter downstream functions of monocytes. Our microarray data also indicated that a number of genes involved in the inhibition of apoptosis are up-regulated following transmigration. Inhibition of apoptosis in transmigrated monocytes is supported by previous studies in neutrophils which have found decreased apoptosis following transmigration [85,86]. Regulation of apoptosis is important for monocytes to prevent premature cell death and to allow monocytes to differentiate into macrophages and dendritic cells. Our microarray data is supported by functional assays revealing reduced apoptosis in transmigrated monocytes and by qRT-PCR confirming up-regulation of NAIP, an inhibitor of apoptosis, following transmigration. We have interpreted this data to indicate that the process of transmigration leads to reduced apoptosis in monocytes. Another possibility is that apoptotic monocytes do not transmigrate as efficiently as non-apoptotic monocytes. However, if this were true, we would expect to see an increase in apoptosis positive cells in the monocyte population which failed to transmigrate. Examination of Figure 11E reveals that the monocytes which failed to transmigrate (unmigrated above) do not have increased levels of apoptosis, thus making it unlikely that early apoptotic monocytes have reduced transmigration efficiency.

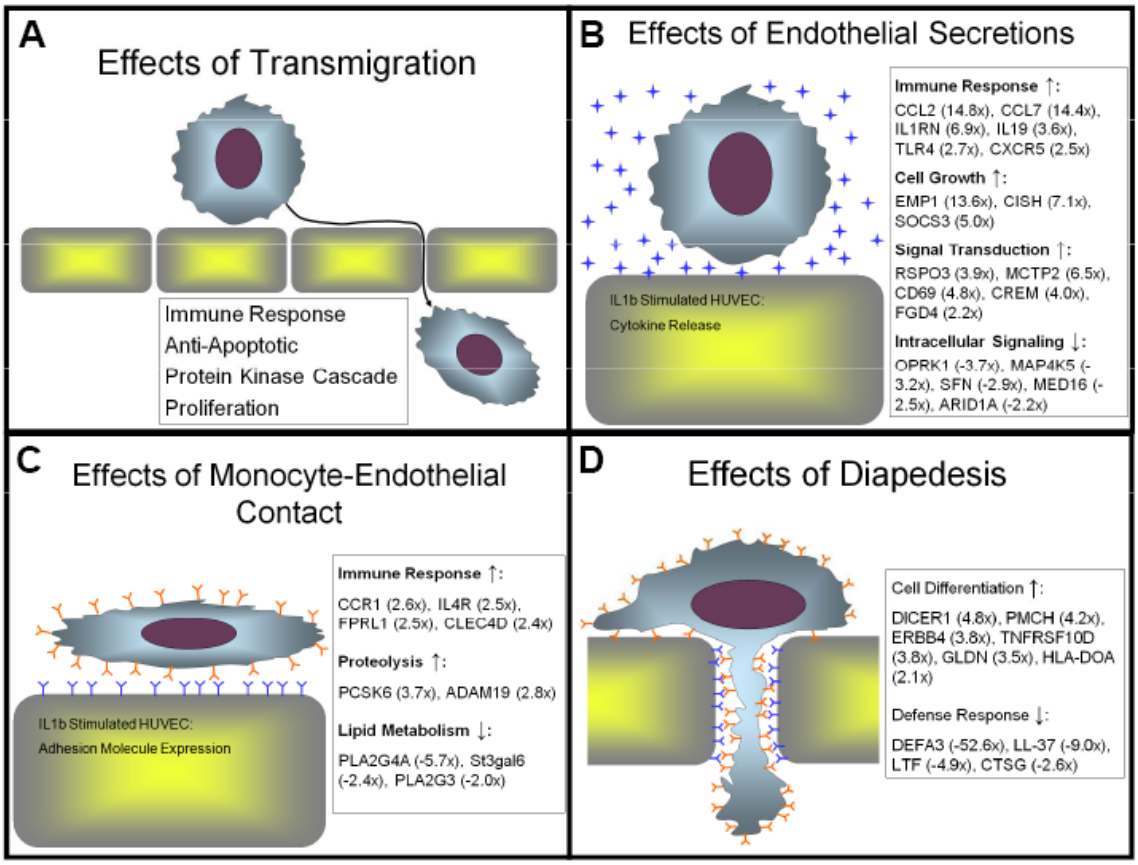

Figure 14: Transmigration alters monocyte gene expression throughout the entire process. (A) Overall effects of monocyte transmigration. (B) Transcriptional effects of monocyte exposure to secretions derived from IL1β stimulated ECs. These genes showed differential expression in monocytes incubated below stimulated ECs, in monocytes which failed to transmigrate, and in transmigrated monocytes as compared to untreated monocytes. (C) Transcriptional effects of monocyte-EC contact. These genes were differentially expressed in monocytes which failed to transmigrate and in transmigrated monocytes as compared to untreated monocytes. (D) Transcriptional effects of diapedesis. These genes were differentially expressed in transmigrated monocytes as compared to untreated monocytes, monocytes which failed to transmigrated, and monocytes incubated below stimulated ECs. Only a portion of the differentially expressed genes for each of the steps of transmigration are shown in this diagram. Genes were chosen for display based on their inclusion in over-represented functional groups. Full lists of differentially expressed genes for each step of transmigration can be found in the supplemental tables. Fold changes listed represent the average fold change for each of the monocyte populations considered as compared to untreated monocytes.

We have also shown that monocyte transcription is affected by each of the steps of transmigration. Monocyte exposure to endothelial secretions leads to increased expression of genes involved in the immune response (Figure 14B). The two most highly up-regulated genes in this study, CCL2 and CCL7, are both chemokines which may promote further recruitment of monocytes. Previous studies have shown that monocyte coculture with naive ECs causes increased expression of CCL2 [87,88]. Takahashi et al. showed that monocytes which failed to adhere to naïve ECs did not show increases in CCL2 staining, leading to the conclusion that monocyte-EC contact induces CCL2 up-regulation. In our study of monocyte interaction with stimulated ECs, similar levels of CCL2 up-regulation were seen in monocytes that had directly contacted the ECs and in monocytes incubated beneath the ECs. This indicates that there are at least two distinct mechanisms responsible for regulating CCL2 expression in monocytes incubated with either naïve or IL1β-stimulated ECs.

Both CCL2 and CCL7 belong to the immune system response functional group (Table 8). Up-regulation of genes within this group may be mediated by a number of cytokines secreted by IL1β-stimulated ECs, including IL6 and fractalkine [80,89,90]. Except for interleukin receptor antagonist (IL1RN), increased expression of each of these genes would lead to increased accumulation of monocytes and other leukocytes within the tissue space during the acute cellular response phase of inflammation. Up-regulation of IL1RN, which inhibits the cellular response to IL1β, may provide a mechanism for limiting long term monocyte recruitment to sites of inflammation [91]. In addition to the immune system response, EC secretions induced expression of genes involved in cellular

component organization and signal transduction. EC secretions also down-regulated signal transduction genes and genes involved in the regulation of transcription (Table 9).

Monocyte-endothelial contact leads to up-regulation of genes involved in signal transduction and the immune response (Figure 14C). Among these genes, increased expression of cytokines and cytokine receptors such as chemokine (C-C motif) receptor 1 [92], formyl peptide receptor-like 1 [93], and pre-B-cell colony enhancing factor [94] may enhance monocyte recruitment to sites of inflammation (Table 10). Monocyte-endothelial contact led to decreased expression of genes involved in lipid metabolism. In particular, both phospholipase A2, group 3 (PLA2G3) and phospholipase A2, group 4A (PLA2G4A), enzymes involved in production of arachidonic acid, were downregulated by monocyte-EC contact. Mishra et al. recently showed that knockdown of PLA2G4A expression leads to a reduction in the rate of monocyte chemotaxis towards CCL2 [95]. Down-regulation of these genes may play an important role in regulating monocyte transmigration and preventing long term monocyte accumulation within sites of inflammation.

Diapedesis induces expression of a number of genes involved in cell differentiation (Figure 14D). We initially hypothesized that monocyte transmigration might drive differentiation towards a macrophage or dendritic cell phenotype. However, in our study genes that are up-regulated by diapedesis and related to cell differentiation are not specific to monocyte differentiation. Recently, Lehtonenen et al. examined the gene expression of monocytes during the late and early stages of macrophage and dendritic

cell differentiation [96]. Comparison of our microarray data to genes differentially expressed in that study reveals that less than five percent of the genes differentially expressed in early macrophage or dendritic cell differentiation were differentially expressed in transmigrated monocytes. None of the common cell surface markers for macrophages (CD14, FcgR1A, CD163) or dendritic cells (CD1a, CD1e, FceR1A/R2, CD1c, CD1b, LY75, CD209) were up-regulated at the mRNA level in our study, while Lehtonen et al. saw up-regulation of mRNA expression for all of these genes at late stages of macrophage and dendritic cell differentiation. These data indicate that additional stimulation beyond transmigration is required for monocyte differentiation into macrophage or dendritic cell phenotypes. This finding is supported by the seminal study of Randolph et al. which examined monocyte differentiation into dendritic cells after a 48 hour incubation period in which monocytes transmigrated and then reverse-transmigrated back to the apical side of ECs grown on a collagen matrix [97]. This work showed that monocyte reverse-transmigration initiates differentiation of monocytes to dendritic cells; but, further stimulation is required for full differentiation to a mature dendritic cell phenotype. In our study differentially regulated genes which are involved in cell differentiation may play an important role in mediating longer term monocyte differentiation in response to transmigration and other extracellular stimuli.

Interestingly, our microarray data revealed that diapedesis leads to down-regulation of anti-microbial proteins (DEFA3, CAMP, CTSG, LTF). These anti-microbial proteins act as an important non-oxidative mechanism of bacterial killing in phagocytic cells [98]. qRT-PCR confirmed our microarray results for each of these proteins. Immunoblots of α-

defensin expression were used to confirm that down-regulation of these genes extends to the protein level. In addition to bacterial killing, anti-microbial proteins have a number of inflammatory effects such as increased leukocyte chemotaxis [99], increased LDL accumulation within the endothelium and interference with vascular smooth muscle cell function [100]. Thus, it is possible that down-regulation of these proteins following transmigration may occur as a cytoprotective effect in order to maintain endothelial homeostasis and limit monocyte recruitment.

Another possible interpretation of our data is that the monocytes which have higher expression levels of anti-microbial proteins are less efficient in transmigrating. In our experimental setup it is impossible to rule out the possibility that the transmigrated monocytes represent a distinct population of monocytes which have an increased capacity for transmigration. However, if so, this population would represent a previously undescribed phenotype comprising approximately 25% of monocytes, a large proportion compared with the largest known subpopulation, CD16+, which represent only 13 percent of all human monocytes[101]. Thus, it is our opinion that a more likely explanation is that diapedesis and monocyte-EC contact cause the observed changes in gene and protein expression rather than separation of high and low anti-microbial-expressing monocytes based on transmigration.

In this study we have shown that freshly isolated human monocytes have decreased levels of apoptosis following transmigration across stimulated ECs. We have also examined the effects of monocyte exposure to EC secretions, monocyte-EC contact, and diapedesis.

This data indicates that monocytes respond to EC secretions with increased production of cytokines, and other inflammatory genes. Monocyte-EC contact also impacted inflammatory gene expression with increased expression of cytokines and cytokine receptors. Finally, diapedesis led to differential expression of genes involved in cell differentiation and bacterial killing. These changes in monocyte gene expression likely serve to prime monocytes for further downstream functions and differentiation outside the bloodstream. Additionally, many of the differentially expressed genes play a role in either mediating or resolving inflammation. Because numerous pathologies, such as arthritis and atherosclerosis, result from chronic inflammation, it is especially important that in monocyte transmigration a careful balance is maintained between inflammatory response and resolution.

CHAPTER 4: REVERSING SHEAR STRESS PROMOTES A MORE INFLAMMATORY AND PROLIFERATIVE PHENOTYPE IN ENDOTHELIAL CELLS THAN STEADY SHEAR STRESS

N.B. Work in this chapter was generated as a joint project with Daniel Conway, a fellow graduate student in the McIntire Lab. I was responsible for the microarray analysis and participated jointly with Daniel in the design of the reversing shear stress system and performance of the monocyte adhesion assay. Daniel performed the flow validation, shear stress experiments, and BrdU cell proliferation assays.

Atherosclerosis is typically localized to the carotid artery sinus, the coronary arteries, the abdominal aorta, and the superficial femoral arteries [102]. These regions have complex blood flow patterns which include flow reversal during each cardiac cycle, leading to the hypothesis that disturbed hemodynamic patterns are atherogenic. Such differences in hemodynamics alter the gene expression profile and ultimately the structure and function of endothelial cells, resulting in modulation of both endothelial cell responses to blood borne factors and endothelial cell interactions with underlying smooth muscle cells, thus increasing the likelihood of atherogenesis [103,104].

Some of the earliest studies comparing "anti-atherogenic" *non-reversing* arterial shear stress to "pro-atherogenic" *reversing* arterial shear stress modeled the reversing shear stress in the form of a sine wave. However, simulations of the wall shear stress of the carotid sinus have shown the wall shear stress is not harmonic, but is a more complex waveform [27,105]. This waveform has a low average shear stress of ~1 dyne/cm^2 with peak

shear stresses as high as +/- 11 dyne/cm^2. Previous studies used high steady shear stress and static conditions as controls for comparison to the proatherogenic waveform [25,27,106]. These studies did not address whether the low average shear stress or the flow reversal found at the wall of the carotid sinus was responsible for observed increases in atherogenesis.

To address the limitations of previous studies, we developed a parallel plate reversing flow system that accurately recreates the physiological form of the reversing shear stress at the carotid sinus wall. Using human umbilical vein endothelial cells, we compared the effects of this shear profile to the effects of steady arterial shear stress (15 dynes/cm^2). Based on our previous work showing few differences between non-reversing pulsatile and steady shear stress [26,107], we chose a steady shear stress of 15 dynes/cm^2 to approximate shear stress in the arteries. We also included a steady low shear stress control (1 dyne/cm^2) to distinguish gene and functional changes that were due to the application of a low average shear stress. Functional analysis confirmed previous findings that reversing shear stress increases cell proliferation and monocyte adhesion; increased cell proliferation was found to be dependent on low average shear stress whereas monocyte adhesion was found to be dependent on fluid reversal. Microarray results indicate that although there are unique sets of genes controlled by both low average shear stress and by reversing flow, more genes were controlled by low average shear stress. We propose that low-time average shear stress, and not fluid reversal/oscillation, may be the more significant mechanical force on endothelial cells.

Materials and Methods

Reversing Shear Stress System Design and Validation

The shear stress profile used in this study (Figure 15) was based on a computer simulation of the wall shear stresses at the carotid bifurcation (time-average 1 dyne/cm^2, maximum +11 dynes/cm^2, minimum -11 dynes/cm^2, 1 Hz) [105]. A custom flow system was designed to reproduce this waveform in a parallel plate flow system (Figure 16). The flow profile was split into two separate waveforms: the steady component of the waveform (-1 dyne/cm^2) and the reversing component of the waveform which had a time-averaged shear stress of 0 dynes/cm^2. A standard syringe pump (Harvard Apparatus 33 Twin Syringe Pump) was used to apply the continuous shear stress component. A 1 mL glass syringe (Becton Dickinson) was mounted to a linear motor (MX80L, Parker Motion). The linear motor controller (ACR9000, Parker Motion) was programmed to deliver the reversing flow component.

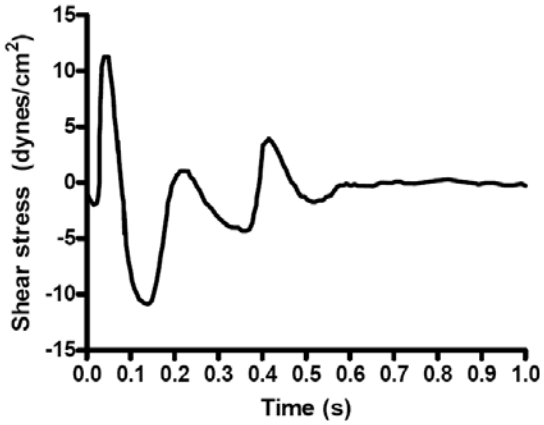

Figure 15: Wall shear stress of the carotid sinus used in the reversing flow system.
A previously published computer simulation[105] of the wall shear stress at the carotid sinus. This shear stress profile was modeled in the reversing flow system.

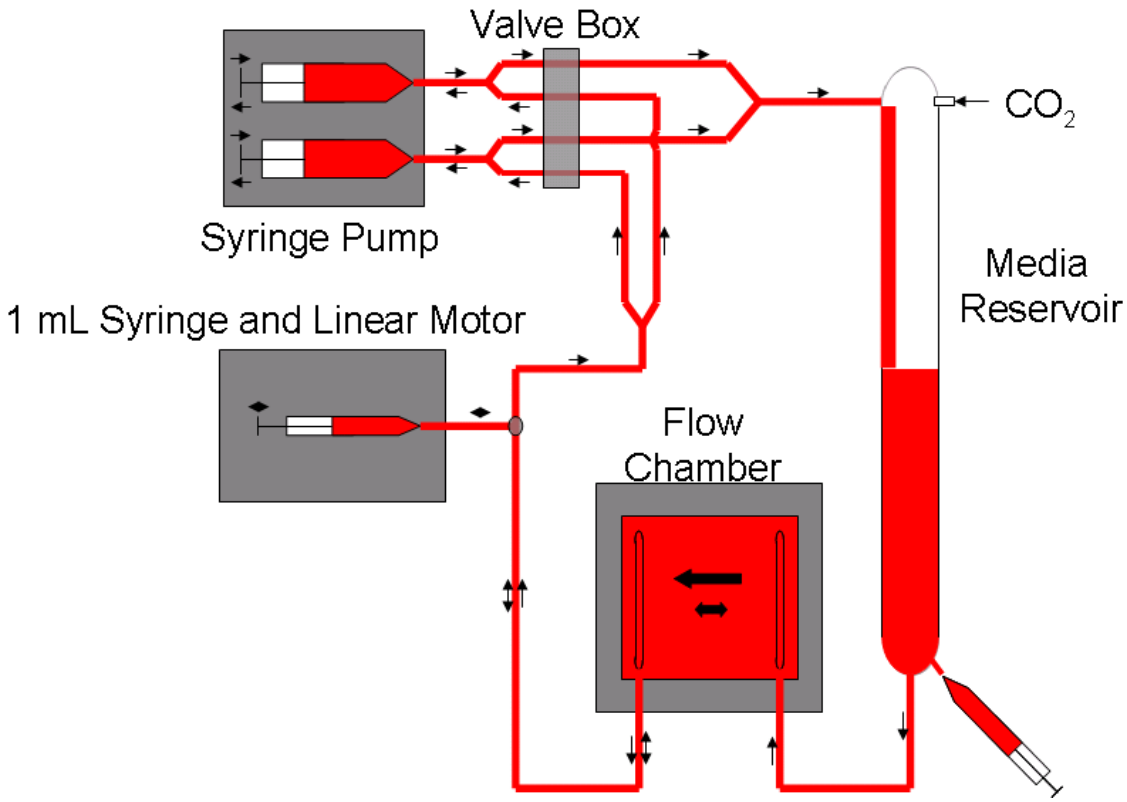

Figure 16: Schematic of the reversing flow system.

To validate the reversing flow system, latex beads (6 μm, Bangs Laboratory) were tracked (Metamorph, Molecular Devices) under high-speed video microscopy (1000 frames per second, (Phantom V4.2, Vision Research) to directly measure the flow rate through the chamber. The focal plane of the microscope was selected to be the center of the parallel plate flow chamber and the velocity of the beads was assumed to represent the maximum velocity through the chamber. Wall shear stress was calculated using Equation 1 (the average velocity was assumed to be two-thirds of the maximal velocity (V_{max}), b is the height of the flow chamber, and μ is the viscosity of the media):

$$\tau = \frac{4V_{max}\mu}{b} \quad \text{Equation 1}$$

The full derivation of Equation 1 is in Appendix A.

Experimental Protocol

HUVEC (passages 3-5) were grown to confluence on glass slides [26], mounted on a parallel plate flow chamber, and exposed to one of four conditions for 24 hours: reversing flow using the newly designed system (RF, 1 dyne/cm^2 +/- 11 dyne/cm^2), arterial high steady shear stress (HSS, 15 dynes/cm^2), low steady shear stress (LSS, 1 dyne/cm^2), and static treatment. RNA and protein were isolated using TRIzol. Microarray analysis was performed on RNA samples (Whole Human Genome arrays, Agilent).

RNA and protein isolation

Immediately after exposure to shear stress total RNA and protein were extracted using TRI-zol (Invitrogen); RNA was further purified with DNase (Qiagen) and RNeasy MinElute Cleanup Kit (Qiagen), according to manufacturers' instructions. The integrity and quantity of the RNA were verified with UV spectrophotometry, accepting only RNA with a 260/280 ratio greater than 1.9. Protein concentration was quantified with DC Protein Assay (Bio-Rad) using bovine serum albumin standards.

Microarray processing

Microarray hybridization and imaging were performed at the Morehouse School of Medicine Functional Genomics Core Facility. Briefly, RNA was linearly amplified to cRNA using Cy3 labeled CTP and a Low RNA Input Fluorescent Linear Amplification Kit (Agilent) according to the manufacturer's instructions. Cy3-labeled cRNA for each sample was hybridized to a 44k Whole Human Genome Microarray (Agilent) according

to the manufacturer's instructions. Slides were dried under nitrogen and scanned on an Agilent DNA Microarray Scanner.

Microarray analysis

Microarray images were analyzed with Agilent Feature Extraction Software according to the manufacturer's instructions. Genes were flagged as either present, marginal, or absent based on criteria such as image saturation, uniformity, population outlier, and uniformity of background. GeneSpring GX 10 software was used to further analyze the microarray data. One way ANOVA assuming equal variances was applied followed by a post-hoc Student-Neuman-Keuls test with a false discovery rate of 5%. Differentially expressed genes were identified as those genes having adjusted p-values of less than 0.05 and flags marked as present or marginal in at least 50% of the samples for conditions with fold changes of at least 1.5 fold.

qRT-PCR

Total RNA from each sample was reverse transcribed into cDNA using SuperScript II (Invitrogen). cDNA was purified with Micro Bio-Spin P-30 Chromatography Columns (BioRad), and diluted in RT-PCR Grade Water (Ambion). Pre-designed PCR primers and Quantitect SYBR Green PCR Master Mix were purchased from Qiagen. Primers were added to the master mix at a ratio of 1:5. Each reaction was performed with 4 µl of diluted cDNA and 6 µl of primers in the master mix. The qRT-PCR reactions were performed on a MyIQ (BioRad) with a 15 minute activation step at 95 ^{o}C; 50 cycles at 94 ^{o}C for 15 seconds, 55 ^{o}C for 30 seconds, 72 ^{o}C for 30 seconds; and a ramped melting

cycle. Fold changes were determined using the ΔΔCt method. qRT-PCR was used to verify gene expression from RNA isolated from five independent experiments.

Cell Proliferation Assays

To measure changes in cell proliferation, shear stress experiments were performed in the presence of 10 μM bromodeoxyuridine (BrdU) (EMD Biosciences). Cells were fixed in 4% paraformaldehyde, treated with 2N HCl and 0.1% Triton-X, stained using a rat anti-BrdU antibody (Abcam), and finally stained with goat anti-rat Alexa Fluor 563 (Invitrogen) and Hoechst (Invitrogen). Standard fluorescent microscopy was used to image the cells. ImageJ (NIH) was used to count BrdU stained cells and Hoechst stained cells in each frame. For each experimental condition 8 frames were analyzed for each experimental replicate with a total of 5 replicates. The percentage of cells that divided under shear stress was determined by dividing the BrdU positive cells by the total number of cells as measured by the Hoechst staining.

Monocyte Adhesion Assays

Monocyte adhesion assays were performed on HUVEC pretreated for 24 hours with one of the four shear stress conditions. Cell tracker orange stained THP-1 (Human acute monocytic leukemia cell line) cells (10^6 cells/mL) were perfused across the pretreated HUVEC at 1 dyne/cm^2 for 5 minutes, stopping the flow for 30 seconds, and rinsing with media for an additional 5 minutes. The number of adherent cells was then counted in ten frames for each replicate.

Results

System Validation

High-speed video tracking of latex beads through the parallel plate chamber allowed for measurement of the average flow rate and the calculation of the wall shear stress in the chamber. Figure 17 provides a visual comparison of the wall shear stress within our parallel plate flow chamber to the in vivo shear stress at the wall of the carotid sinus as determined by computer simulations performed by Perktold and Rappitsch[105]. This comparison shows that our system accurately recreates the in vivo reversing shear stress found at the wall of the carotid sinus. Because this area of the vasculature is particularly prone to atherosclerosis, validation of our system's ability to model flow within the carotid sinus indicates that our system is appropriate for studying the effects of this altered flow type on endothelial cells.

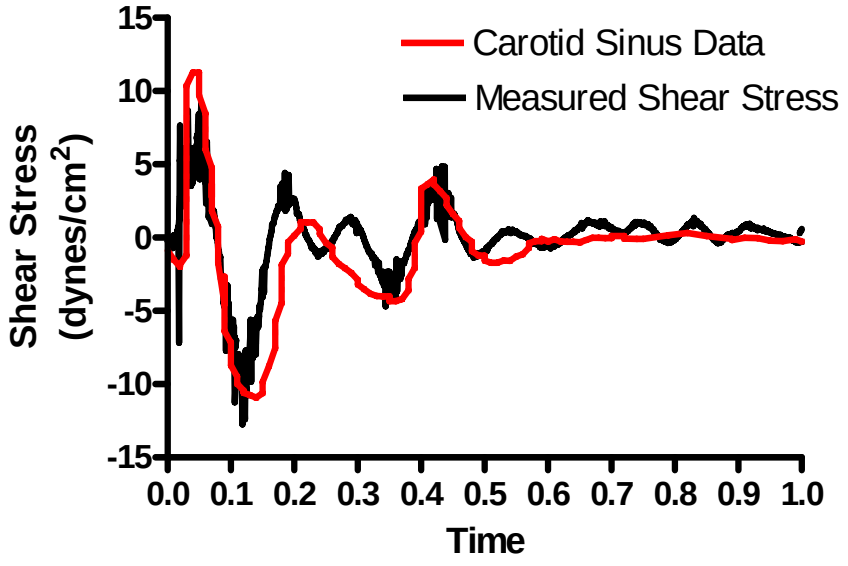

Figure 17: Comparison of in vitro parallel plate shear stress to in vivo shear stress.
In vitro parallel plate shear stress was estimated by tracking latex beads within the flow chamber using high speed video microscopy. In vivo shear stress was estimated by Perktold and Rappitsch using computer simulations of fluid flow within the carotid sinus.

Cellular Morphology

ECs treated with steady shear stress of 15 dyne/cm^2 for 24 hours aligned parallel to the flow direction (Figure 18). ECs exposed to 1 dyne/cm^2 were randomly aligned and slightly elongated in comparison to static conditions. Under reversing flow, the cells exhibited a cobblestone morphology which is quite similar to that seen under static conditions.

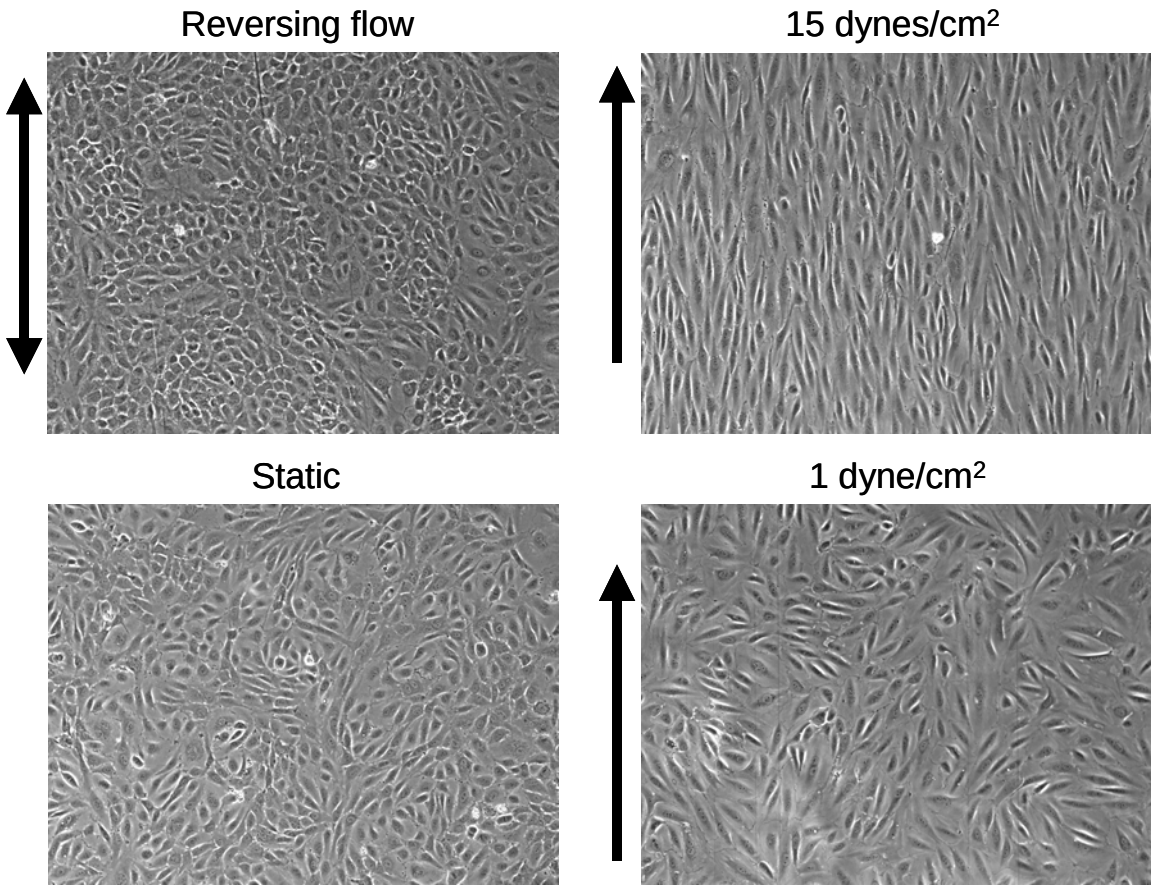

Figure 18: Variations in fluid flow patterns cause altered EC morphology.
Phase contrast images of ECs exposed to 15 dynes/cm^2 shear stress for 24 h reveal an elongated morphology which is aligned with shear stress. ECs exposed to 1 dyne/cm^2 have an elongated morphology but do not align with shear stress. ECs exposed to reversing flow exhibit a cobblestone like morphology that is very similar to the morphology of cells grown under static conditions.

Microarray Results

A comparison of HUVEC exposed to 24 hours of reversing flow (RF), high steady shear (HSS), low steady shear (LSS), and static culture (STAT) was performed with a whole human genome microarray. One way ANOVA with a false discovery rate of 5% revealed 4767 genes with statistically significant differences between at least two of the treatment conditions. A post hoc Student-Newman-Keuls test was performed to determine which conditions were significantly different from each other for each gene. Differentially expressed genes were identified as those that passed the Student-Newman-Keuls test and had flags present or marginal in at least 50% of the samples for conditions having greater than 1.5 fold changes in expression between at least two of the four HUVEC treatment conditions. A total of 4017 differentially expressed genes were identified. Table 12 contains the number of differentially expressed genes between each condition. (See Supplemental Table 8 for lists of gene names and fold changes associated with each of these comparisons.)

Table 12: Number of Differentially Expressed Genes Between Conditions

	Static	HSS	LSS
HSS	3,026	--	--
LSS	2,998	194	--
RF	3,102	365	57

ECs exposed to fluid flow differentially expressed ~3000 genes as compared to ECs exposed to static conditions. This high number of differentially expressed genes compared to static was independent of the type of fluid flow that ECs were exposed to. On the other hand, a comparison of gene expression between fluid flow types revealed

that the largest number of differentially expressed genes can be found in a comparison of reversing flow to high shear stress, with 365 differentially expressed genes. When reversing flow was compared to low shear stress, less than 100 genes were found to be differentially expressed.

Differentially expressed genes for each of the 3 flow conditions compared to static are shown on the proportional Venn diagram in Figure 19 [108]. 57 % of the total number of genes found in these three comparisons are differentially expressed in all of the shear stress conditions. Further examination of these genes shows that there is 100% agreement for all of the flow conditions in the direction of differential expression as compared to static. This indicates that exposure to shear stress determines whether these genes will be up- or down-regulated as compared to the static condition. Thus, the type of shear stress that ECs are exposed to regulates the value of the fold change rather than the direction of the fold change that occurs when comparing gene expression in shear stress conditions to static conditions. Table 13 contains a list of twenty genes which are most up- and down-regulated by fluid flow as compared to static.

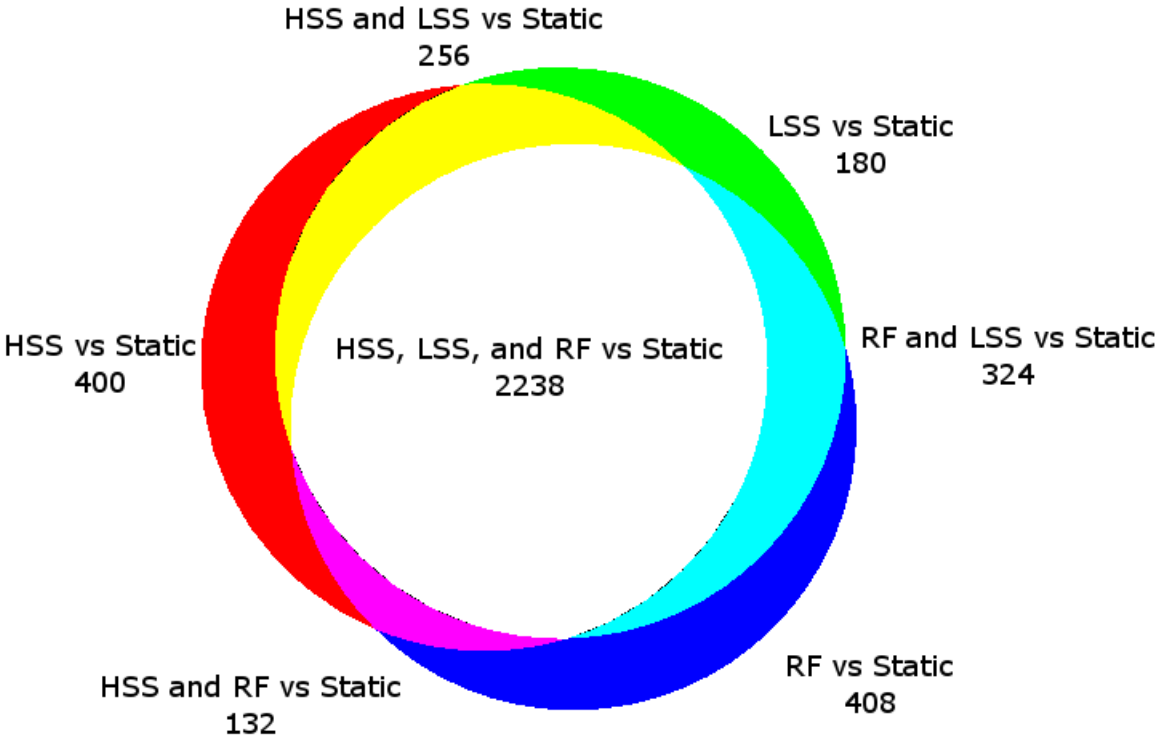

Figure 19: Proportional Venn diagram of differentially expressed genes in a comparison of RF, HSS, and LSS to static culture.
Genes found within the white area of the Venn diagram are differentially expressed by all three fluid flow types as compared to static culture.

Table 13: Top 10 Genes Up- and Down-Regulated by Fluid Flow

Gene Symbol	Gene Name	Average Fold Change* (Flow vs Static)
GPR83	G protein-coupled receptor 83	57.2
CYP1B1	Cytochrome P450, family 1, subfamily B, polypeptide 1	54.1
KCNK3	Potassium channel, subfamily K, member 3	39.8
IL11	Interleukin-11	22.4
ID2	Inhibitor of DNA binding 2	20.8
FREM3	FRAS1 related extracellular maxtrix 3	20.6
GLI2	GLI-Kruppel family member 2	18.3
SAMD11	Sterile alpha motif domain containing 11	17.8
AKR1C1	Aldo-keto reductase family member 1C	16.9
SMAD7	SMAD family member 7	16.6
CD34	CD34 molecule	-32.7
XLKD1	Extracellular link domain containing 1	-38.0
PPP1R9A	Protein phosphatase 1 regulatory subunit 9A	-42.0
PRND	Prion protein 2	-50.3
CHRNA1	Cholinergic receptor nicotinic alpha 1	-50.5
DHRS3	Dehydrogenase/reductase (SDRfamily) member 3	-62.4
CYP26B1	Cytochrome P450, family 26, subfamily B, polypeptide 1	-68.0
KIT	v-kit Hardy Zuckerman 4 feline sarcoma viral oncogene homolog	-76.0
MYO5C	Myosin VC	-89.9
C10Orf10	Chromosome 10 Open reading frame 10	-143.1

*Fold changes represent the average of the average fold change in comparison to static for reversing flow, high shear stress, and low shear stress.

Hierarchical clustering applied to the four EC culture conditions provides further evidence that the largest differences in gene expression are seen between ECs exposed to fluid flow of any type and ECs grown under static conditions. Figure 20 reveals that HSS, LSS, and RF cluster on a branch separate from static culture. From there HSS and LSS cluster separately from RF, indicating that ECs exposed to high shear stress or low shear stress are more similar to each other in terms of gene expression than ECs exposed to reversing flow.

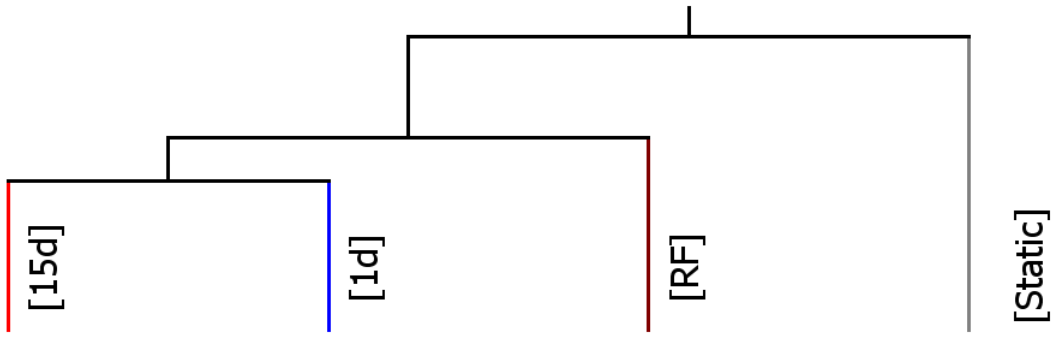

Figure 20: ECs exposed to fluid flow cluster on a branch separate from ECs grown in static culture.

In Table 12, the greatest number of differentially expressed genes is found in a comparison of RF and HSS, with 365 differentially expressed genes. Comparison of HSS to LSS showed 194 genes were differentially expressed, while only 57 genes were differentially expressed when RF and LSS were compared. These differences in the number of differentially expressed genes are indicative of the large changes in EC phenotype that can be found between ECs growing on the wall of the carotid sinus and ECs located in other regions of the vasculature which do not experience blood flow disturbances caused by curvature of the vessels or branching. The Venn diagram shown in Figure 21 depicts the overlap among these three comparisons.

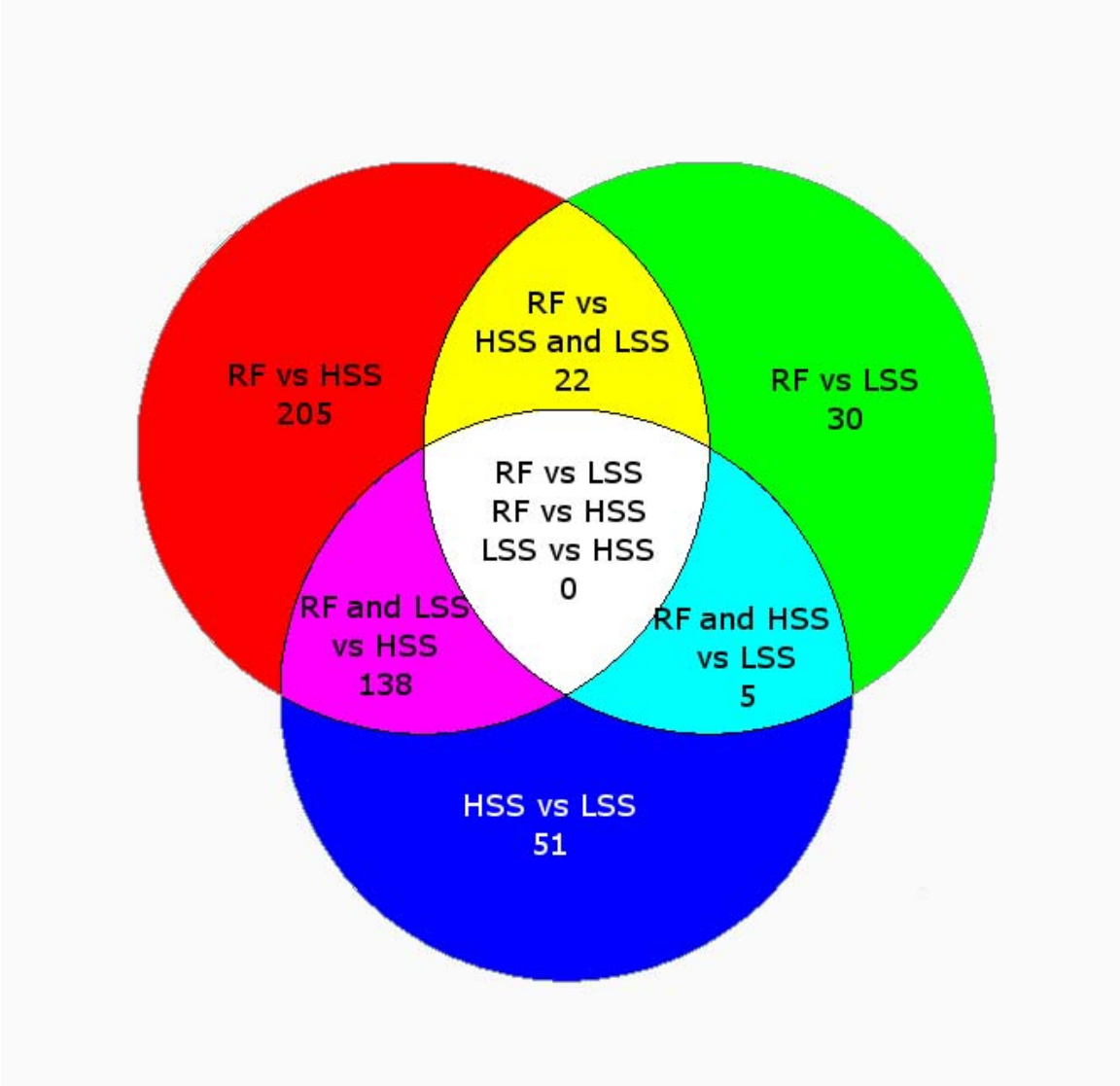

Figure 21: Venn diagram of differentially expressed genes in a comparison of RF to HSS, RF to LSS, and HSS to LSS.
Differentially expressed genes found in the purple region of overlap are regulated by low average flow while genes found within the yellow region of overlap are regulated by flow reversal. Genes located within the light blue area are regulated by high average shear stress.

In our study there are two conditions which have low average shear stress, LSS and RF. Examination of the purple portion of Figure 21 shows that when either LSS or RF is compared to HSS there are 138 genes that are found in both lists. Further examination shows that in all of these genes both LSS and RF generate the same direction of either up- or down-regulation compared to HSS. Based on this similar response to both LSS

and RF as compared to HSS, these genes can be termed "regulated by low average shear stress" (Supplemental Table 9, list of genes with fold changes). DAVID functional annotation clustering was used to group down-regulated and up-regulated genes based on function. These functional groups are shown in Figure 22 and Figure 23 as hierarchical clusters of associated genes and conditions.

These hierarchical clusters include down-regulation by low average shear stress of genes associated with anatomical structure development, cell communication, response to external stimuli, blood vessel morphogenesis, chemical homeostasis, hydrolase activity, and actin filament organization (Figure 22). Genes up-regulated by low average shear stress were associated with metallothioneins and cell cycle phase (Figure 23).

These hierarchical clusters show clustering of both genes and conditions associated with functional groups regulated by low average shear stress. In all of the hierarchical clusters shown, ECs exposed to reversing flow and ECs exposed to low shear stress cluster on a branch which is separate from ECs exposed to high shear stress. It should be noted that clustering of the reversing flow and low shear stress conditions on a single branch is in contrast to the clustering results obtained when all of the genes on the microarray were incorporated into the clustering algorithm. This is a further indication that these genes are regulated by low average shear stress.

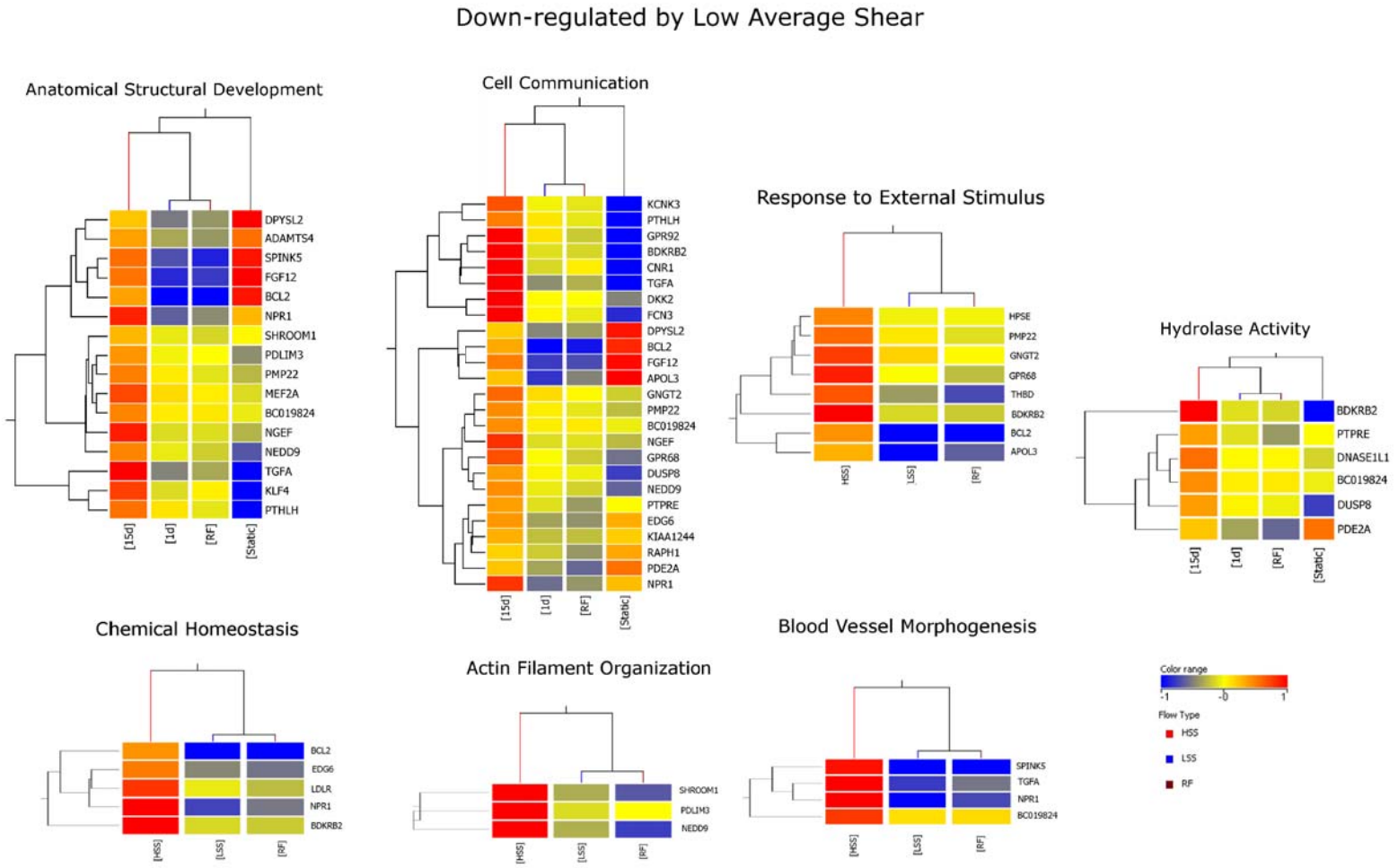

Figure 22: Heirarchical clusters of functional groups down-regulated by low average shear stress.
Flow conditions and genes associated with functional groups identified by DAVID were clustered according to expression patterns. . The color range shown is indicative of the normalized natural log transformed signal values for each gene.

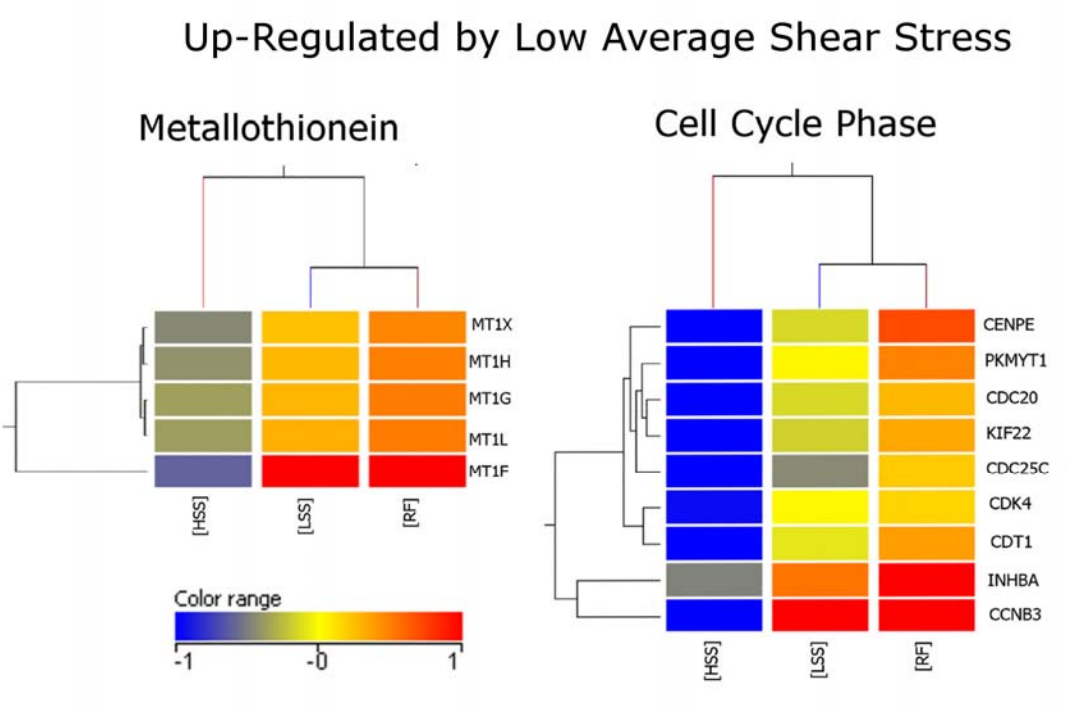

Figure 23: Hierarchical clusters of functional groups up-regulated by low average shear stress. Flow conditions and genes associated with functional groups identified by DAVID were clustered according to expression patterns. The color range shown is indicative of the normalized natural log transformed signal values for each gene.

In our study RF was compared to both HSS and LSS. The yellow portion of Figure 21 shows that there are 22 genes which overlap between these two comparisons. 100% of the genes showed similar directions of up-or down-regulation in response to reversing flow as compared to both HSS and LSS. Based on this these genes can be termed "regulated by reversing flow" (Table 14). DAVID functional annotation clustering was used to group these genes based on function. Differentially regulated functional groups are shown in Figure 24 as hierarchical clusters of associated genes and conditions. In these hierarchical clusters, ECs exposed to reversing flow clustered on a branch separate from ECs exposed to high shear stress or low shear stress. This pattern coincides with the clustering results obtained from analysis of the entire array as shown in Figure 20.

Table 14: Genes regulated by flow reversal

Gene Symbol	Gene Name	Fold Change (RF/HSS)
AK023086	Unannotated	3.1
GGTLA1	gamma-glutamyltransferase-like activity 1	2.5
PRIM2A	primase, polypeptide 2A	2.5
FLJ14712	Unannotated	2.4
CCNE2	cyclin E2	2.4
CEP55	centrosomal protein 55kDa	2.1
APOM	apolipoprotein M	1.9
RRM1	ribonucleotide reductase M1 polypeptide	1.9
KRTAP19-1	keratin associated protein 19-1	1.8
ATAD5	ATPase family, AAA domain containing 5	1.8
PIF1	PIF1 5'-to-3' DNA helicase homolog	1.8
KIF21A	kinesin family member 21A	1.8
BC020241	Unannotated	1.8
C21orf2	chromosome 21 open reading frame 2	1.7
CASC5	cancer susceptibility candidate 5	1.7
JPH2	junctophilin 2	1.7
PRKACB	protein kinase, cAMP-dependent, catalytic, beta (PRKACB), transcript variant 3, mRNA [NM_207578]	1.6
BC017350	Unannotated	-1.6
CDC42EP3	CDC42 effector protein (Rho GTPase binding) 3	-1.8
SLC26A2	solute carrier family 26 (sulfate transporter), member 2	-1.8
THC2722466	Unannotated	-1.9
FGF16	fibroblast growth factor 16	-2.8

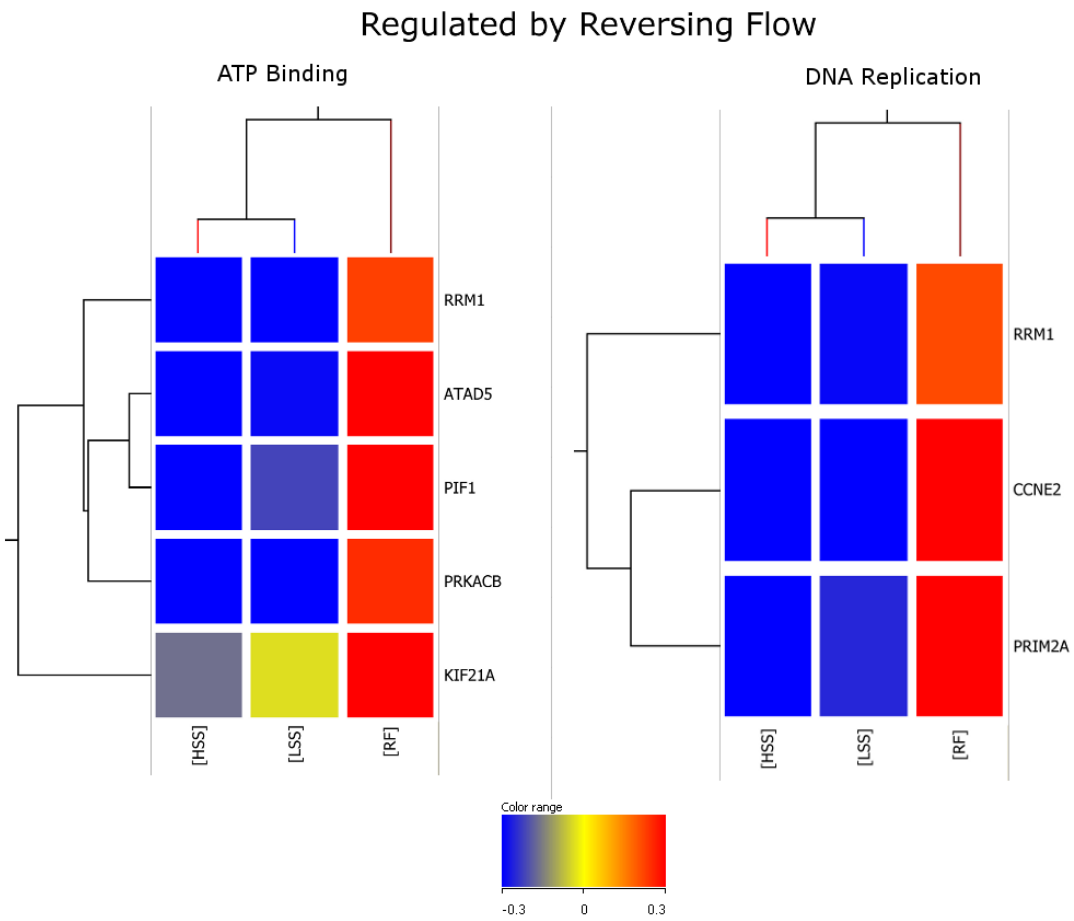

Figure 24: Hierarchical clusters of functional groups regulated by reversing flow.
Flow conditions and genes associated with functional groups identified by DAVID were clustered according to expression patterns. The color range shown is indicative of the normalized natural log transformed signal values for each gene.

Further examination of Figure 21 shows that in the light blue section there are 5 genes which overlap. This portion of the Venn diagram represents genes which are differentially expressed in a comparison of HSS to LSS and RF to LSS. In this case both HSS and RF have been exposed to high shear stresses for at least some period of time during each cycle. As with the other genes in overlapping lists described previously, exposure to HSS and RF induced differential expression compared to LSS in the same direction of either up- or down-regulation. Thus, these 5 genes may be regulated by

exposure to high shear stress despite the fact that the average shear stress applied to RF is low.

qRT-PCR

Microarray data was confirmed with qRT-PCR on two genes up-regulated by low average shear stress, metallothionein 1F (MT1F) and cyclin B3 (CCNB3), along with two genes down-regulated by low average shear stress, Kruppel-like factor 2 (KLF2) and natriuretic peptide receptor A (NPR1). Additionally, two genes up-regulated by reversing flow, primase polypeptide 2A (PRIM2A) and cyclin E2 (CCNE2), were chosen for qRT-PCR confirmation. Comparisons of qRT-PCR data and microarray data are shown in Figure 25. The genes regulated by low average shear stress had very similar changes in expression as measured by either qRT-PCR or microarray. Of the two genes which were up-regulated by reversing flow, only PRIM2A had qRT-PCR data similar to microarray data. CCNE2 showed no significant change in expression between the three flow conditions when measured by qRT-PCR.

Cell Proliferation

To further investigate cell cycle changes, cells exposed to either static culture, HSS, LSS, or RF were assayed for cell proliferation via incubation with BrdU followed by staining for BrdU incorporation into the DNA. Although static control cultures had the greatest fraction of BrdU positive cells, comparisons among the shear stress conditions showed that the number of BrdU positive cells was increased over two-fold under reversing shear stress and 1 dyne/cm^2 when compared to 15 dynes/cm^2 (Figure 26). This data indicates

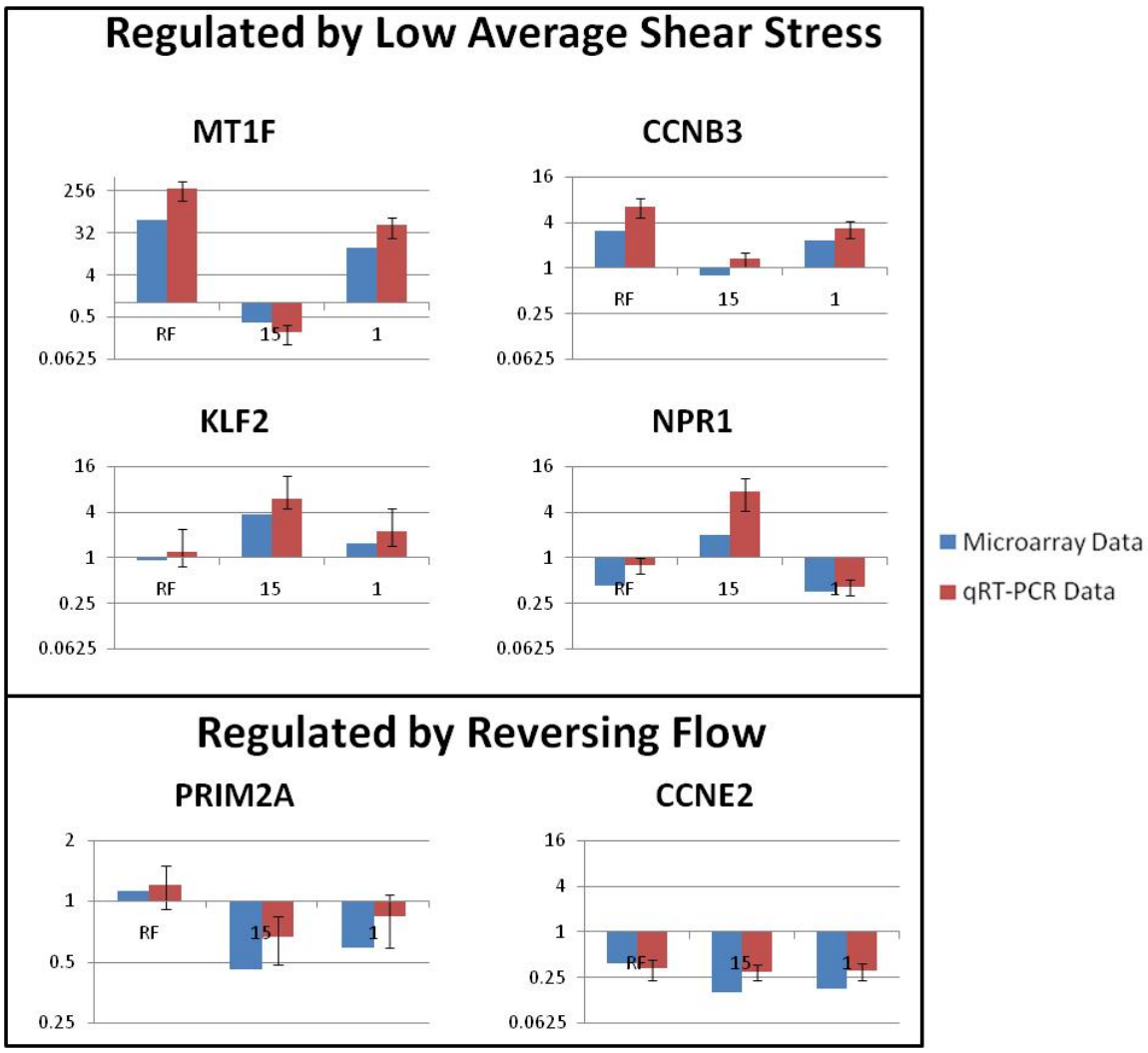

Figure 25: qRT-PCR Confirmation of Microarray Results
Four genes regulated by low average shear stress and two genes regulated by reversing flow were chosen for confirmation of microarray results with qRT-PCR. Blue bars are microarray data and red bars are qRT-PCR data. Note that not all axes share the same value.

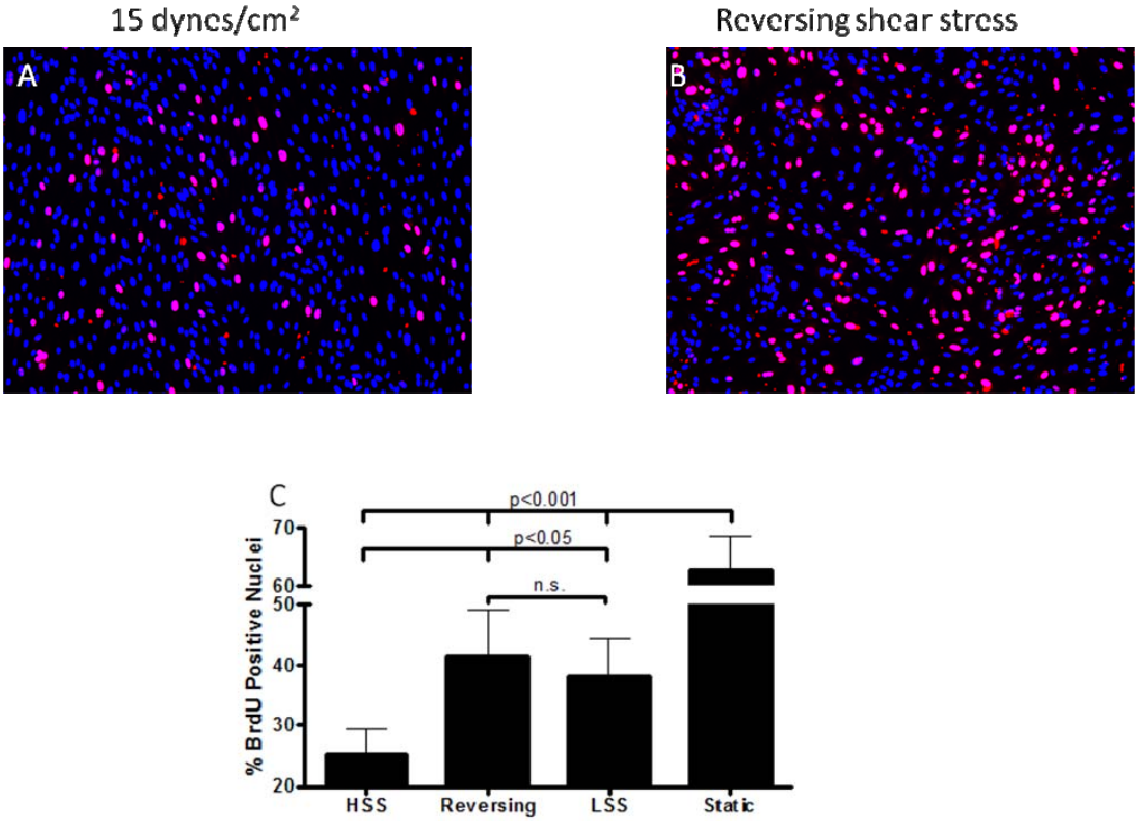

Figure 26: Cell proliferation is inhibited by high shear stress compared to low average shear stress. ECs were stained for BrdU incorporation (red) and the presence of nuclear DNA using Hoechst 33258 (blue) following culture in either static or flow conditions. Nuclei appearing pink are indicative of positive staining for both DNA and BrdU. (A) A representative image of ECs cultured at 15 dynes/cm^2 for 24 hours and stained for BrdU incorporation and nuclear DNA. (B) A representative image of ECs cultured under reversing shear stress for 24 hours and stained for BrdU incorporation and nuclear DNA. (C) Fluid flow caused a reduction in BrdU incorporation. Exposure to high shear stress caused the greatest reduction in BrdU incorporation. The percentage of nuclei which stained positively for BrdU was determined by counting nuclei in 5 experiments with 8 frames per experiment.

that exposure of ECs to shear stress causes inhibition of cell proliferation. In comparison to HSS, both RF and LSS cause increased cell proliferation in ECs, indicating that low time average shear stress is involved in regulating cell division.

Monocyte Adhesion

To assess the ability of reversing shear stress to lead to increased inflammation and leukocyte recruitment, a monocyte adhesion assay was performed on HUVEC pretreated with all shear stress conditions. Significantly increased monocyte adhesion was observed under reversing flow, but not under other conditions (Figure 27).

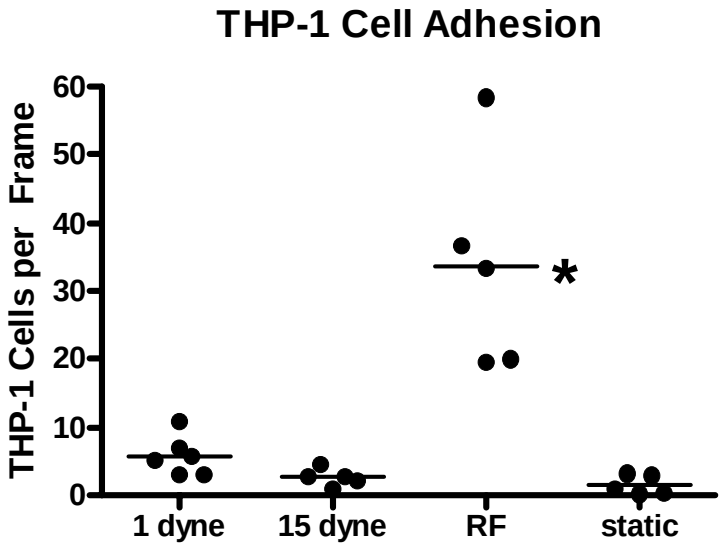

Figure 27 THP-1 cells have greater adhesion to ECs exposed to reversing flow.
THP-1 cells were counted in 10 frames each of five to six separate experiments. Dots shown on the graph represent the average number of adherent cells in each experiment. The line shown on the graph represents the median number of adherent cells for all experiments. *$p<0.001$ between reversing flow and all three other conditions.

Discussion

We describe herein the design and application of a novel reversing shear stress system using a parallel plate flow chamber. Other studies have used a variety of parallel plate or cone and plate systems to study the effects of either disturbed or oscillating flow on endothelial cell gene expression[25,27,106,109-111]. Some of these studies comparing the effects of steady shear stress to reversing shear stress have modeled the reversing shear stress waveform as an oscillating sine wave function. While this is a simpler shear stress to implement in an *in vitro* system, the physiological shear stress is not harmonic, and includes much more rapid changes in shear stress direction. Also, the time-average shear stress in some models was set at zero,[110] and as a result there was no net forward movement across the cells, a situation that does not occur *in vivo*. Another limiting factor of previous studies is the lack of a steady low shear stress control, which would allow for differentiation of responses that are due only to time-average low shear stress from those due to fluid shear stress reversal.

The shear stress profile chosen for our system was based on computer simulated data of the shear stress at the carotid sinus[105] and is similar to that of the atheroprone waveform developed by Dai, et al.[27]. However, unlike the system by Dai, et al., we designed our system to use a parallel plate chamber instead of a cone and plate. A parallel plate chamber allowed us to perform a flow-based monocyte adhesion assay on cells pre-treated with different shear stress conditions. Although we have chosen to use this system to model the reversing shear stress at the carotid sinus, the linear motor can be easily programmed to deliver other equally complex shear stress waveforms.

With this system we investigated changes in cell morphology, gene expression, cell proliferation, and monocyte adhesion under reversing flow as compared to high shear stress, low shear stress, and static culture. ECs exposed to reversing flow exhibited a cobblestone like appearance in contrast to ECs exposed to high shear stress which were elongated and aligned with flow. Similar differences in cell morphology are seen in vivo when comparing porcine ECs found in the descending thoracic aorta (undisturbed unidirectional flow) and porcine ECs found adjacent to a branch of the aorta (separated disturbed flow)[112], providing further evidence that our reversing flow system mimics in vivo fluid flow disturbances found in branching regions of the vasculature.

In our system, fluid flow induced differential gene expression in approximately 7% of all human genes. This number of differentially expressed genes is similar to, although slightly higher, than previous reports which indicate that shear stress affects between 1% and 6% of genes[23,25,106,111,113]. Differences in the number of genes reported as differentially expressed can be attributed to microarray analysis techniques, microarray platforms, and differences in experimental setup. In our system a comparison of fluid flow to static flow revealed that 57% of differentially expressed genes were similarly up- or down-regulated by high shear stress, low shear stress, and reversing flow as compared to static flow. This indicates that up- or down-regulation of these genes is controlled simply by the presence of flow while the type of flow determines the magnitude of response rather than the direction of response as compared to static culture. This is

further validated in Figure 20 by clustering of the three flow conditions on a branch separate from static culture.

In order to validate our microarray data, we have compared our data to data from other groups who have looked at a comparison of endothelial cell gene expression under shear stress and static culture. Our data comparing high shear stress to static culture confirmed 72 percent of the genes reported by Ohura et al. to be up-regulated in HUVEC by 15 dynes/cm^2 laminar shear stress as compared to static culture[106]. McCormick et al. reported transcriptional changes in HUVEC exposed to 25 dynes/cm^2. Our data confirmed differential expression for 47 percent of the genes reported by McCormick et al. which had fold changes of at least 1.5 fold at 24 hours[23]. This agreement of our data with previously published reports on steady shear stress provides further validation of our microarray results.

Comparisons of ECs exposed to different fluid flow regimes are more relevant to understanding vascular pathologies than comparison to static culture because static culture is not representative of a known physiological state. Therefore gene expression of ECs exposed to reversing flow, high steady shear stress, and low steady shear stress were compared. Comparison of reversing flow to high steady shear stress identified 365 differentially expressed genes between the two conditions. The reversing flow profile which we used has a low time averaged shear stress of approximately 1 dyne/cm^2. Therefore, further comparisons were performed to determine whether differential gene expression was induced by low average shear stress or flow reversal. 138 genes were

identified as being regulated by low average shear stress, while only 22 genes were identified as being regulated by flow reversal.

Flow reversal caused up-regulation of three genes related to DNA replication (Figure 24). RRM1 is a gene which encodes for one of two subunits that make up ribonucleotide diphosphate reductase, an enzyme required for the production of deoxyribonucleotides prior to DNA synthesis[114]. CCNE2 encodes for cyclin E2 which regulates CDK2 activity and is involved in the G1 to S phase transition[115]. Finally, PRIM2A is responsible for synthesis of small RNA primers necessary for Okazaki fragments made during DNA replication[116]. Up-regulation of these genes by flow reversal may play an important role in regulating cell proliferation.

The reversing flow profile which we have studied is similar to the "athero-prone" waveform studied by Dai et al[27]. This group used a cone and plate device to apply either athero-prone reversing flow or athero-protective pulsatile non-reversing flow to ECs. This group found 159 genes which were differentially regulated in a comparison of ECs exposed to either athero-prone or athero-protective flow profiles. In our system a comparison of reversing flow to high steady shear stress revealed differential regulation of 13 of these same genes. Our data further reveals that 10 of these 13 genes are regulated by low average shear stress rather than flow reversal (APOL3, CD34, CD58, CRIP1, CYP1B1, KLF2, MEF2A, PTHLH, CDC20, and metallothioneins).

Our lab has recently further examined CYP1B1 expression and confirmed regulation of CYP1B1 by low average shear stress [117]. KLF2 has been shown to be attenuated under reversing shear stress as compared to non-reversing shear stress[27]; however, other published work has shown KLF2 is also equally attenuated under low shear stress[118,119] supporting our observation that KLF2 is regulated by low average shear stress. Regulation of metallothioneins was also reported by Ohura et al. who examined the effects of turbulent flow in comparison to high steady laminar flow [106]; however, in their system turbulent flow caused down-regulation of metallothionein expression while in our system reversing shear stress caused up-regulation of metallothioneins. Our lab has also shown metallothioneins to be one of the few genes differentially regulated by non-reversing pulsatile shear stress compared to steady shear stress.[107] These differences indicate that metallothionein expression is highly sensitive to variations in endothelial shear stress, which may be important for regulation of downstream signaling events.

Our results indicate that a number of genes which regulate the cell cycle are up-regulated by low average shear stress in comparison to high steady shear stress. We performed an analysis of BrdU incorporation in order to assess the effects of differential expression of these genes on cell cycle progression. The increased BrdU incorporation suggests that cell cycle progression can be up-regulated under reversing shear stress. Interestingly similar results were observed for the low shear stress control, suggesting that the time-average low shear stress may regulate cell cycle progression.

We also observed increased monocyte adhesion to ECs following exposure to reversing shear stress. This increase in monocyte adhesion was not found in ECs following exposure to low steady shear stress, indicating that fluid reversal is responsible for the development of a more adhesive and activated endothelial cell phenotype. Previous studies of EC exposure to oscillatory flow have shown a similar increase in monocyte adhesion [109,110,120]. These studies examined monocyte adhesion following a 45 minute incubation with ECs exposed to oscillatory shear stress. In our study we have examined monocyte adhesion under flow; monocytes were perfused across ECs at 1 dyne/cm^2 for five minutes and an assessment of monocyte rolling or firm adhesion revealed no binding between the flowing monocytes and the ECs. However, when fluid flow was stopped for 30 seconds and then returned to 1 dyne/cm^2, monocytes firmly adhered to ECs exposed to reversing flow and did not firmly adhere to ECs grown in static culture or exposed to high or low steady shear stress. These data indicate that flow reversal fails to induce expression of selectins or other molecules involved in initial leukocyte binding; however, exposure to reversing flow leads to increased firm adhesion likely mediated by integrin ligands such as ICAM1 and VCAM1.

In summary we have developed a physiological reversing shear stress system which can be used to reproduce the wall shear stress at the carotid sinus. Using a low steady shear stress control, we show that most gene expression changes in cells exposed to reversing shear stress are regulated by the low time average shear stress and not fluid shear stress reversal. We also show that low time average shear stress is the major force responsible for increases in cell proliferation as compared to cells exposed to arterial levels of steady

shear stress. Interestingly, we showed increased monocyte adhesion only in cells exposed to reversing shear stress. Our findings provide further insight into endothelial responses to mechanical forces and may be important in understanding mechanisms of atherosclerotic development and localization to regions of disturbed flow.

CHAPTER 5: SUMMARY AND DISCUSSION

Summary

In this project, I have examined endothelial and leukocyte responses to inflammatory stimuli and leukocyte transmigration. Key findings from each chapter are presented below.

Chapter 2: Gene expression of endothelial cells due to interleukin-1 beta stimulation and neutrophil transmigration

- Identified over 2500 genes differentially expressed in HUVEC following IL1β stimulation
- IL1β induced differential expression of genes related to apoptosis, cell cycle, NFκb cascade, chemotaxis, and the immune response
- Claudin-1 mRNA and protein are up-regulated by IL1β
- Occludin mRNA and claudin-5 mRNA and protein are down-regulated by IL1β
- PBEF mRNA and protein are up-regulated following IL1β stimulation
- Neutrophil transmigration had little impact on EC gene expression in comparison to the large effects induced by IL1β

Chapter 3: Transmigration across activated endothelium induces transcriptional changes in monocytes

- Identified over 600 genes differentially expressed in transmigrated monocytes as compared to untreated monocytes
- Transmigration induced differential expression of genes related to numerous cell functions including the immune response and inhibition of apoptosis
- AnnexinV labeling showed reduced apoptosis in monocytes following transmigration
- qRT-PCR confirmed increased expression of NAIP, an inhibitor of apoptosis, in monocytes following transmigration
- Identified 89 genes regulated by the process of diapedesis
- Confirmed down-regulation of antimicrobial mRNA and protein expression following monocyte transmigration

Chapter 4: Reversing shear stress promotes a more inflammatory and proliferativer phenotype in endothelial cells than steady shear stress

- Developed a parallel plate flow system to accurately recreate the shear stress found at the wall of the carotid sinus
- Identified ~3000 genes differentially expressed in ECs treated with shear stress as compared to static culture
- Identified 138 genes regulated by exposure to low average shear stress
- Genes regulated by low average shear stress are involved in cell cycle regulation, metallothioneins, cell communication, and anatomical structure development

- Identified 22 genes regulated by exposure to reversing flow which are involved in DNA replication and ATP binding
- ECs exposed to low steady shear stress or reversing flow exhibited increased cell proliferation in comparison to ECs exposed to high steady shear stress
- Increased monocyte adhesion on ECs exposed to reversing flow as compared to high steady shear stress, low steady shear stress, or static culture.

Future Work

This work has used microarray analysis in combination with other techniques to analyze leukocyte and endothelial responses to chemical and mechanical stimuli relevant to inflammation. As with all research, this project has also revealed numerous questions which remained unanswered. In Chapter 2 I showed up-regulation of claudin-1 and down-regulation of claudin-5 and occludin following treatment with IL1β. These proteins are all found at cell-cell junctions between endothelial cells and are thought to play an important role in regulating endothelial permeability and transendothelial resistance. It is clear that the endothelium maintains tight control over expression of these cell junction molecules and further studies are necessary to understand how they work together to regulate endothelial junctions during inflammation, particularly during transmigration. In Chapter 2, I also showed up-regulation of PBEF which is a cytokine thought to be involved in leukocyte recruitment and regulation of the endothelial barrier. The importance of this protein for regulating the endothelium and leukocyte transmigration is not well understood and deserves further study. Finally our work showed that neutrophil transmigration had little impact on EC transcription compared to

the large impact of IL1β stimulation. However, recent studies have provided more evidence of EC intracellular responses to leukocyte transmigration and adhesion. Thus while ECs do not appear to significantly alter transcriptional patterns in response to IL1β induced transmigration, they certainly undergo changes in cytoskeletal organization, adhesion molecule clustering, and activation of signal transduction pathways. Further studies are necessary to gain a full understanding of how ECs respond to inflammatory processes.

In Chapter 3 my work focused on monocyte responses to transmigration. In this work I showed that monocytes have reduced apoptosis following transmigration. In addition I showed that NAIP, a key inhibitor of apoptosis found within the apoptosis pathway, is up-regulated following transmigration. This suggests that NAIP is involved in the inhibition of apoptosis following transmigration. To further substantiate this, activity of caspase 3 and 9 should be examined. More research is necessary in order to understand the mechanisms by which diapedesis causes up-regulation of NAIP expression. My work also showed down-regulation of antimicrobial proteins following transmigration. Further studies are necessary to determine whether the same response is seen in monocytes exposed to bacteria following transmigration. In addition the respiratory burst and bacterial killing ability of transmigrated monocytes should be further examined.

In Chapter 4 I examined the endothelial response to reversing flow. Comparison to low and high shear stress controls revealed that a number of transcriptional changes are regulated by exposure to low average shear stress rather than flow reversal. This data

also showed increased cell proliferation in ECs exposed to low average shear stress as compared to high steady shear stress. Further studies are required to understand the mechanisms involved in regulating cell proliferation and leukocyte adhesion.

APPENDIX A: CALCULATION OF WALL SHEAR STRESS

The measurement of fluid shear stress was accomplished through the use of latex beads filmed under high speed video microscopy (1000 frames per second). This appendix explains how the measured velocity of these individual beads was used to determine wall shear stress.

Calculation of shear stress:

Navier-Stokes Equation

$$\rho\left(\frac{\partial v_x}{\partial t}+v_x\frac{\partial v_x}{\partial x}+v_y\frac{\partial v_x}{\partial y}+v_z\frac{\partial v_x}{\partial z}\right)=\frac{-\partial P}{\partial x}-\mu\left(\frac{\partial^2 v_x}{\partial x^2}+\frac{\partial^2 v_x}{\partial y^2}+\frac{\partial^2 v_x}{\partial z^2}\right)+\rho g_x$$

The Navier-Stokes Equation can be simplified for the fluid flow through a parallel plate chamber based on the following assumptions:

1. Steady state

$$\frac{\partial v_x}{\partial t}=0$$

2. Fully developed flow

$$v_x\frac{\partial v_x}{\partial x}=0 \quad \frac{\partial^2 v_x}{\partial x^2}=0$$

3. Laminar flow

$$v_y=0 \quad v_z=0$$

4. Side wall effects can be ignored

$$\frac{\partial^2 v_x}{\partial z^2}=0$$

5. No gravity in the x direction

$$pg_x = 0$$

The Navier-Stokes equation is then reduced to:

$$\frac{\partial P}{\partial x} = \mu \frac{\partial^2 v_x}{\partial y^2}$$

If the pressure drop is assumed to be constant over the entire length of the chamber, this can be reduced to

$$-\frac{\Delta P}{\mu L} = \frac{\partial\, v_x}{\partial y^2}$$

Separate the variables and integrate to obtain:

$$\frac{-\Delta P}{\mu L} y + C_1 = \frac{\partial v_x}{\partial y}$$

Separate the variables again and integrate to obtain:

$$-\frac{\Delta P}{2\mu L} y^2 + C_1 y + C_2 = v_x$$

Use the following boundary conditions to solve for C_1 and C_2.

$\frac{\partial v_x}{\partial y} = 0$ at y = 0 and $v_x = 0$ at y = b/2

Inserting boundary condition 1:

$$-\frac{\Delta P}{\mu L} y + C_1 = \frac{\partial v_x}{\partial y}$$

$$-\frac{\Delta P}{\mu L}(0) + C_1 = 0$$

$$C_1 = 0$$

Boundary condition 2 can be used to solve for C_2:

$$-\frac{\Delta P}{2\mu L} y^2 + C_1 y + C_2 = v_x$$

$$-\frac{\Delta P}{2\mu L} y^2 + C_2 = v_x$$

$$-\frac{\Delta P}{2\mu L}\left(\frac{b}{2}\right)^2 + C_2 = 0$$

$$C_2 = \frac{\Delta P b^2}{8\mu L}$$

$$v_x = -\frac{\Delta P}{2\mu L} y^2 + \frac{\Delta P b^2}{8\mu L}$$

Solve for the volumetric flow rate by substituting in the velocity equation to the following:

$$Q = \int_{-w/2}^{w/2} \int_{-b/2}^{b/2} v_x \, dy dz$$

$$v_x = -\frac{\Delta P}{2\mu L}\left(y^2 - \frac{b^2}{4} \right)$$

$$Q = \int_{-w/2}^{w/2} \int_{-b/2}^{b/2} -\frac{\Delta P}{2\mu L}\left(y^2 - \frac{b^2}{4} \right) dy dz$$

$$Q = \int_{-b/2}^{b/2} -\frac{\Delta P}{2\mu L}\left(y^2 - \frac{b^2}{4} \right)\left(\frac{w}{2} + \frac{w}{2} \right) dy$$

$$Q = \left(-\frac{\Delta P w}{6\mu L} y^3 + \frac{\Delta P w b^2}{8\mu L} y \right)\Bigg|_{y=-\frac{b}{2}}^{y=\frac{b}{2}}$$

$$Q = \frac{\Delta P w b^3}{12\mu L}$$

Solve for ΔP:

$$\Delta P = \frac{12 Q \mu L}{w b^3}$$

Solve for the shear rate at y = +/-b/2:

$$\gamma = \frac{\partial v_x}{\partial y} = \frac{\Delta P}{\mu L} y$$

$$\gamma = \frac{12 Q \mu L}{w b^3} * \frac{1}{\mu L} * \frac{b}{2}$$

$$\gamma = \frac{6Q}{w b^2}$$

The shear stress, τ, is the shear rate multiplied by the fluid viscosity.

$$\tau = \gamma\mu = \frac{6Q\mu}{wb^2}$$

Relationship between fluid velocity and shear stress

To focus the high speed video camera at the center of the flow chamber, a mark was made on the glass slide and also on the surface of the flow chamber. The focus knob was marked at each position and then adjusted to the middle. The velocity at the middle of the chamber (y=0) represents the maximum velocity, and the measured beads were assumed to be at the maximum velocity of the fluid flow through the chamber.

$$v_x = -\frac{\Delta P}{2\mu L} y^2 + \frac{\Delta P b^2}{8\mu L}$$

$$y = 0$$

$$V_x^{\max} = \frac{\Delta P b^2}{8\mu L}$$

Using the previous derivation of shear stress, find a similar term for the average velocity:

$$Q = \frac{\Delta P w b^3}{12\mu L}$$

$$V_x^{avg} = \frac{Q}{A}$$

$$A = bw$$

$$V_x^{avg} = \frac{\frac{\Delta P w b^3}{12\mu L}}{bw} = \frac{\Delta P b^2}{12\mu L}$$

Finding the ratio of V_x^{avg} to V_x^{max}:

$$\frac{V_x^{avg}}{V_x^{\max}} = \frac{\frac{\Delta P b^2}{12\mu L}}{\frac{\Delta P b^2}{8\mu L}} = \frac{2}{3}$$

$$V_x^{\max} = \frac{3}{2} V_x^{avg}$$

$$V_x^{\max} = \frac{3}{2} \frac{\tau b}{6\mu}$$

$$\tau = \frac{4 V_x^{\max} \mu}{b}$$

REFERENCES

1. Hordijk P. Endothelial signaling in leukocyte transmigration. Cell Biochem Biophys. 2003;38:305-322.

2. Rose DM, Alon R, Ginsberg MH. Integrin modulation and signaling in leukocyte adhesion and migration. Immunol Rev. 2007;218:126-134.

3. Zhao B, Stavchansky SA, Bowden RA, Bowman PD. Effect of interleukin-1beta and tumor necrosis factor-alpha on gene expression in human endothelial cells. Am J Physiol Cell Physiol. 2003;284:C1577-1583.

4. Mayer H, Bilban M, Kurtev V, et al. Deciphering regulatory patterns of inflammatory gene expression from interleukin-1-stimulated human endothelial cells. Arterioscler Thromb Vasc Biol. 2004;24:1192-1198.

5. Bandman O, Coleman RT, Loring JF, Seilhamer JJ, Cocks BG. Complexity of inflammatory responses in endothelial cells and vascular smooth muscle cells determined by microarray analysis. Ann N Y Acad Sci. 2002;975:77-90.

6. van Buul JD, Kanters E, Hordijk PL. Endothelial signaling by Ig-like cell adhesion molecules. Arterioscler Thromb Vasc Biol. 2007;27:1870-1876.

7. Etienne S, Adamson P, Greenwood J, Strosberg AD, Cazaubon S, Couraud PO. ICAM-1 signaling pathways associated with Rho activation in microvascular brain endothelial cells. J Immunol. 1998;161:5755-5761.

8. Huang AJ, Manning JE, Bandak TM, Ratau MC, Hanser KR, Silverstein SC. Endothelial cell cytosolic free calcium regulates neutrophil migration across monolayers of endothelial cells. J Cell Biol. 1993;120:1371-1380.

9. Goldbeter A, Dupont G, Berridge MJ. Minimal model for signal-induced Ca2+ oscillations and for their frequency encoding through protein phosphorylation. Proc Natl Acad Sci U S A. 1990;87:1461-1465.

10. Marcus BC, Hynes KL, Gewertz BL. Loss of endothelial barrier function requires neutrophil adhesion. Surgery. 1997;122:420-426; discussion 426-427.

11. Cepinskas G, Savickiene J, Ionescu CV, Kvietys PR. PMN transendothelial migration decreases nuclear NFkappaB in IL-1beta-activated endothelial cells: role of PECAM-1. J Cell Biol. 2003;161:641-651.

12. Read MA, Whitley MZ, Williams AJ, Collins T. NF-kappa B and I kappa B alpha: an inducible regulatory system in endothelial activation. J Exp Med. 1994;179:503-512.

13. Collins T, Read MA, Neish AS, Whitley MZ, Thanos D, Maniatis T. Transcriptional regulation of endothelial cell adhesion molecules: NF-kappa B and cytokine-inducible enhancers. FASEB J. 1995;9:899-909.

14. Hansson GK, Libby P. The immune response in atherosclerosis: a double-edged sword. Nat Rev Immunol. 2006;6:508-519.

15. Libby P, Ridker PM, Maseri A. Inflammation and atherosclerosis. Circulation. 2002;105:1135-1143.

16. Steinberg D. Low density lipoprotein oxidation and its pathobiological significance. J Biol Chem. 1997;272:20963-20966.

17. Edfeldt K, Swedenborg J, Hansson GK, Yan ZQ. Expression of toll-like receptors in human atherosclerotic lesions: a possible pathway for plaque activation. Circulation. 2002;105:1158-1161.

18. Lessner SM, Galis ZS. Matrix metalloproteinases and vascular endothelium-mononuclear cell close encounters. Trends Cardiovasc Med. 2004;14:105-111.

19. Hashimoto S, Suzuki T, Dong HY, Yamazaki N, Matsushima K. Serial analysis of gene expression in human monocytes and macrophages. Blood. 1999;94:837-844.

20. Li J, Pritchard DK, Wang X, et al. cDNA microarray analysis reveals fundamental differences in the expression profiles of primary human monocytes, monocyte-derived macrophages, and alveolar macrophages. J Leukoc Biol. 2006.

21. VanderLaan PA, Reardon CA, Getz GS. Site specificity of atherosclerosis: site-selective responses to atherosclerotic modulators. Arterioscler Thromb Vasc Biol. 2004;24:12-22.

22. Gimbrone MA, Jr., Topper JN, Nagel T, Anderson KR, Garcia-Cardena G. Endothelial dysfunction, hemodynamic forces, and atherogenesis. Ann N Y Acad Sci. 2000;902:230-239; discussion 239-240.

23. McCormick SM, Eskin SG, McIntire LV, et al. DNA microarray reveals changes in gene expression of shear stressed human umbilical vein endothelial cells. Proc Natl Acad Sci U S A. 2001;98:8955-8960.

24. McCormick SM, Frye SR, Eskin SG, et al. Microarray analysis of shear stressed endothelial cells. Biorheology. 2003;40:5-11.

25. Garcia-Cardena G, Comander J, Anderson KR, Blackman BR, Gimbrone MA, Jr. Biomechanical activation of vascular endothelium as a determinant of its functional phenotype. Proc Natl Acad Sci U S A. 2001;98:4478-4485.

26. Yee A, Sakurai Y, Eskin SG, McIntire LV. A validated system for simulating common carotid arterial flow in vitro: alteration of endothelial cell response. Ann Biomed Eng. 2006;34:593-604.

27. Dai G, Kaazempur-Mofrad MR, Natarajan S, et al. Distinct endothelial phenotypes evoked by arterial waveforms derived from atherosclerosis-susceptible and -resistant regions of human vasculature. Proc Natl Acad Sci U S A. 2004;101:14871-14876.

28. Brown Z, Gerritsen ME, Carley WW, Strieter RM, Kunkel SL, Westwick J. Chemokine gene expression and secretion by cytokine-activated human microvascular endothelial cells. Differential regulation of monocyte chemoattractant protein-1 and interleukin-8 in response to interferon-gamma. Am J Pathol. 1994;145:913-921.

29. Scholz D, Devaux B, Hirche A, et al. Expression of adhesion molecules is specific and time-dependent in cytokine-stimulated endothelial cells in culture. Cell Tissue Res. 1996;284:415-423.

30. Montesano R, Orci L, Vassalli P. Human endothelial cell cultures: phenotypic modulation by leukocyte interleukins. J Cell Physiol. 1985;122:424-434.

31. Molony L, Armstrong L. Cytoskeletal reorganizations in human umbilical vein endothelial cells as a result of cytokine exposure. Exp Cell Res. 1991;196:40-48.

32. Springer TA. Traffic signals for lymphocyte recirculation and leukocyte emigration: the multistep paradigm. Cell. 1994;76:301-314.

33. Abbassi O, Kishimoto TK, McIntire LV, Anderson DC, Smith CW. E-selectin supports neutrophil rolling in vitro under conditions of flow. J Clin Invest. 1993;92:2719-2730.

34. Lawrence MB, Smith CW, Eskin SG, McIntire LV. Effect of venous shear stress on CD18-mediated neutrophil adhesion to cultured endothelium. Blood. 1990;75:227-237.

35. Jones DA, Abbassi O, McIntire LV, McEver RP, Smith CW. P-selectin mediates neutrophil rolling on histamine-stimulated endothelial cells. Biophys J. 1993;65:1560-1569.

36. Hentzen E, McDonough D, McIntire L, Smith CW, Goldsmith HL, Simon SI. Hydrodynamic shear and tethering through E-selectin signals phosphorylation of p38 MAP kinase and adhesion of human neutrophils. Ann Biomed Eng. 2002;30:987-1001.

37. Hentzen ER, Neelamegham S, Kansas GS, et al. Sequential binding of CD11a/CD18 and CD11b/CD18 defines neutrophil capture and stable adhesion to intercellular adhesion molecule-1. Blood. 2000;95:911-920.

38. Schenkel AR, Mamdouh Z, Chen X, Liebman RM, Muller WA. CD99 plays a major role in the migration of monocytes through endothelial junctions. Nat Immunol. 2002;3:143-150.

39. Ostermann G, Weber KS, Zernecke A, Schroder A, Weber C. JAM-1 is a ligand of the beta(2) integrin LFA-1 involved in transendothelial migration of leukocytes. Nat Immunol. 2002;3:151-158.

40. Vestweber D. Adhesion and signaling molecules controlling the transmigration of leukocytes through endothelium. Immunol Rev. 2007;218:178-196.

41. Schenkel AR, Mamdouh Z, Muller WA. Locomotion of monocytes on endothelium is a critical step during extravasation. Nat Immunol. 2004;5:393-400.

42. Frye SR, Yee A, Eskin SG, Guerra R, Cong X, McIntire LV. cDNA microarray analysis of endothelial cells subjected to cyclic mechanical strain: importance of motion control. Physiol Genomics. 2005;21:124-130.

43. Zimmerman GA, McIntyre TM, Prescott SM. Thrombin stimulates the adherence of neutrophils to human endothelial cells in vitro. J Clin Invest. 1985;76:2235-2246.

44. Dennis G, Jr., Sherman BT, Hosack DA, et al. DAVID: Database for Annotation, Visualization, and Integrated Discovery. Genome Biol. 2003;4:P3.

45. Baggiolini M, Walz A, Kunkel SL. Neutrophil-activating peptide-1/interleukin 8, a novel cytokine that activates neutrophils. J Clin Invest. 1989;84:1045-1049.

46. Rao RM, Yang L, Garcia-Cardena G, Luscinskas FW. Endothelial-dependent mechanisms of leukocyte recruitment to the vascular wall. Circ Res. 2007;101:234-247.

47. Smith WL, DeWitt DL, Garavito RM. Cyclooxygenases: structural, cellular, and molecular biology. Annu Rev Biochem. 2000;69:145-182.

48. Herrmann J, Lerman LO, Lerman A. Ubiquitin and ubiquitin-like proteins in protein regulation. Circ Res. 2007;100:1276-1291.

49. Schulz C, Schafer A, Stolla M, et al. Chemokine fractalkine mediates leukocyte recruitment to inflammatory endothelial cells in flowing whole blood: a critical role for P-selectin expressed on activated platelets. Circulation. 2007;116:764-773.

50. Karin M, Lin A. NF-kappaB at the crossroads of life and death. Nat Immunol. 2002;3:221-227.

51. Winn RK, Harlan JM. The role of endothelial cell apoptosis in inflammatory and immune diseases. J Thromb Haemost. 2005;3:1815-1824.

52. Cozzolino F, Torcia M, Aldinucci D, et al. Interleukin 1 is an autocrine regulator of human endothelial cell growth. Proc Natl Acad Sci U S A. 1990;87:6487-6491.

53. Ott LW, Resing KA, Sizemore AW, et al. Tumor Necrosis Factor-alpha- and interleukin-1-induced cellular responses: coupling proteomic and genomic information. J Proteome Res. 2007;6:2176-2185.

54. Dunne A, O'Neill LA. The interleukin-1 receptor/Toll-like receptor superfamily: signal transduction during inflammation and host defense. Sci STKE. 2003;2003:re3.

55. Skop B, Sobczak A, Drozdz M, Kotrys-Puchalska E. Comparison of the action of transforming growth factor-beta 1 and interleukin-1 beta on matrix metabolism in the culture of porcine endothelial cells. Biochimie. 1996;78:103-107.

56. Lee KY, Ito K, Hayashi R, Jazrawi EP, Barnes PJ, Adcock IM. NF-kappaB and activator protein 1 response elements and the role of histone modifications in IL-1beta-induced TGF-beta1 gene transcription. J Immunol. 2006;176:603-615.

57. Naldini A, Carraro F. Role of inflammatory mediators in angiogenesis. Curr Drug Targets Inflamm Allergy. 2005;4:3-8.

58. Dinarello CA. Biologic basis for interleukin-1 in disease. Blood. 1996;87:2095-2147.

59. Burke-Gaffney A, Keenan AK. Modulation of human endothelial cell permeability by combinations of the cytokines interleukin-1 alpha/beta, tumor necrosis factor-alpha and interferon-gamma. Immunopharmacology. 1993;25:1-9.

60. Marcus BC, Wyble CW, Hynes KL, Gewertz BL. Cytokine-induced increases in endothelial permeability occur after adhesion molecule expression. Surgery. 1996;120:411-416; discussion 416-417.

61. Bazzoni G. Endothelial tight junctions: permeable barriers of the vessel wall. Thromb Haemost. 2006;95:36-42.

62. Abe T, Sugano E, Saigo Y, Tamai M. Interleukin-1beta and barrier function of retinal pigment epithelial cells (ARPE-19): aberrant expression of junctional complex molecules. Invest Ophthalmol Vis Sci. 2003;44:4097-4104.

63. Duffy HS, John GR, Lee SC, Brosnan CF, Spray DC. Reciprocal regulation of the junctional proteins claudin-1 and connexin43 by interleukin-1beta in primary human fetal astrocytes. J Neurosci. 2000;20:RC114.

64. Nitta T, Hata M, Gotoh S, et al. Size-selective loosening of the blood-brain barrier in claudin-5-deficient mice. J Cell Biol. 2003;161:653-660.

65. Fontijn RD, Rohlena J, van Marle J, Pannekoek H, Horrevoets AJ. Limited contribution of claudin-5-dependent tight junction strands to endothelial barrier function. Eur J Cell Biol. 2006;85:1131-1144.

66. Ognjanovic S, Ku TL, Bryant-Greenwood GD. Pre-B-cell colony-enhancing factor is a secreted cytokine-like protein from the human amniotic epithelium. Am J Obstet Gynecol. 2005;193:273-282.

67. Nemeth E, Tashima LS, Yu Z, Bryant-Greenwood GD. Fetal membrane distention: I. Differentially expressed genes regulated by acute distention in amniotic epithelial (WISH) cells. Am J Obstet Gynecol. 2000;182:50-59.

68. Ognjanovic S, Bao S, Yamamoto SY, Garibay-Tupas J, Samal B, Bryant-Greenwood GD. Genomic organization of the gene coding for human pre-B-cell colony enhancing factor and expression in human fetal membranes. J Mol Endocrinol. 2001;26:107-117.

69. Ye SQ, Zhang LQ, Adyshev D, et al. Pre-B-cell-colony-enhancing factor is critically involved in thrombin-induced lung endothelial cell barrier dysregulation. Microvasc Res. 2005;70:142-151.

70. Tesfamariam B, DeFelice AF. Endothelial injury in the initiation and progression of vascular disorders. Vascul Pharmacol. 2007;46:229-237.

71. van Wetering S, van den Berk N, van Buul JD, et al. VCAM-1-mediated Rac signaling controls endothelial cell-cell contacts and leukocyte transmigration. Am J Physiol Cell Physiol. 2003;285:C343-352.

72. van Buul JD, Hordijk PL. Signaling in leukocyte transendothelial migration. Arterioscler Thromb Vasc Biol. 2004;24:824-833.

73. Williams MR, Kataoka N, Sakurai Y, Powers CM, Eskin SG, McIntire LV. Gene expression of endothelial cells due to interleukin-1 beta stimulation and neutrophil transmigration. Endothelium. 2008;15:73-165.

74. Leon B, Ardavin C. Monocyte migration to inflamed skin and lymph nodes is differentially controlled by L-selectin and PSGL-1. Blood. 2008;111:3126-3130.

75. Kukreti S, Konstantopoulos K, Smith CW, McIntire LV. Molecular mechanisms of monocyte adhesion to interleukin-1beta-stimulated endothelial cells under physiologic flow conditions. Blood. 1997;89:4104-4111.

76. Imhof BA, Aurrand-Lions M. Adhesion mechanisms regulating the migration of monocytes. Nat Rev Immunol. 2004;4:432-444.

77. Shi C, Simon DI. Integrin signals, transcription factors, and monocyte differentiation. Trends Cardiovasc Med. 2006;16:146-152.

78. Mahoney TS, Weyrich AS, Dixon DA, McIntyre T, Prescott SM, Zimmerman GA. Cell adhesion regulates gene expression at translational checkpoints in human myeloid leukocytes. Proc Natl Acad Sci U S A. 2001;98:10284-10289.

79. Maurer M, von Stebut E. Macrophage inflammatory protein-1. Int J Biochem Cell Biol. 2004;36:1882-1886.

80. Popovic M, Laumonnier Y, Burysek L, Syrovets T, Simmet T. Thrombin-induced expression of endothelial CX3CL1 potentiates monocyte CCL2 production and transendothelial migration. J Leukoc Biol. 2008;84:215-223.

81. Sozzani S, Locati M, Zhou D, et al. Receptors, signal transduction, and spectrum of action of monocyte chemotactic protein-1 and related chemokines. J Leukoc Biol. 1995;57:788-794.

82. Dangerfield J, Larbi KY, Huang MT, Dewar A, Nourshargh S. PECAM-1 (CD31) homophilic interaction up-regulates alpha6beta1 on transmigrated neutrophils in vivo and plays a functional role in the ability of alpha6 integrins to mediate leukocyte migration through the perivascular basement membrane. J Exp Med. 2002;196:1201-1211.

83. Hochberg Y, Tamhane AC. Multiple comparison procedures. New York: Wiley; 1987.

84. Snedecor GW, Cochran WG. Statistical methods (ed 8th). Ames: Iowa State University Press; 1989.

85. Hu M, Miller EJ, Lin X, Simms HH. Transmigration across a lung epithelial monolayer delays apoptosis of polymorphonuclear leukocytes. Surgery. 2004;135:87-98.

86. Watson RW, Rotstein OD, Nathens AB, Parodo J, Marshall JC. Neutrophil apoptosis is modulated by endothelial transmigration and adhesion molecule engagement. J Immunol. 1997;158:945-953.

87. Takahashi M, Masuyama J, Ikeda U, et al. Induction of monocyte chemoattractant protein-1 synthesis in human monocytes during transendothelial migration in vitro. Circ Res. 1995;76:750-757.

88. Thomas-Ecker S, Lindecke A, Hatzmann W, Kaltschmidt C, Zanker KS, Dittmar T. Alteration in the gene expression pattern of primary monocytes after adhesion to endothelial cells. Proc Natl Acad Sci U S A. 2007;104:5539-5544.

89. Biswas P, Delfanti F, Bernasconi S, et al. Interleukin-6 induces monocyte chemotactic protein-1 in peripheral blood mononuclear cells and in the U937 cell line. Blood. 1998;91:258-265.

90. Romano M, Sironi M, Toniatti C, et al. Role of IL-6 and its soluble receptor in induction of chemokines and leukocyte recruitment. Immunity. 1997;6:315-325.

91. Kovalovsky D, Paez Pereda M, Sauer J, et al. The Th1 and Th2 cytokines IFN-gamma and IL-4 antagonize the inhibition of monocyte IL-1 receptor antagonist by glucocorticoids: involvement of IL-1. Eur J Immunol. 1998;28:2075-2085.

92. Weber C, Weber KS, Klier C, et al. Specialized roles of the chemokine receptors CCR1 and CCR5 in the recruitment of monocytes and T(H)1-like/CD45RO(+) T cells. Blood. 2001;97:1144-1146.

93. Migeotte I, Communi D, Parmentier M. Formyl peptide receptors: a promiscuous subfamily of G protein-coupled receptors controlling immune responses. Cytokine Growth Factor Rev. 2006;17:501-519.

94. Luk T, Malam Z, Marshall JC. Pre-B cell colony-enhancing factor (PBEF)/visfatin: a novel mediator of innate immunity. J Leukoc Biol. 2008;83:804-816.

95. Mishra RS, Carnevale KA, Cathcart MK. iPLA2beta: front and center in human monocyte chemotaxis to MCP-1. J Exp Med. 2008;205:347-359.

96. Lehtonen A, Ahlfors H, Veckman V, Miettinen M, Lahesmaa R, Julkunen I. Gene expression profiling during differentiation of human monocytes to macrophages or dendritic cells. J Leukoc Biol. 2007;82:710-720.

97. Randolph GJ, Beaulieu S, Lebecque S, Steinman RM, Muller WA. Differentiation of monocytes into dendritic cells in a model of transendothelial trafficking. Science. 1998;282:480-483.

98. Harder J, Glaser R, Schroder JM. Human antimicrobial proteins effectors of innate immunity. J Endotoxin Res. 2007;13:317-338.

99. Oppenheim JJ, Tewary P, de la Rosa G, Yang D. Alarmins initiate host defense. Adv Exp Med Biol. 2007;601:185-194.

100. Kougias P, Chai H, Lin PH, Yao Q, Lumsden AB, Chen C. Defensins and cathelicidins: neutrophil peptides with roles in inflammation, hyperlipidemia and atherosclerosis. J Cell Mol Med. 2005;9:3-10.

101. Passlick B, Flieger D, Ziegler-Heitbrock HW. Identification and characterization of a novel monocyte subpopulation in human peripheral blood. Blood. 1989;74:2527-2534.

102. Wootton DM, Ku DN. Fluid mechanics of vascular systems, diseases, and thrombosis. Annu Rev Biomed Eng. 1999;1:299-329.

103. Chien S. Effects of disturbed flow on endothelial cells. Ann Biomed Eng. 2008;36:554-562.

104. Davies PF. Endothelial transcriptome profiles in vivo in complex arterial flow fields. Ann Biomed Eng 2008;36:563-570.

105. Perktold K, Rappitsch G. Computer simulation of local blood flow and vessel mechanics in a compliant carotid artery bifurcation model. J Biomech. 1995;28:845-856.

106. Ohura N, Yamamoto K, Ichioka S, et al. Global analysis of shear stress-responsive genes in vascular endothelial cells. J Atheroscler Thromb. 2003;10:304-313.

107. Yee A, Bosworth KA, Conway DE, Eskin SG, McIntire LV. Gene expression of endothelial cells under pulsatile non-reversing vs. steady shear stress; comparison of nitric oxide production. Ann Biomed Eng. 2008;36:571-579.

108. Chow S, Rodgers P. Applet For Drawing 3 Set Area-Proportional Venn Diagrams. Vol. 2008; 2005.

109. Chappell DC, Varner SE, Nerem RM, Medford RM, Alexander RW. Oscillatory shear stress stimulates adhesion molecule expression in cultured human endothelium. Circ Res. 1998;82:532-539.

110. Sorescu GP, Sykes M, Weiss D, et al. Bone morphogenic protein 4 produced in endothelial cells by oscillatory shear stress stimulates an inflammatory response. J Biol Chem. 2003;278:31128-31135.

111. Brooks AR, Lelkes PI, Rubanyi GM. Gene expression profiling of human aortic endothelial cells exposed to disturbed flow and steady laminar flow. Physiol Genomics. 2002;9:27-41.

112. Davies PF. Endothelial transcriptome profiles in vivo in complex arterial flow fields. Ann Biomed Eng. 2008;36:563-570.

113. Chen BP, Li YS, Zhao Y, et al. DNA microarray analysis of gene expression in endothelial cells in response to 24-h shear stress. Physiol Genomics. 2001;7:55-63.

114. Mann GJ, Musgrove EA, Fox RM, Thelander L. Ribonucleotide reductase M1 subunit in cellular proliferation, quiescence, and differentiation. Cancer Res. 1988;48:5151-5156.

115. Payton M, Coats S. Cyclin E2, the cycle continues. Int J Biochem Cell Biol. 2002;34:315-320.

116. Dehde S, Rohaly G, Schub O, et al. Two immunologically distinct human DNA polymerase alpha-primase subpopulations are involved in cellular DNA replication. Mol Cell Biol. 2001;21:2581-2593.

117. Conway DE, Sakurai Y, Weiss D, et al. Expression of CYP1A1 and CYP1B1 in human endothelial cells: regulation by fluid shear stress. Cardiovasc Res. 2009.

118. Dekker RJ, van Thienen JV, Rohlena J, et al. Endothelial KLF2 links local arterial shear stress levels to the expression of vascular tone-regulating genes. Am J Pathol. 2005;167:609-618.

119. Wang N, Miao H, Li YS, et al. Shear stress regulation of Kruppel-like factor 2 expression is flow pattern-specific. Biochem Biophys Res Commun. 2006;341:1244-1251.

120. Sorescu GP, Song H, Tressel SL, et al. Bone morphogenic protein 4 produced in endothelial cells by oscillatory shear stress induces monocyte adhesion by stimulating reactive oxygen species production from a nox1-based NADPH oxidase. Circ Res. 2004;95:773-779.